UNIVERSITY OF OKLAHOMA

GRADUATE COLLEGE

INVESTIGATIONS OF INTERSPECIES ELECTRON TRANSFER MECHANISMS IMPORTANT TO SYNTROPHIC METABOLISM

A DISSERTATION

SUBMITTED TO THE GRADUATE FACULTY

In partial fulfillment of the requirements for the

Degree of

DOCTOR OF PHILOSOPHY

By

JESSICA RHEA SIEBER
Norman, Oklahoma
2011

Downloaded from SHAREOK. Persistent Handle URL: https://hdl.handle.net/11244/319167

INVESTIGATIONS OF INTERSPECIES ELECTRON TRANSFER MECHANISMS IMPORTANT TO SYNTROPHIC METABOLISM

A DISSERTATION APPROVED FOR THE
DEPARTMENT OF BOTANY AND MICROBIOLOGY

BY

_____
Dr. Michael McInerney, Chair

_____
Dr. Joseph Suflita

_____
Dr. David Nagle

_____
Dr. Elizabeth Karr

_____
Dr. Keith Strevett

© Copyright by JESSICA RHEA SIEBER 2011
All Rights Reserved.

ACKNOWLEDGEMENTS

I have had an incredible amount of support during my PhD program. Dr. McInerney has been more than a guiding hand in my research, but has taught me that I am always capable of more. I will always appreciate the opportunities he gave me that most graduate students do not get including studying in Germany, working with multiple collaborators, and writing reviews. He taught me patience, cautiousness, and how to help others realize their potential.

I have been fortunate to have a very supportive and insightful committee. Dr. Suflita taught me the importance of having several lines of evidence before drawing a conclusion. Dr. Nagle taught me that sometimes the simplest of experiments is the best approach to answer a question. Dr. Karr helped me to keep the methanogens in mind. Syntrophy requires two organisms, but many of us focus only on the syntrophic organism. Dr. Strevett always reminded me that there are many ways to think about a question.

I could not have gotten this far without my many lab mates and friends in the department for their challenging conversations and interesting approaches. I particularly want to thank Kim, Bryan, and Huynh. I think we have learned to work very well as a team, which has kept our lab on the forefront of anaerobic physiology.

All of my family has been incredibly patient with Cody and I. The support we have had from our parents, siblings, and extended family, has pushed us to seek success.

I also need to thank my husband, Cody Sheik. He has helped me maintain and balance my life inside and outside of science. He has always had a different way of thinking about things, which has broadened my approach to science and life. He has made me a better person and a better scientist.

TABLE OF CONTENTS

Acknowledgments iv

List of Tables viii

List of Figures x

Preface xii

Abstract xvi

Chapter I. Methanogenesis: syntrophic metabolism

- Summary 2
- Introduction 3
- Bioenergetic Considerations 5
- Interspecies Electron Transfer 9
- Biochemical Pathways for Syntrophic Metabolism 12
- Potential mechanisms for reverse electron transfer 19
- Conclusions 23

Chapter II. The genome of *Syntrophomonas wolfei*: new insights into syntrophic metabolism and biohydrogen production

- Summary 27
- Introduction 28
- Results and Discussion 31
- Conclusions 56
- Methods 57
- Supplementary Materials 59

Chapter III. Proteomic analysis of the syntrophic, fatty acid-oxidizing organism, *Syntrophomonas wolfei*

- Summary 95
- Introduction 96

Results and Discussion 98

Conclusions 130

Methods 131

Supplemental Materials 138

Chapter IV. Interspecies electron transfer during syntrophic fatty acid- and aromatic acid metabolism

Summary 142

Introduction 143

Results 147

Discussion 171

Methods 176

References 184

LIST OF TABLES

Chapter I

Table 1. Reactions involved in syntrophic metabolism 7

Chapter II

Table 1. General features of the *Syntrophomonas wolfei* genome 32

Table 1S. General features of the *S. wolfei* genome in comparison to other genomes 59

Table 2S. List of genes involved in key metabolic step in *S. wolfei* 60

Table 3S. List of genes involved in electron transfer and formation of ion gradients and those predicted to have transmembrane helices in *S. wolfei* 69

Table 4S. List of genes involved in transport in *S. wolfei* 72

Table 5S. List of sigma factor genes in *S. wolfei* 80

Table 6S. List of genes involved in motility and chemotaxis in *S. wolfei* 81

Table 7S. List of genes involved in sporulation in *S. wolfei* 85

Chapter III

Table 1. Thermodynamics of syntrophic butyrate metabolism 97

Table 2. Abundance of peptides detected only during growth with a methanogenic partner 103

Table 3. The most abundant peptides detected in each condition 111

Table 4. Proteins detected only during syntrophic growth on butyrate 126

Table 1S. Probability of differential abundance during syntrophic growth 138

Table 2S. Probability of differential abundance during growth on crotonate regardless of the presence of a methanogen 139

Table 3S. Abundance of proteins assigned to COG categories 140

Chapter IV

Table 1. Specific activities for hydrogenase and formate dehydrogenase in whole cells of *S. wolfei* 149

Table 2. Localization of hydrogenase and formate dehydrogenase activity in *S. wolfei* by cell fractionation 151

Table 3. Specific activities for hydrogenase and formate dehydrogenase in whole cells of *S. aciditrophicus* 153

Table 4. Localization of hydrogenase and formate dehydrogenase activity in *S. aciditrophicus* by cell fractionation 155

Table 5. Inhibition of washed cell suspensions of *M. hungatei* with hydrogen and CO_2, formate, or formate, hydrogen and CO_2 as substrates for methane production 157

Table 6. Summary of *S. aciditrophicus* and *M. hungatei* washed cell suspension inhibition experiments 159

Table 7. Inhibition of washed cell suspensions of *S. wolfei* and *M. hungatei* with butyrate or crotonate. 161

Table 8. Primers for Q-RT-PCR analysis of the hydrogenases and formate dehydrogenases of *S. wolfei* 163

Table 9. Primers for Q-RT-PCR analysis of the hydrogenases and formate dehydrogenases of *S. aciditrophicus* 168

LIST OF FIGURES

Chapter I

Figure 1. The β-oxidation pathway for butyrate metabolism in *Syntrophomonas wolfei* 14

Figure 2. Pathway for syntrophic benzoate metabolism 17

Figure 3. Proposed models for reversed electron transfer chains 22

Chapter II

Figure 1. Overview of the metabolism of *S. wolfei* 38

Figure 2. Comparison of *S. wolfei* hydrogenase and formate dehydrogenase gene clusters that contain NADH dehydrogenase genes 42

Figure 3. Illustration of the candidates for reverse electron transfer in the genome of *S. wolfei* 47

Figure 1S. Phylogeny of *S. wolfei* 88

Figure 2S. Circular representation of the *S. wolfei* genome 89

Figure 3S. Ribosomal RNA gene clusters of *S. wolfei* 90

Figure 4S. Best reciprocal protein hits for *S. wolfei* ORFs with other genomes 91

Figure 5S. Best Blast hit distribution of *S. wolfei* ORFs with other genomes 92

Figure 6S. Phylogenetic analysis of predicted coding sequences of the membrane-bound FeS oxidoreductase potentially involved in reverse electron transfer in S. wolfei 93

Chapter III

Figure 1. Growth of *S. wolfei* on crotonate and butyrate 99

Figure 2. Number of peptides detected under each condition 102

Figure 3. Non-metric multidimentional scaling of syntrophy protein profiles 106

Figure 4. Peptides detected under each growth condition mapped against the genome for *S. wolfei* 108

Figure 5. Representation of peptides detected in the *S. wolfei* proteome by assignment to major functional classes (COG) 114

Figure 6. The β-oxidation pathway in *S. wolfei* and abundance of the corresponding peptides detected in the proteome 117

Figure 7. Potential routes for interspecies hydrogen transfer 119

Figure 8. Potential routes for interspecies formate transfer 121

Figure 9. Abundance of peptides potentially involved in reverse electron transfer 124

Chapter IV

Figure 1. Response of hydrogenases and formate dehydrogenases gene expression to growth condition for *S. wolfei* 166

Figure 2. Response of hydrogenases and formate dehydrogenases gene expression to growth condition for *S. aciditrophicus* 170

PREFACE

The main goal of this research is investigate the core mechanisms of syntrophy. Previous research on syntrophic organisms has emphasized that syntrophic metabolism, particularly hydrogen or formate production, would be thermodynamically unfavorable unless energy is invested. The processes involved in ion translocation and reverse electron transfer are poorly understood. In order to further our understanding of these mechanisms, including interspecies electron transfer and reverse electron transfer, genomic, proteomic and mRNA expression analyses were conducted along with the more classic routes of enzyme assays and the use of inhibitors. This work has focused on two organisms capable of syntrophy, *Syntrophomonas wolfei* and *Syntrophus aciditrophicus.*

Chapter 1 is a compilation of what we know to date about syntrophy. The focus was on the bioenergetic constraints and the mechanisms involved in overcoming those hurdles. This includes looking at how various organisms capable of syntrophy transfer electrons to their partner organism, how they conserve energy during metabolism (i.e. using CoA transferases instead of CoA ligases and novel benzoyl-CoA reductases), and complexes potentially involved in reverse electron transfer. This review is a portion of a book chapter published in the Handbook of Hydrocarbon and Lipid Microbiology in 2010, in collaboration with Caroline Plugge, Bernard Schink, and Robert Gunsalus. This

chapter is a condensed version focusing on fatty acid and aromatic acid metabolism, interspecies electron transfer, and reverse electron transfer.

Chapter 2 is an analysis of the genome sequence of S. wolfei. This genome was the first syntrophic fatty acid oxidizer to be published. Novel aspects of *S. wolfei*'s lifestyle were discovered in the genome. Confurcating hydrogenases and formate dehydrogenases were discovered. A novel FeS oxidoreductase potentially involved in transferring electrons from acyl-CoA dehydrogenase linked electron transfer flavoproteins to hydrogen, via a cytochrome b linked hydrogenase, that is highly conserved among sequenced organisms capable of syntrophy. One of the more fascinating discoveries was the redundancy encoded into the genome, including nine acyl-CoA dehydrogenases, six formate dehydrogenases, three sets of ribosomal RNA operons, and three sets of electron transfer flavoprotiens. This research was done in collaboration with the Joint Genome Institute and Dr. Robert Gunsalus's lab at UCLA. JGI carried out the sequencing, gap closing, and automated annotation. Dr. Gunsalus's lab aided in analysis of signal transduction and genes and comparisons to other bacterial genomes. It was published in 2010 in *Environmental Microbiology*.

Chapter 3 is an analysis of the proteome of *S. wolfei*. *S. wolfei* was grown under three conditions; syntrophically on butyrate with the methanogen *M. hungatei*, syntrophically on crotonate with the methanogen M. hungatei, and axenically on crotonate. The proteome revealed multiple systems for

interspecies electron transfer and reverse electron transfer including a confurcating hydrogenase, a putative membrane-bound hydrogenase, and a novel FeS oxidoreductase thought to serve as an electron transfer flavoprotein:quinone oxidoreductase. This work demonstrates that *S. wolfei* expresses multiple enzyme systems for fatty acid metabolism, interspecies electron transfer, and energy conservation under all growth conditions. Shotgun proteomics were carried out by Dr. Gregory Hurst at Oak Ridge National Lab, while down stream data analysis was performed in collaboration with Bryan Crable. Dr. Cody Sheik aided in statistical modeling.

Chapter 4 investigates interspecies electron transfer more in depth. A combination of gene expression, enzymatic analyses and inhibitor-based approaches were used to test whether syntrophic benzoate and cyclohexane carboxylate metabolism by *Syntrophus aciditrophicus* and syntrophic butyrate oxidation by *Syntrophomonas wolfei* involves transfer of H_2 and/or formate, or direct electron transfer by nanowires. *S. aciditrophicus* and *S. wolfei* both contained activity for hydrogenase and formate dehydrogenase. Q-RT-PCR revealed that while all the hydrogenases and formate hydrogenases were expressed in both organisms, two hydrogenase systems in *S. wolfei* are the most differentially expressed during syntrophic growth. In *S. aciditrophicus*, three formate dehydrogenases were the most differentially expressed during syntrophic growth. Syntrophic benzoate metabolism by *S. aciditrophicus* and *M. hungatei* depends on formate transfer, while cyclohexane carboxylate

metabolism depends on hydrogen and formate transfer. Syntrophic butyrate metabolism by *S. wolfei* and *M. hungatei* depends on hydrogen transfer.

ABSTRACT

Syntrophy is a tightly coupled mutualistic interaction among microorganisms that is essential for the global cycling of carbon in essentially all anaerobic environments. Syntrophic degradation of aromatic, alicyclic and fatty acids by microorganisms capable of syntrophic metabolism requires a partner organism, usually a methanogen, to maintain extremely low concentrations of H_2 and/or formate so that the degradation of the initial substrate is thermodynamically favorable. However, recent evidence that syntrophic ethanol metabolism involves direct electron transfer through nanowires raises doubt about the importance of interspecies hydrogen and/or formate transfer. A combination of genomic, gene expression, and enzymatic analyses along with inhibitor studies were used to test whether syntrophic metabolism by the fatty acid degrader, *Syntrophomonas wolfei*, and the aromatic and alicyclic acid degrader, *Syntrophus aciditrophicus*, involves transfer of H_2 and/or formate or direct electron transfer. Genomic analysis showed that both *S. wolfei* and *S. aciditrophicus* are capable of producing hydrogen and formate as interspecies electron carriers, but lack the pilus and cytochrome system needed for direct electron transfer. *S. wolfei* has six formate dehydrogenase and three hydrogenase gene clusters. Formate dehydrogenase activity was found to be higher than hydrogenase activity in whole cells of *S. wolfei* grown syntrophically or axenically. Two hydrogenase genes of *S. wolfei* were up-regulated during syntrophic growth. *S. aciditrophicus* contains two hydrogenase and four formate

dehydrogenase gene clusters. The genes for all of the major subunits of the hydrogenases and formate dehydrogenases were expressed under all growth conditions. Only *fdhII* was differentially expressed with a 2-fold higher expression ratio during syntrophic benzoate growth. Hydrogenase activity in *S. aciditrophicus* was as high, if not higher, than formate dehydrogenase activity, except with cells grown on cyclohexane carboxylate. Inhibitor studies showed the importance of hydrogen transfer for syntrophic butyrate metabolism by *S. wolfei*, formate transfer for syntrophic benzoate metabolism *S. aciditrophicus* and hydrogen and formate transfer for syntrophic cyclohexane carboxylate metabolism by *S. aciditrophicus*.

Analysis of the *S. wolfei* genome revealed potentially novel types of hydrogenases and formate dehydrogenases, including a unique energy conservation mechanism by confurcation of electrons and many other novel features of the syntrophic lifestyle. *S. wolfei* contains multiple homologs for the enzymes involved in butyrate metabolism, many of which were detected later in the proteomic analysis. Many possibilities for reverse electron transfer mechanisms including a novel iron-sulfur oxidoreductase, an electron transfer flavoprotein:quinone oxidoreductase, and a bifurcating butyryl-CoA dehydrogenase were discovered in the genome and latter detected in the proteome of *S. wolfei*. This research shed light on the metabolic machinery involved in reverse electron transfer, which is essential for syntrophic metabolism. The research also showed that the importance of H_2 versus

formate transfer depends on the substrate and organism involved and that *S. wolfei* expresses multiple enzyme systems for fatty acid metabolism, interspecies electron transfer, and energy conservation.

CHAPTER I

METHANOGENESIS: SYNTROPHIC METABOLISM

SUMMARY

Syntrophy is a mutualistic interaction in which two metabolically different types of microorganisms are linked by the need to keep metabolites exchanged between the two partners at low concentrations to make the overall metabolism of both organisms feasible. In most cases, the cooperation is based on the transfer of hydrogen, formate, or acetate from fermentative bacteria to methanogens to make the degradation of electron-rich substrates thermodynamically favorable. Syntrophic metabolism proceeds at very low Gibbs' free energy changes, close to the minimum free energy change needed to conserve energy biologically, which is the energy needed to transport one proton across the cytoplasmic membrane. Pathways for syntrophic degradation of fatty acids predict the net synthesis of about one third of an ATP per round of catabolism. Syntrophic metabolism entails critical oxidation-reduction reactions in which hydrogen or formate production would be thermodynamically unfavorable unless energy is invested. The membrane processes involved in ion translocation and reverse electron transfer are poorly understood. While much evidence supports interspecies transfer of hydrogen and formate, other mechanisms of interspecies electron transfer exist including cysteine cycling and possibly direct electron transfer by electrically conductive pili.

INTRODUCTION

Syntrophic metabolism is an essential, but the least energetically favorable, step in the conversion of organic matter to methane and carbon dioxide in anoxic environments. Biological methane production, also termed methanogenesis, is an important process in the global carbon cycle, accounting for about 1–2% of the carbon fixed annually by photosynthesis (Hedderich and Whitman, 2006). Annual global methane emissions into the atmosphere are large, about 500–600 Teragram (Tg) (1 Tg equals 10^{12} g), and more than 70% (350–400 Tg) of these emissions are due to microbial activity (Ehhalt et al., 2001). Syntrophic metabolism is often the rate-limiting step in methanogenesis (McCarty, 1971; McInerney and Bryant, 1981b) and, thus, is an important process controlling the global carbon flux. The degradation of natural polymers such as polysaccharides, proteins, nucleic acids, and lipids to CO_2 and CH_4 involves a complex microbial community (McInerney and Bryant, 1981b; Schink and Friedrich, 1994). Fermentative bacteria hydrolyze the polymeric substrates such as polysaccharides, proteins, and lipids, and ferment the hydrolysis products to acetate and longer-chain fatty acids, CO_2, formate, H_2. Propionate and longer-chain fatty acids, alcohols, and some amino acids and aromatic compounds are syntrophically metabolized to the methanogenic substrates: H_2, formate, and acetate (Schink, 1997; Schink and Stams, 2006). Lastly, two different groups of methanogens, the hydrogenotrophic methanogens and the acetotrophic methanogens, complete the process, converting acetate, formate

and hydrogen produced by other microorganisms to methane and carbon dioxide.

Syntrophy is an energetically limited interaction between cells of different species, e.g., the fatty acid degrader and the methanogen (Table 1) (Schink, 1997; Schink and Stams, 2006; McInerney et al., 2008). The mutual dependence between the two metabolic types of organisms is so extreme that neither one functions without the activity of its partner. Together, the partners perform functions that neither one can do alone. The degradation of the respective substrate, in this case, a fatty or aromatic acid (Table 1), is thermodynamically unfavorable if the product concentrations are at standard conditions (1 M concentration, or 1 atm for gases). The function of methanogens is to consume hydrogen, for example, to low steady-state pressure (10^{-4}–10^{-5} atm) to make fatty and aromatic acid oxidation thermodynamically favorable (Table 1). The syntrophic degradation of fatty and aromatic acids accounts for much of the carbon flux in methanogenic environments (McCarty, 1971; Pavlostathis and Giraldo-Gomez, 1991). Initial anaerobic transformations of aromatic compounds (Heider and Fuchs, 1997b, a; Schink, 2000) generally lead to the conversion of diverse aromatic compounds into benzoyl-coenzyme A (CoA) (Merkel et al., 1989; Gallert and Winter, 1994; Gibson et al., 1994; Gibson et al., 1997; Breese and Fuchs, 1998; Hirsch et al., 1998). In methanogenic environments, the reduction and cleavage of the aromatic ring are catalyzed by syntrophic associations of benzoate-

degrading microorganism and hydrogen- and/or formate-using methanogens (Ferry and Wolfe, 1976; Mountfort and Bryant, 1982; Szewzyk and Schink, 1989).

BIOENERGETIC CONSIDERATIONS

Syntrophy is a fascinating process from a bioenergetic perspective. Even if methanogenic activity is high and hydrogen levels are low, syntrophic metabolism releases very little free energy, which must be shared among the partners (Schink, 1997). Organisms capable of syntrophic metabolism operate at free energy changes very close to the minimum increment of energy required for ATP synthesis (Schink, 1997; Hoehler, 2004). The minimum amount of energy needed for ATP synthesis is predicted to be about -23 kJ mol^{-1} although this value maybe as low as -15 to -20 kJ mol^{-1}. Most of the free energy changes observed during syntrophic metabolism are in this range (Schink, 1997) although some studies have found free energy changes less than -10 kJ mol^{-1} (Dwyer et al., 1988; Scholten and Conrad, 2000).

An important question is how these organisms exploit such small free energy changes for growth. The second fascinating feature of syntrophic metabolism is the need for reverse electron transfer. In syntrophic metabolism, there are critical oxidation-reduction reactions that are thermodynamically unfavorable, e.g., result in a negative $\Delta E'$. For example, the production of hydrogen (E' of -261 mV at 1 Pa H_2) or formate (E' of -258 mV at 1 mM formate)

(Schink, 1997) from electrons generated from the oxidation of acyl CoA intermediates to their respective enoyl-CoA intermediates (E' of -10 mV) (Sato et al., 1999) has a $\Delta E'$ of about -250 mV.

Table 1. Reactions involved in syntrophic metabolism.

Reactions	$\Delta G^{o'}$ [a] (kJ/mol)	$\Delta G'$ [b] (kJ/mol)
Methanogenic reactions		
$4\ H_2 + HCO_3^- + H^+ \rightarrow CH_4 + 3\ H_2O$	-135.6	-15.8
$4\ HCOO^- + H_2O + H^+ \rightarrow CH_4 + 3\ HCO_3^-$	-130.4	-11.8
Syntrophic Oxidations		
$Acetate^- + 4\ H_2O \rightarrow 2\ HCO_3^- + H^+ + 4\ H_2$	+104.6	-1.5
$Propionate^- + 3\ H_2O \rightarrow Acetate^- + HCO_3^- + H^+ + 3\ H_2$	+76.1	-16.9
$Butyrate^- + 2\ H_2O \rightarrow 2\ Acetate^- + H^+ + 2\ H_2$	+48.6	-39.2
$Benzoate^- + 7\ H_2O \rightarrow 3\ Acetate^- + HCO_3^- + 3\ H^+ + 3\ H_2$	+70.1	-68.5

[a] Calculated from the data in Thauer et al. (1977) with the free energy of formation for benzoate given in Kaiser and Hanselmann (1982).

[b] Calculated on the basis of the following conditions observed in methanogenic ecosystems: partial pressures of H_2 of 1 Pa and of CH_4 of 50 kPa, 50 mM bicarbonate, and the concentrations of the substrates and acetate at 0.1 mM each.

A hydrogen partial pressure of about 10^{-5} Pa would make this reaction thermodynamically favorable (Schink, 1997). The syntrophic metabolism of propionate by *Syntrophobacter wolinii* by the methylmalonyl-CoA pathway (Houwen et al., 1990) involves the oxidation of succinate to fumarate (E°' of + 33 mV) (Thauer et al., 1977). Here again, a very low hydrogen partial pressure (10^{-6} Pa) is needed for hydrogen production to be thermodynamically favorable (Schink, 1997). Methanogens cannot generate such low hydrogen partial pressures because hydrogenotrophic methanogenesis reaches thermodynamic equilibrium at 0.2 Pa H_2. Hydrogen or formate production can occur only with energy input, a process called reverse electron transfer. The most likely energy source for this energy input is an ion gradient. Consistent with the requirement for an ion gradient for hydrogen production, the protonophore (CCCP) and the ATP synthase inhibitor (DCCD) inhibited hydrogen production from butyrate by *Syntrophomonas wolfei* and from benzoate by *Syntrophus buswellii* (Wallrabenstein, 1994). Similarly, hydrogen formation from glycolate by membrane vesicles of *Syntrophobotulus glycolicus* (Friedrich et al., 1996) required ATP or a proton gradient (Friedrich and Schink, 1993, 1995). While it is clear that reverse electron transfer is needed for syntrophic metabolism, the nature of this system is not known.

How do syntrophic microbial associations operate at low energy conditions? Do they have novel mechanisms for energy conservation or are they more efficient at conserving energy than other microorganisms? We will

analyze what is known about syntrophic metabolism in an attempt to answer these questions. Further details on the physiology of the organisms capable of syntrophic metabolism are available in several comprehensive reviews (Schink, 1997, 2006; McInerney et al., 2008).

INTERSPECIES ELECTRON TRANSFER

Above, we defined syntrophy based on the exchange of H_2 between the syntrophic partners. However, other mechanisms to exchange electrons equivalents exist. Most hydrogenotrophic methanogens use formate or hydrogen or both (Hedderich and Whitman, 2006; Liu and Whitman, 2008). There is very little difference in free energy change for methane production when hydrogen versus formate serves as the electron donor (Table 1). The conclusion of many studies is that syntrophic metabolism can involve either interspecies transfer of hydrogen and/or formate. Syntrophic metabolism by hydrogen transfer was shown for glycolate metabolism by *Syntrophobotulus glycolicus* (Friedrich et al., 1996), sugar metabolism by *Syntrophococcus sucromutans* (Krumholz and Bryant, 1986), acetate metabolism by a thermophilic, syntrophic acetate-oxidizing strain AOR (Lee and Zinder, 1988) and ethanol metabolism by S-organism (Bryant et al., 1967), by culturing these organisms with a methanogen that uses only hydrogen. In a similar fashion, syntrophic metabolism by formate transfer was shown for an amino acid degrader by using a sulfate-reducing partner that uses formate but not H_2

(Zindel et al., 1988). Syntrophic propionate degradation by *Syntrophobacter fumaroxidans* (Dong et al., 1994b; Dong and Stams, 1995b) and syntrophic butyrate degradation by *Syntrophomonas (Syntrophospora) bryantii* (Dong et al., 1994a) occurred only with a methanogen that used both hydrogen and formate, and not with a methanogen that used only hydrogen, implicating the need for formate metabolism. Proteomic and enzymatic analyses showed high levels of expression of formate dehydrogenase in both *S. fumaroxidans* and its methanogenic partner, arguing for the importance of formate metabolism (de Bok et al., 2002a; de Bok et al., 2002b; de Bok et al., 2003). Flux analysis of this coculture (de Bok et al., 2002a) and of a butyrate degrading coculture (Boone et al., 1989) indicated that the H_2 diffusion was too slow to account for the rates of syntrophic metabolism. The use of hydrogen and/or formate as the interspecies electron carrier provides an explanation why so many methanogens use both hydrogen and formate. Genomic analysis supports the involvement of both compounds because the genomes of *Syntrophus aciditrophicus*, *Syntrophomonas wolfei* and *Methanospirillum hungatei*, the methanogenic partner most often observed in syntrophic associations, have multiple formate dehydrogenase and hydrogenase genes (McInerney et al., 2007; Sieber et al., 2010b). Molecules other than hydrogen or formate may be involved in interspecies electron transfer and their use may circumvent the need for reverse electron transfer. An acetate-oxidizing coculture of *Geobacter sulfurreducens* and *Wolinella succinogenes* used cysteine as the interspecies

electron carrier (Kaden et al., 2002). Cysteine is commonly used as a reductant in anaerobic media, which could explain why it was overlooked as an electron carrier.

Another possibility is direct electron transfer between the syntrophic partners by electron conductive pili or nanowires (Reguera et al., 2005; Gorby et al., 2006). Interspecies electron transfer by nanowires is difficult to prove in syntrophic associations because we do not have the ability to mutate the pilus genes in either of the syntrophic partners at this time. However, nanowire-like structures connecting the syntrophic propionate degrader, *Pelotomaculum thermopropionicum* with its methanogenic partner have been observed by electron microscopy (Ishii et al., 2005; Gorby et al., 2006) and scanning tunneling microscopy showed that these structures were electron transmissive (Gorby et al., 2006). Some researchers point to aggregation of cells in cocultures as proof of direct electron transfer (Logan and Regan, 2006), but aggregation also reduces the distance between the syntrophic partners, which would increase the rate of hydrogen or formate transfer (Conrad et al., 1985; Thiele and Zeikus, 1988; Ishii et al., 2005).

BIOCHEMICAL PATHWAYS FOR SYNTROPHIC METABOLISM

The pathways for several syntrophic metabolisms are known and an analysis of the bioenergetics of these pathways illustrates how small amounts of energy are conserved during syntrophic metabolism (Schink, 1997).

Butyrate Metabolism

Organisms capable of syntrophic butyrate metabolism include all species of *Syntrophomonas* (McInerney et al., 1981b; Lorowitz et al., 1989; Zhang et al., 2004, 2005; Sobieraj and Boone, 2006; Wu et al., 2006b, a; Sousa et al., 2007; Wu et al., 2007), *Thermosyntropha lipolytica* (Svetlitshnyi et al., 1996), and *Syntrophothermus lipocalidus* (Sekiguchi et al., 2000). Syntrophic butyrate metabolism proceeds via the β-oxidation pathway (Fig. 1) (Wofford et al., 1986). Similar to syntrophic propionate metabolism, butyrate is activated to butyryl-CoA by the transfer of the CoA group from acetyl-CoA; butyryl-CoA is then β-oxidized to two acetyl-CoA molecules (Wofford et al., 1986). One of the acetyl-CoA molecules is used to activate butyrate and the other is used for ATP synthesis. The oxidation of butyryl-CoA to crotonyl-CoA produces reduced electron transfer flavoprotein ($E0^0$ of -10 mV) (Sato et al., 1999) and the oxidation of L-3-hydroxylbutyryl-CoA to 3-oxobutyryl-CoA produces NADH. Hydrogen production (E^0 of -292 mV at 10 Pa H_2) from electrons derived from NADH (E^0 of -320 mV) (Thauer et al., 1977) is favorable at the partial pressures maintained by methanogens (about 1^{-10} Pa), but hydrogen production from the

electrons from the oxidation of butyryl-CoA to crotonyl-CoA requires reverse electron transfer (Wallrabenstein, 1994). About two-thirds of the ATP is needed to overcome this energy barrier, which leaves about one-third of an ATP available to support growth. The measured free energy changes available during syntrophic butyrate metabolism ranged from -5 to -17 kJ mol^{-1} (Dwyer et al., 1988; Jackson and McInerney, 2002), somewhat lower than that predicted to conserve energy (-14 to -23 kJ mol^{-1}) (Schink, 1997).

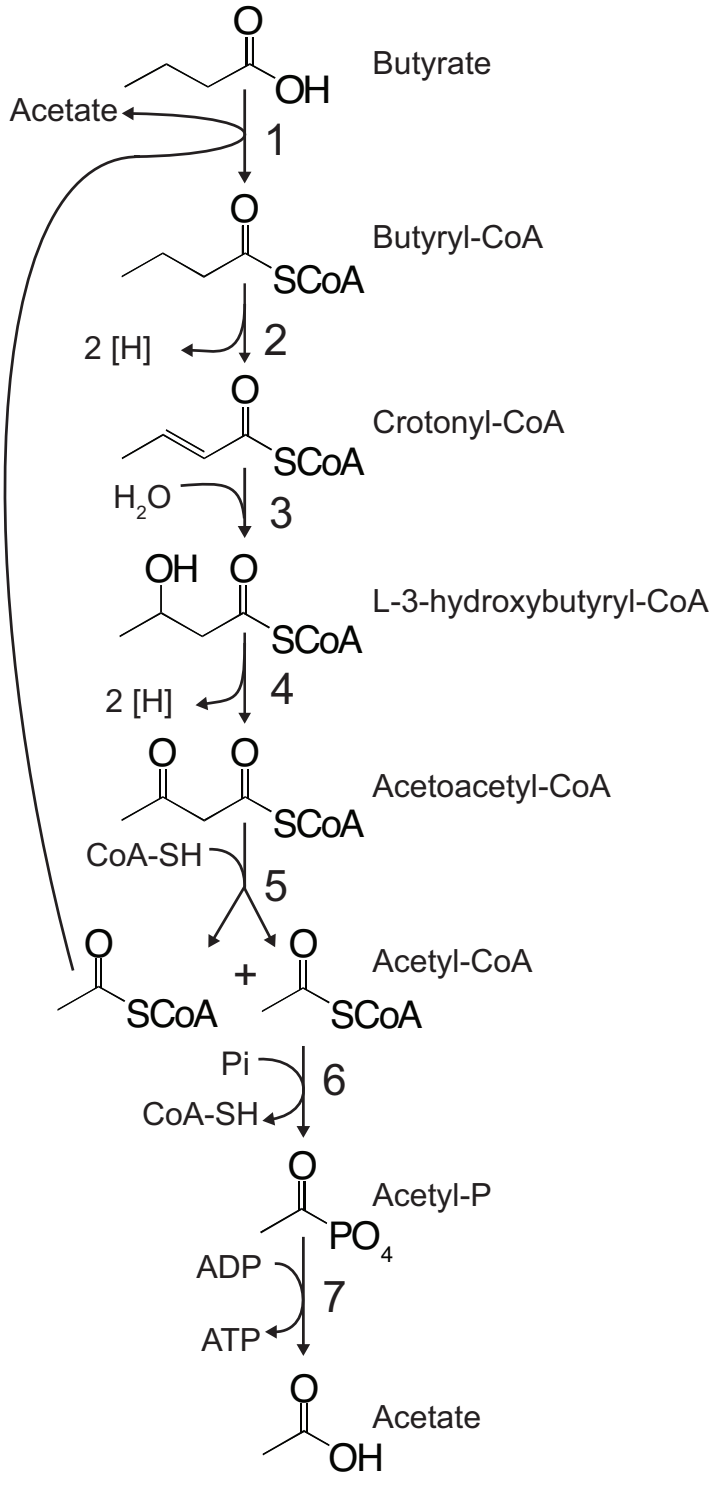


Figure 1. The β-oxidation pathway for butyrate metabolism in *Syntrophomonas wolfei*. Adapted from Wofford et al. (1986). The enzymes involved are: (1) CoA transferase; (2) acyl-CoA dehydrogenase; (3) enoyl-CoA hydratase; (4) L-(+)-3-hydroxybutyryl-CoA dehydrogenase; (5) 3-ketoacyl-CoA thiolase; (6) phosphotransacetylase; (7) acetate kinase. [H] is reducing equivalents.

Benzoate Metabolism

Syntrophic benzoate degraders include three species of *Syntrophus*: *S. buswellii*, *S. gentianae* and *S. aciditrophicus*, and *Sporotomaculum syntrophicum*, *Pelotomaculum terephthalicicum* and *Pelotomaculum isophthalicicum* (McInerney et al., 2008). The reduction of benzoyl-CoA represents a considerable energy barrier for anaerobic microorganisms because the midpoint potential of the first electron transfer is about -1.8 V (Heider and Fuchs, 1997b), which is well below that of most physiological electron donors (-0.4 V) (Boll and Fuchs, 1998; Boll et al., 2000). In *Thauera aromatica*, benzoyl-CoA reduction requires the hydrolysis of two ATP molecules per electron pair to overcome this barrier (Boll et al., 1997). *Geobacter metallireducens* (Wischgoll et al., 2005), *Desulfococcus multivorans* (Peters et al., 2004) and *S. aciditrophicus* (McInerney et al., 2007) most likely use a completely different type of enzyme to reduce benzoyl-CoA. Previous studies detected 2-hydroxycyclohexane carboxylate, cyclohex-1-ene carboxylate and pimelate in culture fluids of *S. aciditrophicus* grown with benzoate and the enzyme activities needed to convert cyclohex-1-ene carboxyl-CoA to pimelyl-CoA in cell-free extracts of *S. aciditrophicus* (Fig. 2) (Elshahed et al., 2001). The intermediates and enzyme activities detected were consistent with the metabolism of cyclohex-1-ene carboxyl-CoA to pimelyl-CoA by the pathway found in *Rhodopseudomonas palustris* (Harwood et al., 1998). However, genes

homologous to those involved in benzoate metabolism in *R. palustris* were not detected in the *S. aciditrophicus* genome (McInerney et al., 2007). Interestingly, the genome of *S. aciditrophicus* contains genes with high homology to those in the *T. aromatica* genome (Fig. 2) (McInerney et al., 2007). The genes for the cyclohex-1,5-diene carboxyl-CoA hydratase and the 6-oxocyclohex-1-ene carboxyl-CoA hydrolase of *S. aciditrophicus* have been cloned and expressed in *Escherichia coli* (Peters et al., 2007; Kuntze et al., 2008). Enzymatic analysis showed that the *S. aciditrophicus* cyclohex-1,5-diene carboxyl-CoA hydratase converted cyclohex-1,5-diene carboxyl-CoA to 6-hydroxycyclohex-1-ene carboxyl-CoA, and that *S. aciditrophicus* 6-oxocyclohex-1-ene carboxyl-CoA hydrolase made 3-hydroxypimelyl-CoA from 6-oxocyclohex-1-ene carboxyl-CoA. Thus, it appears that *S. aciditrophicus* uses a two-electron reduction reaction to convert benzoyl-CoA to cyclohex-1,5-diene carboxyl-CoA, which is then metabolized to 3-hydroxypimelyl-CoA in a manner analogous to that found in *T. aromatica*.

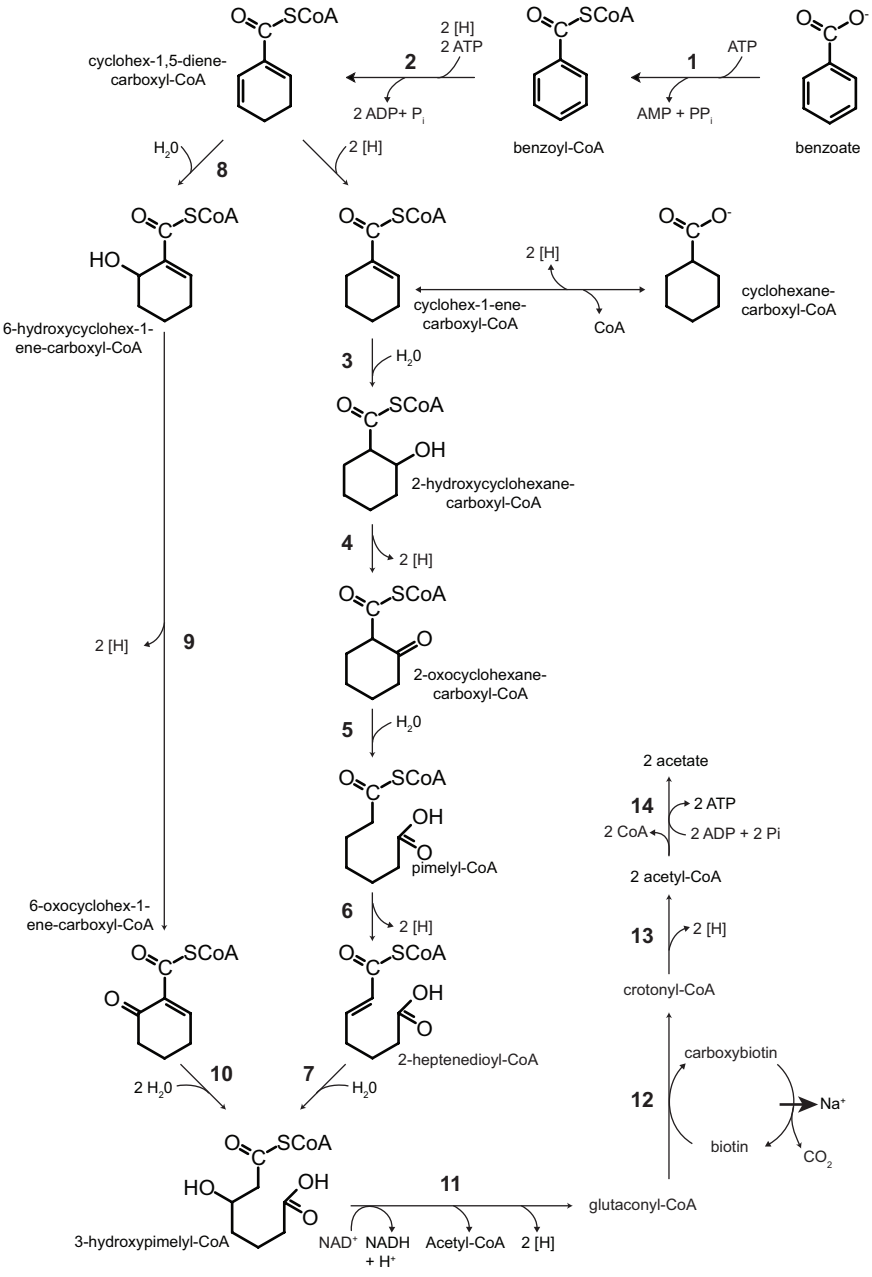


Figure 2. Pathway for syntrophic benzoate metabolism. Adapted from McInerney et al. (2007). The enzymes involved are: (1) benzoyl-CoA ligase; (2) benzoyl-CoA reductase; (3) cyclohex-1-carboxyl-CoA hydratase; (4) 2-hydroxycyclohexane carboxyl-CoA dehydrogenase; (5) 2-oxocyclohexane-carboxyl-CoA hydrolase; (6) pimelyl-CoA dehydrogenase; (7) enoyl-CoA hydratase; (8) cyclohex-1,5-dienoyl-CoA hydratase; (9) 6-hydrocyclohex-1-ene-carboxyl-CoA dehydrogenase; (10) 6-oxocyclohex-1-ene-carboxyl-CoA hydrolase; (11) β-oxidation enzymes; (12) glutaconyl-CoA decarboxylase; (13) β-oxidation enzymes (see Fig. 1 for more detail); (14) acetate kinase/phosphotransacetylase. [H] are reducing equivalents.

It is not clear yet how net energy is conserved during syntrophic benzoate metabolism. Benzoate activation, benzoyl-CoA reduction and hydrogen production from acyl-CoA intermediates require more ATP (greater than 4 ATP per benzoate) than is produced by the known ATP-producing reactions, e.g., substrate-level phosphorylation from acetate (3 ATPs), proton translocation by a membrane-bound pyrophosphatase (equivalent to 1/3 ATP per benzoate) (Schöcke and Schink, 1998), and the decarboxylation of glutaconyl-CoA linked to sodium-ion translocation (1/3 of an ATP per benzoate) (Beatrix et al., 1990; Schöcke and Schink, 1998). Nevertheless, syntrophic benzoate degraders grow. The measured free energy changes during syntrophic benzoate metabolism range from about -30 to -45 kJ of energy (Warikoo et al., 1996; Schöcke and Schink, 1997), which suggest that about one-third of an ATP or more could be formed.

In addition to the bioenergetics, there is still much that we do not understand of syntrophic benzoate metabolism. Cyclohexane carboxylate accumulates to very high concentration during syntrophic benzoate metabolism (Elshahed et al., 2001). Is it possible that another mechanism for benzoyl-CoA reduction exists in *S. aciditrophicus*, which may be energetically more favorable? Cyclohexane carboxylate and benzoate formation were observed when *S. aciditrophicus* was grown with crotonate (Mouttaki et al., 2007). Intermediates detected during crotonate metabolism were the same as those detected during syntrophic benzoate metabolism, suggesting that the pathway

for benzoate metabolism is reversible and operates at high-energy efficiency.

POTENTIAL MECHANISMS FOR REVERSE ELECTRON TRANSFER

Several mechanisms have been proposed for reverse electron transfer during syntrophic metabolism (Fig. 3). *S. wolfei* contains menaquinone (Wallrabenstein, 1994) which could function as the electron carrier between a membrane-associated acyl-CoA dehydrogenase and a cytoplasmically-oriented hydrogenase (Schink and Friedrich, 1994) (Fig. 3a). In this model, inward movement of protons by the quinone loop is used to drive reverse electron transfer. The second model (Fig. 3b) directly links electron flow from the membrane-bound acyl-CoA dehydrogenase to an externally oriented hydrogenase (Schink and Friedrich, 1994). The consumption of protons on the outside of the cell membrane drives reverse electron transfer. The external orientation of the hydrogenase in *S. wolfei* was confirmed by $CuCl_2$ inhibition studies (Wallrabenstein, 1994). A third variation is possible if a soluble acyl-CoA dehydrogenase is used (Fig. 3c). In this model, a membrane-bound oxidoreductase would be necessary to aid electron transfer to the hydrogenase. This model could employ menaquinone or another electron carrier and would involve the proton gradient as the driving force for reverse electron transfer. Another possibility to produce H_2 from thermodynamically difficult substrates was recently proposed by Prof. Buckel's laboratory and confirmed by Prof. Thauer's laboratory in *Clostridium kluyveri* (Herrmann et al., 2008; Li et al.,

2008). C. kluyveri ferments ethanol and acetate to butyrate and small amounts of H_2. A soluble enzyme complex in *C. kluyveri* couples the energetically favorable reduction of crotonyl-CoA to butyryl-CoA by NADH with the unfavorable reduction of ferredoxin (Fd) by NADH (Fig. 3d) (1):

$$\text{Crotonyl-CoA} + Fd_{ox} + 2NADH + 2H^+ \rightarrow \text{Butyryl-CoA} + Fd_{red} + 2NAD^+ \quad (1)$$

This enzyme complex was purified and shown to be FAD dependent (Li et al., 2008). Once $FADH_2$ is formed, there is a bifurcation of electron flow with some electrons used for the exergonic reduction of crotonyl-CoA ($E0^0$ = ⁻10 mV), which drives the endergonic reduction of ferredoxin ($E0^0$ = ⁻410 mV). The reversal of this reaction could accomplish reverse electron transfer during syntrophic oxidation.

A possible model for reverse electron transfer during syntrophic propionate metabolism is suggested by studies in *Bacillus subtilis* (Fig. 3e) (Schirawski and Unden, 1998). *B. subtilis* has menaquinone (E^0 of ⁻70 mV) and not ubiquinone (E^0 of + 100 mV) so the oxidation of succinate to fumarate (E^0 of + 33 mV) is coupled to menaquinone reduction and requires reverse electron transfer. The binding site for menaquinone of the membrane-bound cytochrome b was located close to the outside of the cell membrane, which would allow the inward movement of protons if menaquinone is oxidized on the cytoplasmic side of the membrane. In syntrophic propionate metabolism, menaquinone oxidation

could be linked to a membrane bound hydrogenase or formate dehydrogenase. *S. fumaroxidans* has a membrane-bound succinate dehydrogenase (Van Kuijk et al., 1998) and formate dehydrogenases and hydrogenases that are membrane-associated (de Bok et al., 2002a; de Bok et al., 2002b; de Bok et al., 2003). These observations are consistent with the reverse electron transfer system as found in *B. subtilis* (Schirawski and Unden, 1998).

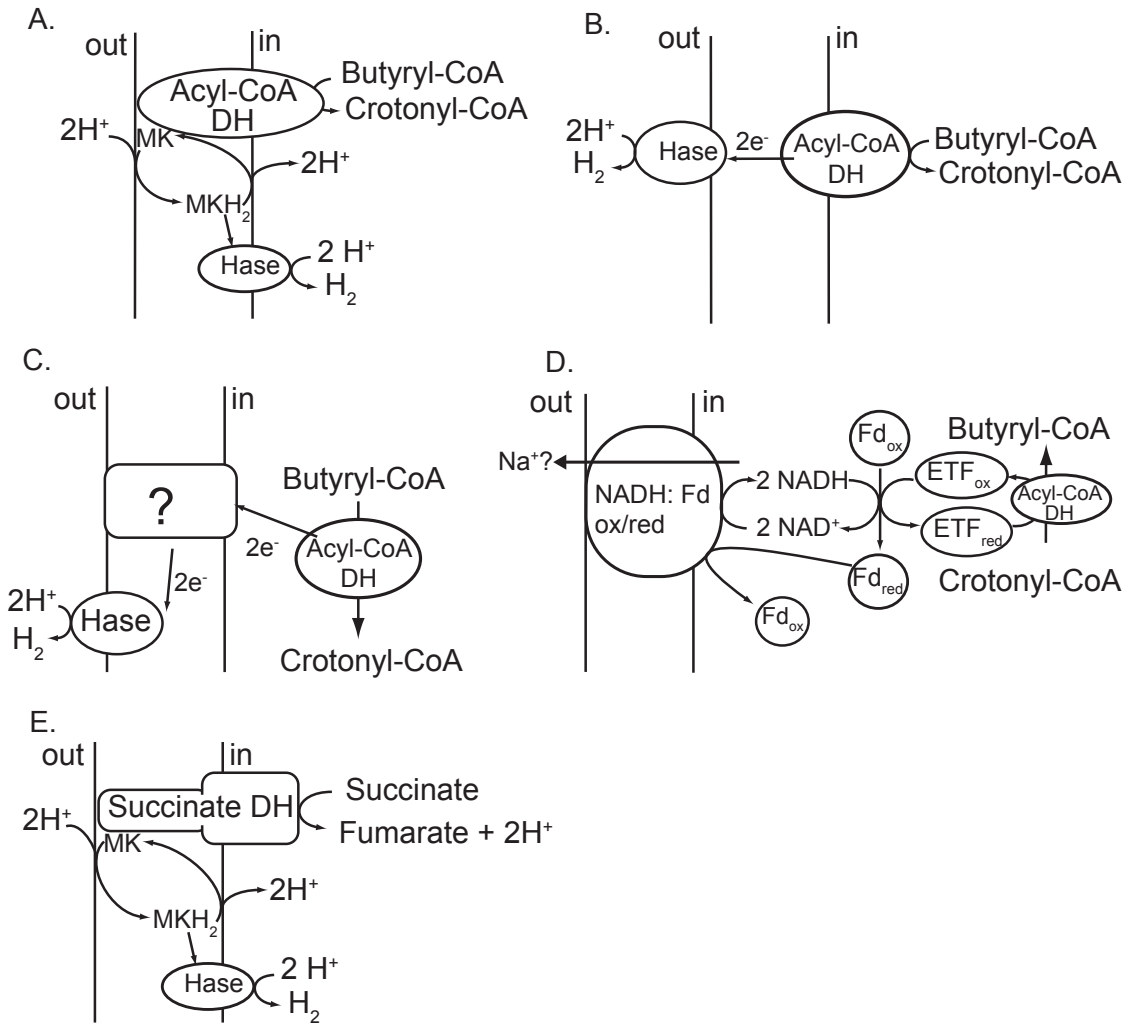


Figure 3. Proposed models for reversed electron transfer chains. (a), (b), and (c) adapted from Schink and Friedrich (1994), (d) adapted from Li et al. (2008), and (e) adapted from Schirawski and Unden (1998). DH, dehydrogenase; Hase, hydrogenase; MK, menaquinone; Fd is ferredoxin; ?, unknown membrane bound oxidoreductase; ox:red, oxidoreductase; in, cytoplasm; out, outside cytoplasmic membrane.

CONCLUSIONS

The concept of a minimum free energy change for energy conservation provides the framework to understand how bacteria exploit small free energy changes. Pathways for syntrophic metabolism of fatty acids predict that ATP can be synthesized at increments of about one-third of an ATP, which is consistent with the measured free energy changes observed for the syntrophic metabolism of these compounds. However, there is still much that we do not understand. For instance, how does net ATP synthesis occur during syntrophic benzoate metabolism and why, in some cases, are free energy changes less than the predicted minimum free energy change needed for energy conservation? We know very little about the biochemistry of reverse electron transfer. Genome sequences of several organisms capable of syntrophic metabolism are available and analysis of these sequences may provide insights into the bioenergetics of syntrophy. Genomic analyses suggest that organisms capable of syntrophic metabolism have multiple mechanisms to generate ion gradients and use different mechanisms for reverse electron transfer. Further work on the role of these membrane complexes in syntrophic metabolism is needed. More research is needed to understand how bacteria exploit small free energy changes for growth. Also unresolved is how reversible metabolic pathways found in some syntrophic metabolizers are linked to ATP synthesis in each direction.

Many syntrophic associations are highly organized, multicellular

structures with the partners in close physical proximity to each other. We know very little about the molecular mechanisms involved in the formation and maintenance of these catalytic units. Regulatory mechanisms that control the development of attached consortia most likely are similar to those involved in biofilm formation. We are beginning to unravel the molecular and biochemical details involved in the syntrophic lifestyle. The combination of computational with functional genomic approaches may allow us to interrogate the regulatory mechanisms involved in establishing and maintaining multispecies associations in order to quantify and predict the behavior of microorganisms and microbial communities in natural ecosystems. A thorough understanding of the formation and structure of dense microbial aggregates is essential for application of methanogenesis. Only in bioreactors in which methanogenic communities operate in dense aggregates can anaerobic wastewater treatment take place at a high volumetric rate.

The research in the next three chapters is focused on answering the following questions. What makes an organism an obligate syntroph? Are there gene systems that are unique to the syntrophic lifestyle? Is hydrogen, formate or both used interspecies electron transfer and does the preference depend on the organism and substrate? Because genetic manipulation is not yet possible in syntrophic metabolizers that degrade the key intermediates in methanogenesis, e.g., fatty, aromatic and alicyclic acids, I used a combination of genomic, proteomic, transcriptomic, and enzymatic analyses to answer these

questions. I used genomic analysis to determine the genetic potential of an organisms capable of syntrophy, proteomic analysis to determine if the gene products were present during syntrophic and axenic growth, transcriptomic analysis to determine if the genes were differentially transcribed, implicating them as important functional genes under the growth conditions tested, and finally enzymatic analysis to demonstrate activities thought to be essential for syntrophy.

CHAPTER II

THE GENOME OF *SYNTROPHOMONAS WOLFEI*: NEW INSIGHTS INTO SYNTROPHIC METABOLISM AND BIOHYDROGEN PRODUCTION

SUMMARY

Syntrophomonas wolfei is a specialist, evolutionarily adapted for syntrophic growth with methanogens and other hydrogen- and/or formate-using microorganisms. This slow growing anaerobe has three putative ribosome RNA operons, each of which has 16S rRNA and 23S rRNA genes of different length and multiple 5S rRNA genes. The genome also contains ten RNA-directed, DNA polymerase genes. Genomic analysis shows that *S. wolfei* relies solely on the reduction of protons, bicarbonate, or unsaturated fatty acids to re-oxidize reduced cofactors. *S. wolfei* lacks the genes needed for aerobic or anaerobic respiration and has an exceptionally limited ability to create ion gradients. An ATP synthase and a pyrophosphatase were the only systems detected capable of creating an ion gradient. Multiple homologs for β-oxidation genes were present even though *S. wolfei* uses a limited range of fatty acids from 4 to 8 carbons in length. *S. wolfei,* other syntrophic metabolizers with completed genomic sequences, and thermophilic anaerobes known to produce high molar ratios of hydrogen from glucose have genes to produce H_2 from NADH by an electron bifurcation mechanism. Comparative genomic analysis also suggests that formate production from NADH may involve electron bifurcation. A membrane-bound, iron-sulfur oxidoreductase found in *S. wolfei* and *Syntrophus aciditrophicus* may be uniquely involved in reverse electron transfer during syntrophic fatty acid metabolism. The genome sequence of *S. wolfei* reveals several core reactions that may be characteristic of syntrophic fatty acid

metabolism and illustrates how biological systems produce hydrogen from thermodynamically difficult reactions.

INTRODUCTION

Syntrophic interactions among microbial species are essential in anaerobic degradation, and syntrophic fatty and aromatic acid metabolism accounts for much of the carbon flux in methanogenic ecosystems (Schink, 1997). Syntrophy is an essential intermediary step in the conversion of natural polymers such as polysaccharides, proteins, nucleic acids, and lipids to CO_2 and CH_4 (McInerney et al., 1981b; Schink, 1997). Syntrophy is usually defined as a thermodynamically based interaction where the degradation of a compound such as a fatty acid (equation 1) occurs only when degradation products of the compound, usually hydrogen, formate and acetate, are maintained at very low concentrations by a second microorganism, usually a methanogen (McInerney et al., 1979; McInerney et al., 1981b; Schink, 1997):

$$Butyrate^- + 2\ H_2O \rightarrow 2\ Acetate^- + H^+ + 2\ H_2 \qquad \text{(eq. 1)}$$

$\Delta G^{o'} = +\ 48.6$ kJ/mol (Thauer et al., 1977)

For example, when the H_2 partial pressure is kept at 1 Pa by the methanogens, the Gibbs free energy change for equation 1 becomes -39.2 kJ/mol, assuming that the concentrations of the butyrate and acetate are each 0.1 mM. Even

under optimal conditions, the Gibbs free energy changes for syntrophic metabolism are close to equilibrium (Schöcke and Schink, 1997; Scholten and Conrad, 2000; Jackson and McInerney, 2002) and this energy must be shared among the syntrophic partners (Schink, 1997). For these reasons, growth rates (<0.005 h^{-1}) and growth yields (2.6 g dry weight $mole^{-1}$ of propionate) (McInerney et al., 1981b; Scholten and Conrad, 2000) are low, which makes biochemical investigations very difficult. How organisms conserve energy and grow when the thermodynamic driving force is very low is an important physiological question. Many syntrophic associations form highly organized, multicellular structures where the partners are in close physical proximity to each other (Sekiguchi et al., 1999; Boetius et al., 2000; Ishii et al., 2006). Little is known about the molecular mechanisms involved in the formation and maintenance of these catalytic units.

Syntrophomonas wolfei and other members of the *Syntrophomonadaceae* form a coherent phylogenetic group that is distantly related to other members of the phylum Firmicutes (Fig. 1S) (Zhao et al., 1990). Members of *Syntrophomonadaceae*, like *S. wolfei*, are metabolic specialists that metabolize fatty acids syntrophically in association with hydrogen /formate-using microorganisms and are unable to use other substrates or electron donor and acceptor combinations (McInerney et al., 2008). Some species are able to grow in pure culture with unsaturated fatty acids such as crotonate (McInerney et al., 2008); (Beaty and McInerney, 1987; Amos and McInerney, 1990).

Members of *Syntrophomonadaceae* are also unusual in that they stain gram-negative and have a complex cell wall ultrastructure although they are members of the Firmicutes (McInerney and Bryant, 1981a). *S. wolfei* serves as the model microorganism for the study of syntrophic fatty acid metabolism. It uses only four to eight-carbon fatty acids and several unsaturated fatty acids in co-culture with hydrogen/formate-using microorganisms (McInerney et al., 1979; McInerney et al., 1981a) and grows in pure culture with unsaturated fatty acids such as crotonate (Beaty and McInerney, 1987; Amos and McInerney, 1990). *S. wolfei* metabolizes fatty acids by the b-oxidation pathway, forms most of its ATP by substrate-level phosphorylation, and has menaquinone and a *c*-type cytochrome (Wofford et al., 1986; McInerney and Wofford, 1992; Wallrabenstein, 1994).

A defining feature of syntrophic metabolism is the need for reverse electron transfer (Mouttaki et al., 2009). Hydrogen (E' of -261 mV at 1 Pa H_2) and formate (E' of -258 mV at 1 μM formate) production from electrons generated in the oxidation of acyl-CoA intermediates to their respective enoyl-CoA intermediates (E' of -10 mV) is energetically unfavorable ($\Delta E'$ of ~ -250 mV) and energy input is required by a process called reverse electron transfer. *Syntrophus aciditrophicus*, which syntrophically degrades fatty and aromatic acids, contains genes for a unique Rnf-type ion-translocating, electron transfer complex and a membrane-bound iron-sulfur oxidoreductase that may function in reverse electron transfer (McInerney et al., 2007). How other syntrophic

metabolizers accomplish reverse electron transfer is not clear although an NADH:acceptor oxidoreductase has been partially purified from syntrophically-grown *S. wolfei* cells that may be involved in reverse electron transfer (Müller et al., 2009).

The *S. wolfei* genome sequence delineates a core set of reactions characteristic of syntrophic fatty acid metabolism and illuminates poorly understood metabolic processes critical for H_2 and formate production and energy conservation from thermodynamically challenging substrates.

RESULTS AND DISCUSSION

General features of the genome

S. wolfei has one circular chromosome consisting of 2.94 mega base pairs (MB) (Table 1: Fig. 2S). The genome size is comparable to the genomes of syntrophic specialists such as *Pelotomaculum thermopropionicum* (3.0 MB) and *Syntrophus aciditrophicus* (3.2 MB) and to metabolic specialists in the class *Clostridia* (Table 1S).

Table 1. General features of the *Syntrophomonas wolfei* genome.

Category	Amount
DNA, total	2,936,195 bp
DNA, coding	2,450,680 bp
G+C Content	44.87%
DNA scaffolds	1
Genes total number	2639
Protein coding genes	2574 (97.5%)
RNA genes	65 (2.5%)
rRNA genes	19
5S rRNA	13
16S rRNA	3
23S rRNA	3
tRNA genes	46
Genes with function prediction	1507 (57.1%)
Genes without function prediction	1067 (40.4%)

The chromosome has a well-defined G+C skew with inflection points at the origin of replication and termination site (see Fig. 2S). Approximately 76.7% of the genes are transcribed from the leading strand as is typical of members of the Phylum Firmicutes (Rocha, 2002). Eighty-five percent of the chromosome is predicted to be coding sequence with 2677 open reading frames (ORFs) of which 2574 ORFs code for proteins and 103 code for RNA genes (Table 1). About 56.3% of the protein-coding sequences (CDS) have functional assignments, slightly lower that most of the genomes in Table 1S; 37.5% of the ORF lack functional assignment but have similarity to sequences in databases. Interestingly, only a small percentage of ORF have no similarity with sequences in databases even though *S. wolfei* is only distantly related to other organisms with completed genomic sequences. Sequence analysis suggests that 201 ORF contain information for translocation to the outside of the cell membrane and 301 ORF contain two or more predicted transmembrane spanning helices. There is one small region of DNA (from 1,505,786 to 1,521,252 bases) with a much lower % G + C content (26-34%) than the average % G + C of ~45. The low % G + C region contains genes for 12 hypothetical proteins (Swol_1303 through Swol_1315) and an integrase gene (Swol_1316) and is flanked by portions of a tRNA gene, consistent with its acquisition by horizontal gene transfer.

There are three putative rRNA operons; each has an unusual

organization in that they contain multiple 5S rRNA genes (see Fig. 3S; Table 1 and 1S). Also, each of the 16S rRNA and 23S rRNA genes has a different length (see Fig. 3S). Kosaka et al. (Kosaka et al., 2008) showed that 23S rRNA genes of *P. thermopropionicum* and *S. wolfei* each contain two intervening sequences. Fragmentation of the 23S rRNA was confirmed in *P. thermopropionicum* (Kosaka et al., 2008). The *S. wolfei* genome has 46 tRNAs, 68 transposase genes, and ten RNA-directed, DNA polymerases (reverse transcriptases) genes. The *S. wolfei* genome has 70 pseudogenes, most of which are partial copies of integrases. *S. wolfei* also has six CRISPR regions, which have recently been shown to provide immunity from foreign nucleic acids (Sorek et al., 2008; Horvath et al., 2009). This is a large number of CRISPR regions for a genome of this size.

Comparison to other genomes

When *S. wolfei* ORFs were compared pair-wise to individual microbial genomes, best reciprocal BLAST (BRB) hits revealed the closest associations to members of the Phylum Firmicutes (see Fig. 4S): *Desulfotomaculum reducens* MI-1 (1213 BRB hits), *Desulfitobacterium hafniense* Y51 (1179), *Pelotomaculum thermopropionicum* SI (1150), and *Alkaliphilus metalliredigens* QYMF (1145). Approximately 1000 genes are well conserved across the Firmicutes species shown in Fig. 4S. The remaining genes (ca. 1500) represent a novel complement within the *S. wolfei* genome.

In another comparison, the best BLAST hit (BBH) to any microbial gene was determined (Fig. 5S) and showed 225, 221, 214, and 179 closest hits to the genomes of *P. thermopropionicum* SI, *D. reducens* MI-1, *Moorella thermoacetica* ATCC 39073, and *Heliobacterium modesticaldum* Ice1, respectively. Like the three other syntrophic metabolizers with completed genomic sequences (*S. fumaroxidans, P. thermopropionicum* and *S. aciditrophicus*), a small number of archaea-related genes were identified by the BBH approach. These included nine BBH's to *Methanosarcina mazei* Go1 and six to *Methanococcus maripaludis* S2, suggesting the possibility of lateral gene transfer events from these potential syntrophic partners. The genes potentially acquired by horizontal gene transfer include ORFs encoding for ABC-type uptake systems, B_{12}-dependent enzymes, and cell surface proteins. Genome to genome comparisons at the protein sequence level revealed a few small regions of synteny between the *S. wolfei* genome and the genomes of *Carboxydothermus hydrogenoformans* Z-2901, *D. reducens* MI-1, and *P. thermopropionicum* SI, but not with the other genomes listed in Table 1S (data not shown). The regions of synteny included genes involved in replication, translation, transcription and biosynthesis. A large region indicative of a core genome characteristic for syntrophy was not detected.

Fatty acid metabolism

A metabolic reconstruction of the core physiological traits of *S. wolfei,* which combines the known enzymatic machinery and predictions based on the

gene inventory can be seen in Figure 1. *S. wolfei* uses only four to eight-carbon fatty acids and several unsaturated fatty acids in co-culture (McInerney et al., 1979) and in pure culture growth occurs only with unsaturated fatty acids such as crotonate (Beaty and McInerney, 1987; Amos and McInerney, 1990). Enzymatic studies showed that *S. wolfei* metabolizes fatty acids by the β-oxidation pathway (Wofford et al., 1986; McInerney and Wofford, 1992) and genes for all of the β-oxidation enzymes were detected (Fig. 1; Table 2S). Surprisingly, there are multiple homologues for all of the β-oxidation genes despite *S. wolfei's* extremely restricted substrate range (see Table 2S). The *S. wolfei* genome contains nine acyl-CoA dehydrogenase genes, five enoyl-CoA hydratase genes, six 3-hydroxyacyl-CoA dehydrogenase genes, and five acetyl-CoA acetyltransferase genes. Müller et al. (Müller et al., 2009) detected acyl-CoA dehydrogenases encoded by Swol_1933 and Swol_2052 in syntrophically grown cocultures. Genome-scale metabolic modeling suggests that metabolically limited organisms, such as *S. wolfei* rely on gene duplication of essential functions rather than the possession of alternate pathways to maintain metabolic robustness in case a deleterious mutation occurs (Mahadevan and Lovley, 2008). Alternatively, *S. wolfei* may express different homologs under different environmental conditions (Strittmatter et al., 2009).

Beta-oxidation of butyrate generates two acetyl-CoA's, one of which is used to make ATP by the action of phosphotransacetylase (Swol_0767 gene product) and acetate kinase (Swol_0768 or Swol_1486 gene products) (Fig. 1;

Table 2S). The second acetyl-CoA is used for the activation of butyrate (Fig. 1). Seven CoA transferase genes are present that could function in fatty acid activation (see Table 1S). Two acyl-CoA synthase (AMP-forming) (ligases) (Swol_1144 and Swol_1180) genes are also present, but their functions are mostly likely in coenzyme A biosynthesis (Swol_1180) and PHA metabolism (Swol_1144). Beta-oxidation of butyrate results in the net synthesis of 1 ATP per butyrate by substrate-level phosphorylation (SLP). Two-thirds of the ATP made by SLP is predicted to be used to drive reverse electron transfer as discussed below (Schink, 1997). The remaining one-third of the ATP made by SLP is available for growth.

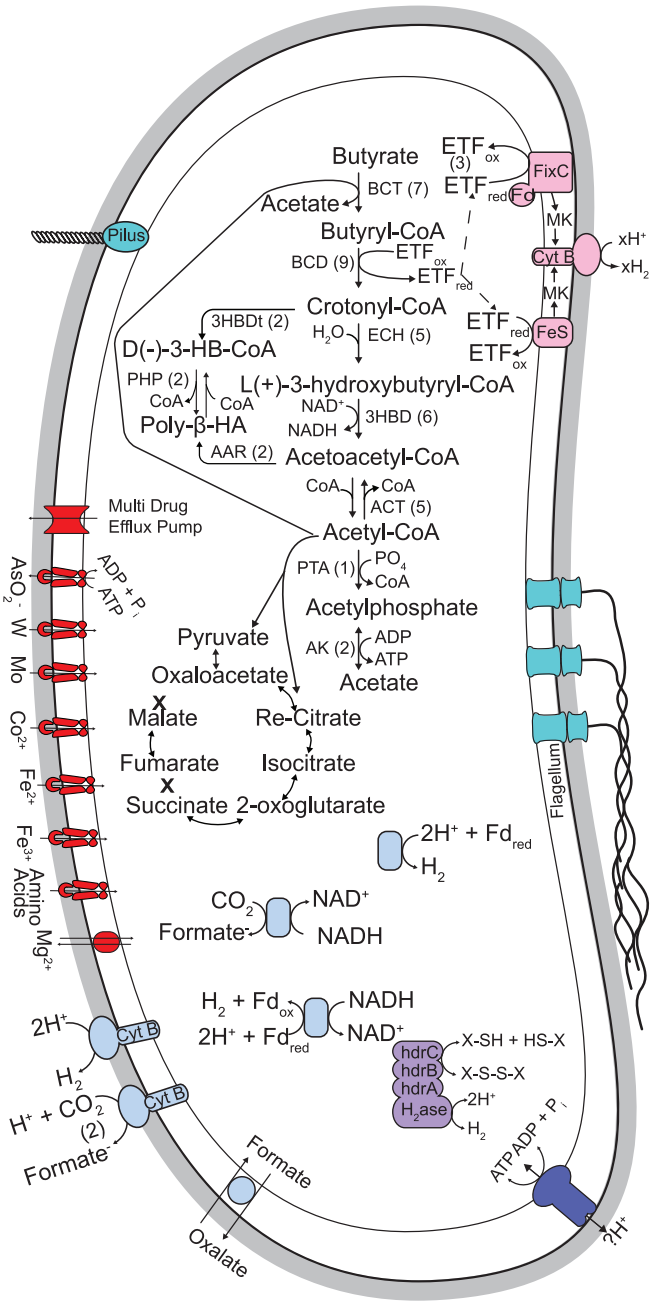


Figure 1. Overview of the metabolism of *S. wolfei*. Primary metabolism reactions are black with the number of homologs in parentheses, cell wall is grey, hydrogenases and formate dehydrogenases are light green, ATP synthase is dark blue, transport and efflux pumps are red, flagella and pili are aqua, heterodisulfide reductase is purple and genes potentially involved in reversed electron transfer are pink. Dashed lines indicate the potential routes for reverse electron transfer. xH^+ and xH_2 could be either hydrogen or formate, in the oxidized or reduced states, respectively. ETF, electron transfer flavoprotein; Fd, ferredoxin; MK, menaquinone

H_2 and Formate Production

Multiple formate dehydrogenase and hydrogenase genes are present, consistent with the reoxidation of reducing equivalents (NADH and reduced electron transfer flavoprotein) generated during β-oxidation for the production of hydrogen or formate (McInerney and Bryant, 1981b; Wallrabenstein, 1994). Genomic analysis predicts that there are five formate dehydrogenases (Fdh), two of which are externally oriented, and three hydrogenases, one of which is externally oriented (see Table 3S; Fig. 1). All three hydrogenases are [FeFe]-type hydrogenases, normally associated with hydrogen production (Vignais et al., 2001). The [NiFe]-type and [NiFeSe]-type hydrogenases, usually associated with H_2 oxidation, were not detected. The presence of cytoplasmic as well as externally oriented hydrogenases and formate dehydrogenases may suggest that a proton motive force could be formed by separation of proton-consuming reactions (H_2 or formate production internally) and proton-producing reactions (H_2 or formate oxidation externally) across the membrane (Odom and Peck, 1981; Heidelberg et al., 2004). However, without NiFe-hydrogenases, it is unclear whether *S. wolfei* can oxidize H_2.

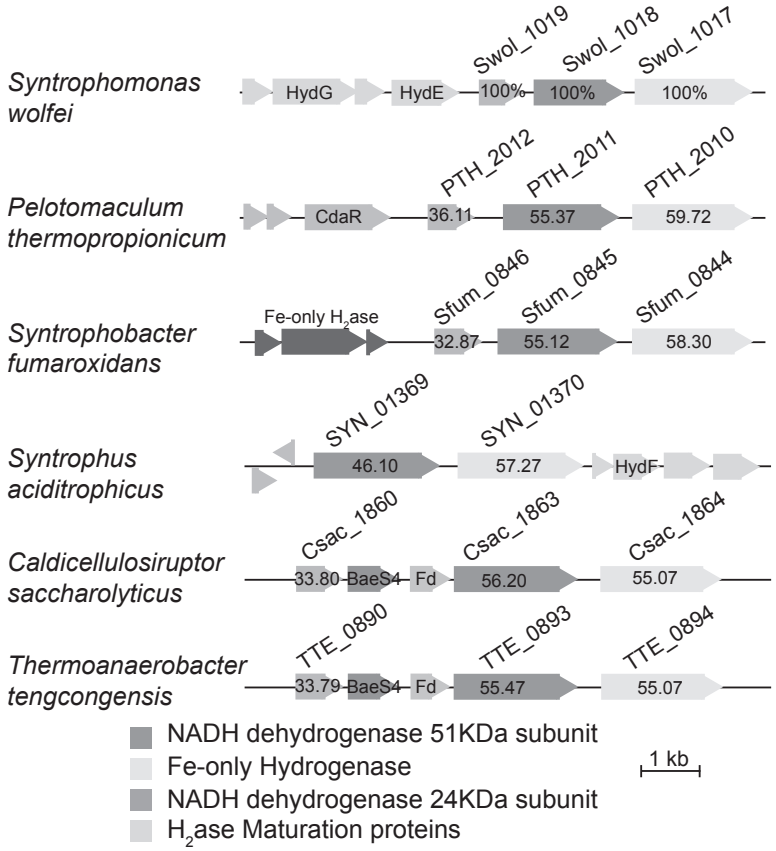
The three cytoplasmic formate dehydrogenases (gene products of Swol_0658, Swol_1028, and Swol_1830) and one of the cytoplasmic hydrogenases (gene products of Swol_1017 and 1019) appear to be NADH-linked because these genes cluster with those that encode subunits of NADH:quinone oxidoreductase (chains E and F) (see Table 3S; Fig. 2).

Recently, a trimeric hydrogenase has been purified from *Thermotoga maritima* that couples the thermodynamically favorable production of H_2 from reduced ferredoxin to drive the unfavorable production of H_2 from NADH by a process called electron bifurcation (Schut and Adams, 2009). Swol_1017-1019 are homologous to the genes for the bifurcating hydrogenase in *T. maritima* (Schut and Adams, 2009). Genes homologous to the electron-bifurcating hydrogenase with the same synteny as found in *S. wolfei* are present in the genomes of the syntrophic metabolizers, *P. thermopropionicum,* and *S. fumaroxidans*, and anaerobes known to produce high molar ratios of hydrogen (>3 H_2 per glucose) from glucose (Fig. 2). In the syntrophic fatty and aromatic acid degrader, *S. aciditrophicus,* the gene for the [FeFe]-hydrogenase is adjacent to a gene for NADH:quinone oxidoreductases subunit (Fig. 2). The [FeFe]-hydrogenase and the NADH dehydrogenase chain F in *S. wolfei* share a high degree of homology at the amino acid level (>57% and >46%, respectively) with their respective counterparts in other syntrophic metabolizers and anaerobes known to produce high molar ratios of hydrogen from glucose even though these organisms are phylogenetically very distinct. The association of the gene for the catalytic subunit of formate dehydrogenase with genes for NADH:quinone oxidoreductases subunits (Fig. 2) suggests that electron bifurcation may also be involved in formate production from NADH.

Recently, a NADH:acceptor oxidoreductase was partially purified from cell-free extracts of *S. wolfei* that contained subunits encoded by Swol_0783,

Swol_0785 and Swol_0786, predicted to encode for the NADH-linked formate dehydrogenase, and Swol_1017, Swol_1018 and Swol_1019, predicted to encode for the NADH-linked hydrogenase (Müller et al., 2009). This experimental evidence coupled with the comparative genomic analyses (Fig. 2) argues that the bifurcation mechanism (Schut and Adams, 2009) may be a universal approach for reverse electron transfer for syntrophic H_2 and formate production from NADH. While the bifurcation mechanism seems quite plausible, it is unclear how *S. wolfei* makes reduced ferredoxin needed to drive the bifurcation mechanism. The *S. wolfei* genome lacks genes for the ion-translocating Rnf complex, which could use the ion gradient to drive the unfavorable reduction of ferredoxin by NADH and has been implicated in reverse electron transfer in *S. aciditrophicus* (McInerney et al., 2007).

NADH Ferredoxin-dependent Hydrogenase



NADH-dependent Formate Dehydrogenase

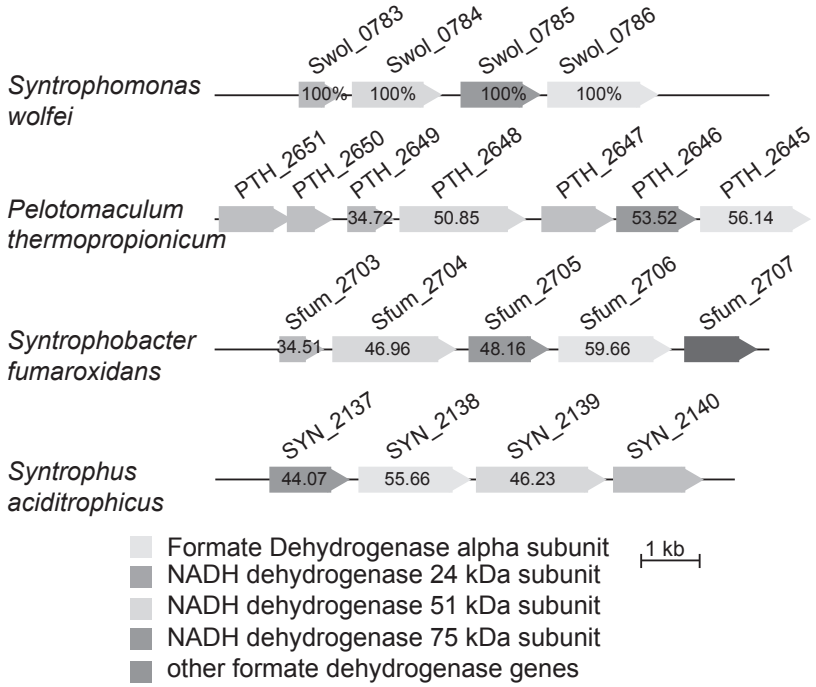


Figure 2. Comparison of *S. wolfei* hydrogenase and formate dehydrogenase gene clusters that contain NADH dehydrogenase genes to similar genes clusters in other bacteria capable of syntrophic metabolism or production of high hydrogen yields from glucose. A) The Swol_1017-1019-type hydrogenase gene cluster, B) the Swol_0783-0786-type formate dehydrogenase gene clusters. Numbers are percent identities at the amino acid level to the respective *S. wolfei* gene product.

Alternatively, *S. wolfei* could use the proton motive force to drive the unfavorable production of H_2 or formate from reduced menaquinone. Such a mechanism is supported by experimental evidence for the presence of menaquinone and an externally oriented hydrogenase (Wallrabenstein, 1994). Hydrogen (E' of -261 mV at 1 Pa H_2) and formate (E' of -258 mV at 1 μM formate) production from reduced menaquinol (E' of -74 mV) (Thauer et al., 1977) would require an energy expenditure of ~36 kJ per mole, which could be provided by the hydrolysis of two-thirds of the ATP made by substrate-level phosphorylation to translocate two protons across the membrane. In support of this hypothesis, *S. wolfei* contains genes predicted to encode for an externally oriented hydrogenase (Swol_1925-1927) and two externally oriented formate dehydrogenases (Swol_0798-800 and Swol_1825-1827). Each gene cluster contains a gene predicted to encode for a membrane-bound *b*-type cytochrome (Table 3S). The gene arrangement suggests that a typical, membrane-bound oxidoreductase complex is formed where the *b*-type cytochrome accepts electrons from menaquinone, transfers the electrons to an iron-sulfur protein,

which then transfers the electrons to the catalytic subunit, either a hydrogenase or a formate dehydrogenase (Jormakka et al., 2002) (Fig. 1).

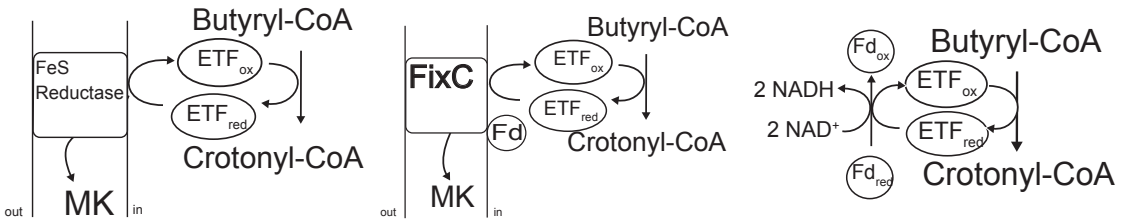
S. wolfei has genes to encode for heterodisulfide reductase subunits A, B, C adjacent to genes for iron-sulfur proteins and an NAD(P)-binding oxidoreductase (Table 3S). In methanogens that lack cytochromes, a soluble Hdr is thought to couple the endergonic reduction of ferredoxin with H_2 with the exergonic reduction of CoM-S-S-CoB with H_2 by a flavin-based electron bifurcation analogous to that for NADH-linked hydrogenases (Schut and Adams, 2009) and acyl-CoA dehydrogenase-electron transfer flavoprotein (Bcd/etfAB) complex (Herrmann et al., 2008; Li et al., 2008). The genes for the *S. wolfei* Hdr are not clustered with those for hydrogenase or formate dehydrogenase, suggesting that Hdr in *S. wolfei* may have a function other than reverse electron transfer to H_2 or formate. In addition, reactions to produce reduced ferredoxin or a disulfide required as substrates by Hdr are not known.

A homolog for the electron-conducting pili gene in *Geobacter sulfurreducens* (Reguera et al., 2005) that could allow direct electron transfer between the syntrophic partners was not detected in the *S. wolfei* genome. Also absent in the *S. wolfei* genome are genes for the inner and outer membrane cytochromes believed to be needed to transfer electrons to nanowires.

Electron flow from acyl-CoA dehydrogenase

The above discussion suggests that reverse electron transfer in *S. wolfei* occurs via menaquinone interacting directly with hydrogenase or formate dehydrogenase complexes or by a NADH:acceptor oxidoreductase (Müller et al., 2009) interacting with hydrogenases or formate dehydrogenases that make H_2 or formate by a bifurcation mechanism (Fig. 1). The remaining question is how *S. wolfei* makes reduced menaquinone from electrons derived in b-oxidation. The *S. wolfei* genome has three gene clusters encoding for electron transfer flavoprotein (ETF) (Fig. 3; Table 2S and 3S). ETF accepts electrons from the acyl-CoA dehydrogenase and typically interacts with membrane ETF:quinone oxidoreductases (Beckmann and Frerman, 1985b, a; Husain and Steenkamp, 1985; Zhang et al., 2004). One set of *S. wolfei* ETF genes is adjacent to a gene predicted to encode for a FeS-oxidoreductase (Table 3S; Fig. 3). This gene arrangement is also observed in the phylogenetically distant *S. aciditrophicus* (McInerney et al., 2007). The amino acid sequences of the *S. aciditrophicus* (SYN_02638) and *S. wolfei* (Swol_0698) gene products share 43.45% sequence identity. Both FeS oxidoreductases contain two 4Fe-4S clusters, two conserved cysteine domains, and six predicted membrane-spanning helices, suggesting that each protein is a membrane-bound FeS oxidoreductase. Based on a comparison to known quinone-binding motifs in photosynthetic systems (Fisher and Rich, 2000), the FeS oxidoreductase may have a quinone-binding site although the sequences for quinone binding are not highly conserved and

difficult to discern from sequence information. Many bacteria contain genes homologous to Swol_0698, but very few have adjacent ETF genes. The organisms with completed genomic sequences that have this type of gene arrangement include: *S. wolfei, S. aciditrophicus, C. hydrogenoformans, Geobacter lovleyi, Desulfococcus oleovorans, Desulfotalea psychrophila, G. sulfurreducens, D. hafniense* (DCB-2 and Y51), *D. reducens, H. modesticaldum*, *G. uraniumreducens,* and *G. metallireducens.* Phylogenetic analysis shows that the *S. wolfei* and *S. aciditrophicus* gene products are closely related to each other and more distantly related to the *C. hydrogenoformans* and *D. hafniense* (DCB-2 and Y51) gene products (Fig. 6S). The high degree of homology between *S. wolfei* and *S. aciditrophicus* gene products and the clustering of the FeS oxidoreductase gene with ETF genes suggests a role in syntrophic fatty acid metabolism. The C-terminal portion of the Swol_0698 gene product was detected in a partially purified acyl-CoA dehydrogenase activity obtained from syntrophically grown *S. wolfei* cells (Müller et al., 2009), consistent with the hypothesis that the Swol_0698 gene product funnels electrons from b-oxidation to membrane redox carriers (McInerney et al., 2007).



Iron-sulfur-binding reductase linked to ETF	
Electron transfer flavoprotein, beta subunit	Swol_0696
Electron transfer flavoprotein, alpha subunit	Swol_0697
Iron-sulfur-binding reductase	Swol_0698

Fix System	
Electron transfer flavoprotein, alpha-subunit	Swol_2121
Electron transfer flavoprotein, beta-subunit	Swol_2122
FixX (ferredoxin)	Swol_2123
FixC (ETF: Quinone Oxidoreductase)	Swol_2124
Acyl-CoA dehydrogenase	Swol_2126

Acyl CoA dehydrogenase linked to ETF	
Electron transfer flavoprotein, beta-subunit	Swol_0266
Electron transfer flavoprotein, alpha-subunit	Swol_0267
Acyl-CoA dehydrogenase	Swol_0268

Figure 3. Illustration of the candidates for reverse electron transfer in the genome of *S. wolfei*. a.) Novel reverse electron transfer system involving electron transfer flavoprotein (ETF) and a membrane-bound iron-sulfur oxidoreductase, b.) Fix system comprised of a ETF, ETF:Quinone oxidoreductase, and ferredoxin, and c.) soluble acyl-CoA dehydrogenase:ETF complex. Gene designations are given below the figure.

A second set of ETF-encoding genes is associated with *fix* genes (Table 3S; Fig. 3). This gene cluster contains genes for the two subunits of the electron transfer flavoprotein (*fixA* and *fixB*), a ferredoxin (*fixX*), and a membrane-bound, ETF-oxidoreductase (*fixC*). In nitrogen-fixing bacteria, Fix catalyzes reverse electron transfer from ETF to ferredoxin (Earl et al., 1987; Weidenhaupt et al., 1996; Edgren and Nordlund, 2004; Sperotto et al., 2004). The Fix system has also been implicated in anaerobic carnitine reduction in *Escherichia coli* where the *caiTABCDE* operon is found adjacent to the *fixABCX* (Eichler et al., 1995; Walt and Kahn, 2002). *S. wolfei* does not fix nitrogen or reduce carnitine, and genes required for these activities were not detected in the genome. The location of the *fix* genes with those for acyl-CoA dehydrogenase, enoyl-CoA hydratase, and a CoA transferase implicates their role in electron transfer during b-oxidation. The Fix system could be used to supply reduced ferredoxin needed for the unfavorable synthesis of pyruvate from acetyl-CoA or for hydrogen and formate production by the bifurcation mechanism.

The third set of ETF genes (Swol_0266-268) is adjacent to a gene for an acyl-CoA dehydrogenase (*bcd/etfAB*) (Table 2S; Fig. 3). None of the gene products are predicted to be membrane-bound. It is possible that the three gene products form a soluble reverse electron transfer complex analogous to that in *Clostridium kluyveri* (Herrmann et al., 2008; Li et al., 2008). In *C. kluyveri*, a soluble Bcd/EtfAB complex couples the energetically favorable reduction of

crotonyl-CoA to butyryl-CoA by NADH with the unfavorable reduction of ferredoxin (Fd) by NADH through a bifurcation mechanism (equation 1).

$$\text{Crotonyl-CoA} + Fd_{ox} + 2\ \text{NADH} \rightarrow \text{Butyryl-CoA} + Fd_{red} + 2NAD^{+}$$

(eq. 3)

In *S. wolfei*, this system would operate in the opposite direction as that shown in equation 3 to reduce NAD^{+} with electrons derived from butyryl-CoA and reduced ferredoxin (Fig. 3). However, the acyl-CoA dehydrogenase partially purified from cell-free extracts of syntrophically grown *S. wolfei* was not a Bcd/etfAB (Müller et al., 2009). The genes (Swol_1933 and Swol_2052) that encode the acyl-CoA dehydrogenases detected in *S. wolfei* cell-free extracts (Müller et al., 2009) are not linked to ETF genes.

Respiratory and other primary ion-translocating systems

Genomic analysis indicates that *S. wolfei* has few options to generate a proton motive force needed for reverse electron transfer, nutrient uptake and motility. The key proton translocating genes found in the genome are an ATP synthase and a pyrophosphatase (Table 3S). *S. wolfei* like *S. aciditrophicus* (McInerney et al., 2007) lacks the genes for aerobic and anaerobic respiration. The cytochrome encoding genes detected were *b*-type cytochromes associated with hydrogenases and formate dehydrogenases and a *c*-type cytochrome associated with genes predicted to encode for a periplasmic, nitrite reductase (Swol_1521 and Swol_1522) with a potential role in detoxification (Greene et al.,

2003). *S. wolfei* does not grow with nitrite (McInerney et al., 1979; McInerney et al., 1981b). There is a cluster of hypothetical genes, some of which are predicted to encode for membrane proteins and/or redox proteins (Swol_1956 to Swol_1968) (Table 3S). The function of these genes in *S. wolfei* is unknown. Most likely, *S. wolfei* uses a proton-transporting ATP synthase to hydrolyze ATP made by substrate-level phosphorylation to generate a proton motive force (Table 3S). A gene for a proton-translocating pyrophosphatase (Swol_1064) is present, but a continual source of pyrophosphate is not available because *S. wolfei* uses a CoA transferase rather than a ligase reaction to activate fatty acids.

Biosynthesis

S. wolfei grows in a defined medium with crotonate as the energy source and thiamine, lipoic acid, cyanocobalamin, and *para*-aminobenzoic acid as required growth factors (Beaty and McInerney, 1990). *S. wolfei* has genes for pyruvate synthase (pyruvate:ferredoxin oxidoreductase) and pyruvate carboxylase that convert acetyl-CoA to pyruvate and pyruvate to oxaloacetate, respectively (Table 2S; Fig. 1). Also present are the genes for pyruvate:phosphate dikinase to convert pyruvate to phosphoenolpyruvate and those to form glucose from phosphoenolpyruvate (Table 2S; Fig. 1). *S. wolfei* uses the oxidative arm of the tricarboxylic acid cycle to synthesize 2-oxoglutarate and succinyl-CoA from acetyl-CoA (Table 2S; Fig. 1). This is an unusual approach for an anaerobe as most strict anaerobes lack the genes for

2-oxoglutarate dehydrogenase. The Swol_0375 gene product shares 25% identity with an E-value of 3E-26 to the CKL_0973 gene product, which has been shown to encode for a *re*-citrate synthase in *C. kluyveri* (Li et al., 2007). The gene cluster, Swol_0375-378, contains genes for a homocitrate synthase, an aconitase and isocitrate dehydrogenase, similar to arrangement found for the *re*-citrate synthase gene cluster in *C. kluyveri* (Li et al., 2007). Genes to encode for *si*-type citrate synthase, succinate dehydrogenase, malate dehydrogenase, fumarate reductase, the glyoxylate shunt, and a complete gamma-aminobutyric acid (GABA) shunt were not detected in the *S. wolfei* genome.

Assignment of the 1507 functionally described genes into pathways revealed that most pathways needed for biosynthetic self-sufficiency (e.g., biosynthesis of amino acids, purines, pyrimidines, membrane lipids, polysaccharides, and some cofactors) are present, but many pathways have missing steps. By manual curation, we were able to detect most of the missing genes involved in amino acid biosynthesis with the exceptions of the genes encoding for threonine-ammonia lyase, methionine synthase, and the arginosuccinate synthase and lyase.

There are forty ATP-binding cassette (ABC) transporters predicted to be involved in nutrient uptake and antibiotic resistance (see Table 4S; Fig. 1) (Ren et al., 2007). There are multiple genes for arsenite resistance, calcium

antiporters, multi-drug pumps and uptake systems for potassium, zinc, ferrous iron, magnesium, phosphate, and sugars (Table 4S).

S. wolfei stains gram-negatively and has a complex cell wall that suggested the presence of an outer membrane (McInerney et al., 1981b). However, phylogenetic analysis placed *S. wolfei* in the Phylum Firmicutes (Zhao et al., 1990), whose members lack lipopolysaccharides. The *S. wolfei* genome contains genes for peptidoglycan synthesis but lacks those for lipopolysaccharide biosynthesis, consistent with the placement of *S. wolfei* in the Phylum Firmicutes.

Regulation and signal transduction

The *S. wolfei* genome contains a prototypical bacterial RNA core polymerase (*rpoA*, *rpoB*, *rpoC*) that along with seventeen sigma factors, confers promoter specificity (Table 5S). The sigma factors include a general housekeeping 70 factor (*rpoD*), a heat shock 32 factor (*rpoH*), a flagella biogenesis 1 factor (*fliA*), and a 54 factor (*rpoN*) similar to that used for general nitrogen control in *E. coli*. The genome contains three sigma 54-interacting transcriptional regulators.

Genes for numerous two-component regulatory systems (11 histidine kinase-type sensor transmitters, 6 response regulatory proteins, and 8 receiver-only domain proteins) are present in the genome. Roughly half are genetically linked to a cognate two-component protein member, which suggests an

interacting partner in sensory transduction. Compared to other gram-positive microbes, *S. wolfei* has a relatively small number of primary transcription factors containing a helix-turn-helix motif (ca. 58 genes). Instead, *S. wolfei* appears to have adopted a minimalist regulatory strategy reliant on a core set of signaling pathways, consistent with its highly specialized metabolism.

Cellular adaptation and stress response

S. wolfei has evolved multiple systems for adapting to stress. This includes motility, PHA formation, and potentially sporulation. Oxidative stress can be dealt with by genes encoding rubrerythrin, (Swol_0670) and superoxide dismutase (Swol_1711), although the catalase gene is absent. Another type of cellular adaptation in syntrophic organisms would be a communication system with a methanogenic partner to initiate syntrophy. The genetic systems necessary for quorum sensing such as acyl-homoserine lactone production are absent. The genome contains a non-ribosomal peptide synthetase gene (Swol_1084) that could be involved in synthesizing short peptides, which can act as signaling molecules. Alternatively a flagellum recognition system, similar to the system in *P. thermopropionicum* (Shimoyama et al., 2009), is possible. *S. wolfei* does produce flagella, but it would be difficult at this point to infer from the genome if the methanogen can recognize the flagellum as a signal to initiate a cooperative relationship.

Motility and taxis

Motility and the presence of flagella have been observed with laboratory cultures (McInerney et al., 1981b). *S. wolfei* has a set of flagellar structural proteins (M-ring, motor, hook, and rod) along with the associated flagellar biogenesis and regulatory genes including a σ 28 and an anti-28 factor (*flgM*) and *E. coli*-type master switch proteins, *flhCD* (see Table 6S). Nine methyl-accepting chemotaxis sensory proteins (three soluble and six membrane associated) act to detect as yet unknown attractants and/or repellants for signal transduction. The genome contains three genes for each of the *cheB*, *cheC*, *cheR*, and *cheW* plus four *cheA* and one *cheD* gene, suggesting potentially parallel signal transduction pathways with differing outputs. No *cheZ* or *cheV* genes were detected.

Synthesis of poly-β-hydroxyalkanoates (PHA)

Members of the genus *Syntrophomonas* are among the few microorganisms within the Firmicutes that make PHA (McInerney, 1992). *S. wolfei* is unique in that most microorganisms produce PHA when nutrients other than carbon, usually nitrogen or oxygen, are limiting for growth (Anderson et al., 1990; McInerney, 1992), while *S. wolfei* synthesizes PHA during the exponential stage of growth in pure culture or co-culture apparently in the absence of any nutrient limitation (Amos and McInerney, 1989). The production of PHA may provide a mechanism for *S. wolfei* to obtain energy when

thermodynamic conditions make the degradation of fatty acids unfavorable (Amos and McInerney, 1989; Beaty and McInerney, 1989; McInerney, 1992). The genome contains all of the genes necessary to synthesize and metabolize PHA. Interestingly, these genes do not appear to be clustered into functional units on the chromosome. There are two genes for 3-hydroxybutyryl-CoA dehydratases (Swol_0650 and Swol_2566) that are distinguishable from the enoyl-CoA hydratases involved in b-oxidation, three genes for poly-(3)-hydroxyalkanoate synthetases (Swol_1099, Swol_1145 and Swol_1241) and two genes for acetoacetyl-CoA reductases (Swol_0650 and Swol_1910). The presence of two sets of genes for poly-(3)-hydroxyalkanoate synthesis is consistent with previous work that showed that *S. wolfei* uses two routes for PHA synthesis (Amos and McInerney, 1993), the condensation of two acetyl-CoA molecules to acetoacetyl-CoA and its subsequent reduction to D(-)-3-hydroxybutyryl-CoA, and the conversion of a b-oxidation intermediate to D(-)-3-hydroxybutyryl-CoA without carbon-carbon bond cleavage. Having two routes for PHA production shows that energy storage is a very important process in *S. wolfei*'s lifestyle.

Spore formation

S. wolfei has not been shown to form spores, yet its genome contains a full complement of genes needed for the developmental programs of spore formation and germination (Table 7S). Sporulation has been shown to occur for other members of the genus *Syntrophomonas* (Wu et al., 2006b, a; Sousa et al.,

2007; Wu et al., 2007), particularly under bicarbonate-limited conditions (Wu et al., 2007). The genome contains 59 genes involved in sporulation, which rivals *C. hydrogenoformans* for lowest number of genes involved in sporulation, if *S. wolfei* in fact forms spores.

CONCLUSIONS

Genomic analysis shows that *S. wolfei* specializes in syntrophic fatty acid metabolism in association with methanogens and other hydrogen- and formate-using microorganisms. The high degree of specialization and acquisition of genes from its methanogenic partner supports the idea that syntrophic metabolizers evolved as syntrophic specialists by interacting with niche-associated methanogens (Kosaka et al., 2008). Its very restricted metabolic potential probably reflects the outcome of evolutionary selection for energy conservation systems that are highly efficient at using small amounts of free energy. The inability to respire and the dearth of primary ion pumps makes the generation of ion gradients difficult, but may be advantageous to syntrophic specialist like *S. wolfei* because there are few routes for proton leakage. This may allow for more effective control of the production and use of the proton motive force.

Genomic comparisons did not reveal a large, contiguous, core set of genes that could be identified as being involved in syntrophy, but did reveal that genes for electron bifurcation for hydrogen (Schut and Adams, 2009) and

possibly formate production are present in genomes of syntrophic metabolizers and anaerobes that yield high amounts of H_2 from glucose (Fig. 2). A second potential set of core syntrophic reactions may be the reactions involved in electron transfer from acyl-CoA dehydrogenases to membrane complexes. By comparative genomic analyses, we identified a novel, membrane-bound, iron-sulfur oxidoreductase that may funnel electrons from reduced ETF to membrane redox carriers (McInerney et al., 2007). While we have made great progress in delineating the genetic systems involved in syntrophic fatty and aromatic acid metabolism (McInerney et al., 2007), we have very little understanding of what other gene systems may be needed for syntrophy. It is unclear whether cell-cell communication systems, specialized recognition factors and/or attachment systems are needed. However, genomic information provides us with the tools to test these hypotheses experimentally.

METHODS

Media and growth conditions

Syntrophomonas wolfei subsp. *wolfei* strain Göttingen DSM 2245B was grown in basal medium (Beaty et al., 1987) without rumen fluid with 20 mM sodium crotonate. Multiple 1-liter cultures were used to obtain cells for DNA isolation, which was performed using the CTAB containing method (Wilson, 2001), which can be found at http://www.jgi.doe.gov.

Genome Sequencing

S. wolfei genomic DNA, isolated by standard methods (above), was sequenced at the Joint Genome Institute (JGI) using a combination of 3 kb, 8 kb and 40 kb DNA libraries. All general aspects of library construction and sequencing performed at the JGI can be found at http://www.jgi.doe.gov. The Phred/Phrap/Consed software package (http://www.phrap.com) was used to assemble all three libraries and to assess quality (Ewing and Green, 1998; Ewing et al., 1998; Gordon et al., 1998). Possible mis-assemblies were corrected, and gaps between contigs were closed by editing in Consed, custom primer walks, or PCR amplification (Roche Applied Science, Indianapolis, IN). The error rate of completed genome sequence of *S. wolfei* is less than 1 in 50,000. Pairwise graphical alignments of whole genome assemblies (e.g. synteny plots) were generated by using the MUMmer system (Delcher et al., 1999a; Delcher et al., 1999b). The sequence of *S. wolfei* can be accessed using the GenBank accession number NC_008346.

Table 1S. General features of the *S. wolfei* genome in comparison to genomes of select members of the Firmicutes and other bacteria capable of syntrophic metabolism.

Genome Name	*Syntrophomonas wolfei wolfei* Goettingen	*Pelotomaculum thermopropionicum* SI	*Thermoanaerobacter tengcongensis* MB4	*Bacillus cereus* ATCC 14579	*Carboxydothermus hydrogenoformans* Z-2901	*Clostridium acetobutylicum* ATCC 824	*Desulfitobacterium hafniense* DCB-2	*Moorella thermoacetica* ATCC 39073	*Syntrophobacter fumaroxidans* MPOB	*Syntrophus aciditrophicus* SB
NCBI Taxon ID	335541	370438	273068	226900	246194	272562	272564	264732	335543	56780
GC Perc	0.45	0.53	0.38	0.35	0.42	0.31	0.47	0.56	0.6	0.51
MBases	2.94	3.02	2.69	5.43	2.4	4.13	5.28	2.63	4.99	3.18
Genes	2677	3018	2719	5513	2738	4022	5042	2634	4179	3226
CDS	2574	2920	2614	5255	2640	3848	4953	2523	4098	3168
RNA	103	98	105	258	98	174	89	111	81	58
5S	13	2	4	13	4	11	5	1	2	1
16S	3	2	4	13	4	11	5	1	2	1
23S	3	2	4	13	4	11	5	1	2	1
tRNA	46	51	55	108	50	73	74	51	51	49
Other RNA	38	41	38	111	36	68	0	57	24	0
Psuedogenes	70	0	26	0	20	0	70	58	34	0
w/ Func Prediction	56.29	56.83	64.55	67.13	64.50	77.10	70.48	69.63	67.22	64.41
w/o Func Pred Sim Perc	37.43	33.66	28.91	28.10	22.83	16.21	27.77	25.36	27.28	22.97
w/o Func Pred No Sim Perc	2.43	6.26	2.68	0.09	9.09	2.36	3.67	0.80	3.57	10.82
Signal P	22.53	20.87	21.07	26.77	22.24	22.40	27.01	23.73	29.27	24.77
TransMb	20.32	20.08	24.27	27.28	12.09	19.92	6.68	21.68	24.61	22.60
CRISPR	6	5	3	1	3	1	5	2	4	2

Table 2S. List of genes involved in key metabolic step in *S. wolfei*.

Function	Gene ID
Beta-oxidation	
Acyl-CoA synthetases (AMP-forming)/AMP-acid ligase II	Swol_1144 Swol_1180
CoA transferase (EC 2.3.1.-)	Swol_0309 Swol_0787 Swol_1014 Swol_1147 Swol_1482 Swol_1734 Swol_1744 Swol_1932 Swol_2128
4-Hydroxybutyryl-CoA transferase	Swol_0436
Acyl-CoA dehydrogenase (EC 1.3.99.3)	Swol_0384 Swol_1933 Swol_2052
Acyl-CoA dehydrogenase, short-chain specific (EC 1.3.99.2)	Swol_0268 Swol_0488 Swol_0788 Swol_1483 Swol_1841 Swol_2126
Enoyl-CoA hydratase (EC 4.2.1.17)	Swol_0650 Swol_0790 Swol_1484 Swol_1936 Swol_2031 Swol_2129 Swol_2566
3-hydroxybutyryl-CoA dehydrogenase (EC 1.1.1.157)	Swol_0307 Swol_0791 Swol_1171 Swol_1485 Swol_1935 Swol_2030
3-Hydroxybutyryl-CoA dehydrogenase (EC 1.1.1.35)	Swol_0435

Acetyl-CoA acetyltransferase (EC 2.3.1.9)	Swol_0308 Swol_0675 Swol_0789 Swol_1934 Swol_2051
Acetate Kinase (EC 2.7.2.1)	Swol_0768 Swol_1486
Phosphotransacetylase (EC 2.3.1.8)	Swol_0767
Transcriptional regulator containing PAS, AAA-type ATPase, and DNA-binding domains	Swol_0437
PHA synthesis	
Acetoacetyl-CoA reductase (EC 1.1.1.36)	Swol_0651 Swol_1910
Poly(3-hydroxyalkanoate) polymerase (EC 2.3.1.-)	Swol_1099 Swol_1145 Swol_1241
ATP synthase	
ATP synthase epsilon chain (EC 3.6.3.14)	Swol_2381
Sodium-transporting two-sector ATPase beta subunit (EC:3.6.3.15)	Swol_2382
Sodium-transporting two-sector ATPase alpha subunit (EC:3.6.3.15)	Swol_2383
Sodium-transporting two-sector ATPase gamma subunit (EC:3.6.3.15)	Swol_2384
ATP synthase delta chain (EC 3.6.3.14)	Swol_2385
ATP synthase B chain (EC 3.6.3.14)	Swol_2386
ATP synthase C chain (EC 3.6.3.14)	Swol_2387
ATP synthase A chain (EC 3.6.3.14)	Swol_2388
ATP synthase protein Z	Swol_2389
Heterodisulfide reductase	
CoB—CoM HDR, subunit C (EC 1.8.98.1)	Swol_0394
CoB—CoM HDR, subunit B (EC 1.8.98.1)	Swol_0395
CoB—CoM HDR, subunit A (EC 1.8.98.1)	Swol_0396*
CoB—CoM HDR, subunit A (EC 1.8.98.1)	Swol_0397*
F420-non-reducing hydrogenase subunit D (EC 1.12.99.-)	Swol_0398*

F420-non-reducing hydrogenase subunit D (EC 1.12.99.-)	Swol_0399*
Formate dehydrogenase beta chain (EC 1.2.1.2)	Swol_0400
Cytochrome-C3 hydrogenase (EC 1.12.2.1)	Swol_0401
Cytochrome-C3 hydrogenase (EC 1.12.2.1)	Swol_0402
Fix System	
Electron transfer flavoprotein alpha-subunit	Swol_2121
Electron transfer flavoprotein beta-subunit	Swol_2122
FixX (ferredoxin)	Swol_2123
FixC (ETF:Quinone Oxidoreductase)	Swol_2124
Acyl-CoA dehydrogenase, short-chain specific (EC 1.3.99.2)	Swol_2126
Acyl CoA dehydrogenase linked to ETF	
Electron transfer flavoprotein beta-subunit	Swol_0266
Electron transfer flavoprotein alpha-subunit	Swol_0267
Acyl-CoA dehydrogenase, short-chain specific (EC 1.3.99.2)	Swol_0268
Iron-sulfur-binding reductase linked to Electron transfer flavoproteins	
electron transfer flavoprotein, beta subunit	Swol_0696
electron transfer flavoprotein, alpha subunit	Swol_0697
iron-sulfur-binding reductase	Swol_0698
Hydrogenases	
Hydrogenase-1 (EC 1.12.7.2)	Swol_1017
NADH dehydrogenase (quinone) (EC:1.6.99.5)	Swol_1018
Fe-hydrogenase	Swol_1019
Hydrogenase-1 (EC 1.12.7.2)	Swol_1925
Hydrogenase-1 (EC 1.12.7.2)	Swol_1926
Formate dehydrogenase, cytochrome B556 subunit (EC 1.2.2.1)	Swol_1927
Fe hydrogenase, large subunit HymC	Swol_2436
Formate Dehydrogenases	

NADH-quinone oxidoreductase chain E (EC 1.6.5.3)	Swol_0783
NADH-quinone oxidoreductase chain F (EC 1.6.5.3)	Swol_0784
NADH dehydrogenase I chain G	Swol_0785
Formate dehydrogenase alpha subunit	Swol_0786
FdhE protein	Swol_0796
Formate dehydrogenase, cyt B556 subunit (EC 1.2.2.1)	Swol_0797
Formate dehydrogenase (cyt b) iron-sulfur subunit (EC 1.2.2.1)	Swol_0798
Formate dehydrogenase (cyt b) major subunit (EC 1.2.2.1)	Swol_0799*
Formate dehydrogenase (cyt b) major subunit (EC 1.2.2.1)	Swol_0800*
Molybdopterin biosynthesis MoeA protein	Swol_0801
Molybdopterin biosynthesis MoeA protein	Swol_0802
NADH-quinone oxidoreductase chain F	Swol_1024
NADH-quinone oxidoreductase chain E	Swol_1025
Molybdopterin biosynthesis MoeA protein	Swol_1026
Molybdopterin biosynthesis enzyme	Swol_1027
Formate dehydrogenase alpha subunit	Swol_1028
NADH-ubiquinone oxidoreductase 75kDa subunit	Swol_1029
FdhD protein	Swol_1030
Molybdate-binding protein	Swol_1821
Formate dehydrogenase formation protein FdhE	Swol_1822
Formate dehydrogenase, cyt B556 subunit (EC 1.2.2.1)	Swol_1823
Formate dehydrogenase (cyt b) iron-sulfur subunit (EC 1.2.2.1)	Swol_1824
Formate dehydrogenase (cyt b) major subunit (EC 1.2.2.1)	Swol_1825*
Formate dehydrogenase (cyt b) major subunit (EC 1.2.2.1)	Swol_1826*
Molybdopterin biosynthesis MoeA protein	Swol_1827
NADH-quinone oxidoreductase chain F (EC 1.6.5.3)	Swol_1828
NADH-quinone oxidoreductase chain E (EC 1.6.5.3)	Swol_1829

Formate dehydrogenase alpha subunit (EC 1.2.1.43)	Swol_1830*
NADH-ubiquinone oxidoreductase 75kDa subunit (EC 1.6.5.3)	Swol_1831*
Ferredoxin	Swol_1832
NADH dehydrogenase (EC 1.6.99.3)	Swol_1833
Ferredoxin	Swol_1834
Aldehyde ferredoxin oxidoreductase(EC:1.2.7.5)	Swol_1835
Nitrite reductase (cytochrome; ammonia-forming)	Swol_1521
Nitrite reductase, small subunit, NrfH	
TCA cycle genes	
Pyruvate synthase porB (EC 1.2.7.1)	Swol_1374 Swol_2234
Pyruvate synthase porA (EC 1.2.7.1)	Swol_1375 Swol_2235
Pyruvate synthase porD (EC 1.2.7.1)	Swol_1376 Swol_2236
Pyruvate synthase porG (EC 1.2.7.1)	Swol_1377 Swol_2237
Pyruvate carboxylase (EC 6.4.1.1)	Swol_0519
putative *re*-citrate synthase	Swol_0375
Aconitate hydratase (EC 4.2.1.3)	Swol_0376
3-isopropylmalate dehydratase, small subunit (EC 4.2.1.33)	Swol_0377
Isocitrate dehydrogenase (EC 1.1.1.42)	Swol_0378
Fumarate hydratase beta subunit (EC 4.2.1.2)	Swol_1628
Fumarate hydratase alpha subunit (EC 4.2.1.2)	Swol_1629
2-oxoglutarate dehydogenase??	Swol_1398
putative keto/oxoacid ferredoxin oxidoreductase, alpha subunit	Swol_0036
putative keto/oxoacid ferredoxin oxidoreductase, beta subunit	Swol_0037
putative keto/oxoacid ferredoxin oxidoreductase, gamma subunit	Swol_0038
cytochrome c assembly protein	Swol_1519

ResB protein required for cytochrome c biosynthesis-like protein	Swol_1520
respiratory nitrite reductase (cytochrome; ammonia-forming) precursor (EC 1.7.2.2)	Swol_1521
respiratory nitrite reductase specific menaquinol--cytochrome-c reductase (NrfH) precursor (EC 1.10.2.-)	Swol_1522
Ferredoxins	
Ferredoxin	Swol_1401 Swol_1440 Swol_1832 Swol_1957 Swol_2105 Swol_2123 Swol_2462
4Fe-4S ferredoxin	Swol_1704 Swol_1834
Genes containing Membrane helices	
Predicted NADH:ubiquinone oxidoreductase, subunit RnfG	Swol_1959
FAD dependent oxidoreductase	Swol_2135
3-hydroxybutyryl-CoA dehydrogenase	Swol_1171
Fatty acid-binding protein, DegV family	Swol_0442 Swol_1050
Polyferredoxin	Swol_1947 Swol_2462
Pumpsand transports	
Pyrophosphatase	Swol_1064
Na/H+ antiporters	Swol_1178 Swol_1590
Na+-driven multidrug efflux pump	Swol_0313 Swol_0316 Swol_0575 Swol_1820 Swol_2061
Multidrug pump	Swol_0960 Swol_1354 Swol_1367 Swol_1713 Swol_2232 Swol_2447-49

Heavy metal efflux	Swol_2086-87
MFS transport	Swol_1903
Na+/H+ antiporter NhaD and related arsenite permeases	Swol_2091-92 Swol_2166
Ca2+/Na+ antiporter	Swol_0654 Swol_2086 Swol_1698
Cation transport ATPase	Swol_0623 Swol_1240
Arabinose efflux permease	Swol_1354
Mg/Co/Ni transporter MgtE (contains CBS domain)	Swol_1082
Cation transport	Swol_0917 Swol_1051 Swol_1889-91
FeII	Swol_0660-662 Swol_1537-39
FeIII	Swol_1187 Swol_1472-73 Swol_1685-87 Swol_2096-97 Swol_2476-77
FeIII citrate	Swol_1676-1679 Swol_1695-96
K+, Trk	Swol_0913-914
Co	Swol_1045-1047 Swol_1947-52 Swol_2300-2302
Sulfonate	Swol_0339-341
Zn	Swol_421 Swol_1139
Mo	Swol_1554-1557
W	Swol_1630-1632
PO4	Swol_1646

Formate transport	Swol_0091
Na/H+ dicarboxylate	Swol_0311
TRAP C4 dicarboxylate	Swol_0329-331
Branched chain amino acid	Swol_0922-923 Swol_2110-2113 Swol_2551-55
Amino acid	Swol_1065-66 Swol_1070-71
Dipeptide	Swol_2012
Maltose	Swol_0403-409
Sugar	Swol_0414-416
Ribose	Swol_0424-426
Thiamine	Swol_2478
AA (Leu, isoleu, etc.)	Swol_2556
Excinuclease	Swol_0251-254
Acriflavin resistance	Swol_0175-176
ABC transporters, general	Swol_0180-182 Swol_0215 Swol_0943 Swol_1207 Swol_1620 Swol_1722-23 Swol_1738-39 Swol_2038 Swol_2094 Swol_2242-43 Swol_2457-58 Swol_2479-81
Periplasmic binding protein	Swol_1687 Swol_1690-1691 Swol_2040
Other Selenocysteine containing proteins	
alkyl hydroperoxide reductase	Swol_2182
hypothetical protein	Swol_2460

selenophosphate synthase	Swol_2542
L-seryl-tRNA(Sec) selenium transferase	Swol_2561
selenocysteine-specific translation elongation factor	Swol_2560

* These genes contain Se cysteine that was originally annotated as a stop codon.

Table 3S. List of genes involved in electron transfer and formation of ion gradients and those predicted to have signal peptides (SigP) and transmembrane helices (TMMH) in *S. wolfei.*

	Locus Tag	Product Name	AA Seq Length	Putative Function	SigP	TMMH
hydI	Swol_1017	Iron hydrogenase, small subunit	574	NADH + $Fd_{red} \leftrightarrow H_2$ +NAD^+ +Fd_{ox}		
	Swol_1018	NADH dehydrogenase subunit	407			
	Swol_1019	Fe-hydrogenase, gamma subunit	148			
hydII	Swol_1925	Hydrogenase-1	387			
	Swol_1926	Hydrogenase-1	135	$MQ \leftrightarrow H_2$	Yes	Yes (1)
	Swol_1927	Cytochrome B556 subunit	220			Yes (4)
hydIII	Swol_2436	(Fe) hydrogenase, large subunit HymC	563	$Fd_{red} \leftrightarrow H_2$		
fdhI	Swol_0656	NADH-quinone oxidoreductase chain E	182		No	No
	Swol_0657	NADH-quinone oxidoreductase chain F	590	$MQ \leftrightarrow H_2$	No	No
	Swol_0658	NADP-dependent formate dehydrogenase beta subunit	688		No	No
fdhII	Swol_0783	NADH-quinone oxidoreductase chain E	148			
	Swol_0784	NADH-quinone oxidoreductase chain F	408	Formate ↔ NADH		
	Swol_0785	NADH dehydrogenase I chain G	353			
	Swol_0786	Formate dehydrogenase alpha subunit	529			
fdhIII	Swol_0796	FdhE protein	275			
	Swol_0797	Formate dehydrogenase, cyt B556 subunit	229			Yes (4)
	Swol_0798	Formate dehydrogenase (cyt b) iron-sulfur subunit	266	Formate ↔ MQ		
	Swol_0799	Formate dehydrogenase (cyt b) major subunit	851			
	Swol_0800	Formate dehydrogenase (cyt b) major subunit	232		Yes	
	Swol_1024	NADH-quinone oxidoreductase chain F	407			

	Swol_1025	NADH-quinone oxidoreductase chain E	148			
fdhIV	Swol_1026	Molybdopterin biosynthesis MoeA protein	402			
	Swol_1027	Molybdopterin biosynthesis enzyme	343			
	Swol_1028	Formate dehydrogenase alpha subunit	536	Formate ↔ NADH		
	Swol_1029	NADH-ubiquinone oxidoreductase 75kDa subunit	358	Formate ↔ MQ		
	Swol_1030	FdhD protein	263			
	Swol_1821	Molybdate-binding protein	294			
	Swol_1822	Formate dehydrogenase formation protein FdhE	256			
fdhV	Swol_1823	Formate dehydrogenase, cyt B556 subunit	219		Yes	Yes (4)
	Swol_1824	Formate dehydrogenase (cyt b) iron-sulfur subunit	270		Yes	Yes (1)
	Swol_1825	Formate dehydrogenase (cyt b) major subunit	808	Formate ↔ MQ		
	Swol_1826	Formate dehydrogenase (cyt b) major subunit	196	Formate ↔ NADH	Yes	
	Swol_1827	Molybdopterin biosynthesis MoeA protein	412			
	Swol_1828	NADH-quinone oxidoreductase chain F	407			
	Swol_1829	NADH-quinone oxidoreductase chain E	148			
fdhVI	Swol_1830	Formate dehydrogenase alpha subunit	536			
	Swol_1831	NADH-ubiquinone oxidoreductase 75kDa subunit	363	Formate ↔ NADH		
	Swol_1832	Ferredoxin	158	ETF ↔ MQ? Or Fd?		
	Swol_1833	NADH dehydrogenase	412			
	Swol_1834	Ferredoxin	168			
	Swol_1835	Aldehyde ferredoxin oxidoreductase	629			

	Swol_2121	Electron transfer flavoprotein alpha subunit	311			
	Swol_2122	Electron transfer flavoprotein beta subunit	251			
fix	Swol_2123	FixX (ferredoxin)	94			
	Swol_2124	FixC (ETF:Quinone Oxidoreductase)	428	ETF ↔ MQ? Or Fd?	Yes	Yes (1)
	Swol_0696	Electron transfer flavoprotein, beta subunit	252	ETF ↔ MQ		
	Swol_0697	Electron transfer flavoprotein, alpha subunit	317			
fsr	Swol_0698	Iron-sulfur-binding reductase	714			Yes (6)
	Swol_1519	Cytochrome c assembly protein	255	ETF ↔ MQ	Yes	Yes (8)
	Swol_1520	ResB protein, cytochrome c biosynthesis-like protein	342		Yes	Yes (4)
CytC	Swol_1521	Respiratory nitrite reductase precursor	416		Yes	Yes (1)
	Swol_1522	Respiratory nitrite reductase specific kq--cyt-c reductase precursor	125		Yes	

Table 4S. List of genes involved in transport in *S. wolfei.*

Protein			Substrate	KEGG	PFAM	SigP	TMMH
The ATP-binding Cassette (ABC) Superfamily							
ABC	membrane	binding protein					
Swol_0323	Swol_0324	Swol_0325	?	K05833 K05832 K01989	00005 02653 04392	No No Yes	No Yes No
Swol_0664	Swol_0665		? (Fe-S assembly/SufBCD system)	K09013 K07033	00005 01458	No No	No No
Swol_0314	Swol_0315	Swol_0316	amino acid (glutamine/glutamate/ aspartate?)	K02028 K02029 K02030	00005 00528 00497	No Yes No	No Yes No
Swol_1059 Swol_1072	Swol_1071	Swol_1070	amino acid (glutamine/glutamate/ aspartate?)	K02028 K02028 K02029	00005 00005 00528 00497	No No No Yes	No No Yes Yes
Swol_1740	Swol_1739		amino aicd (glutamine/glutamate/ aspartate?)	K10041	00005 00528	No Yes	No Yes
Swol_2110	Swol_2111 Swol_2112	Swol_2113	branched-chain amino acid	K01995 K01998 K01997 K01999	00005 02653 02653 01094	No Yes No Yes	No Yes Yes Yes
Swol_2552 Swol_2553	Swol_2554 Swol_2555	Swol_2556	branched-chain amino acid	K01996 K01995 K01998 K01997 K01999	00005 00005 02653 02653 01094	No No Yes Yes Yes	No Yes No Yes No
Swol_0245	Swol_0246		cell division	K09812 K09811	00005 02687	No Yes	No Yes
Swol_1472	Swol_1473	Swol_1187	cobalamin/Fe3+-siderophores	K02013 K02015 K02016	00005 01032 01497	No No Yes	No No Yes
	Swol_1676	Swol_1673 Swol_1675 Swol_1679 Swol_2097 Swol_2486	cobalamin/Fe3+-siderophores	K02015 K02016 K02016 K02016 K02016 K02016	01032 01497 01497 01497 01497 01497	Yes Yes Yes Yes Yes Yes	Yes Yes Yes Yes No No

Swol_1694	Swol_1695	Swol_1687 Swol_1690 Swol_1691	cobalamin/Fe3+-siderophores	K02013 K02015 K02016	00005 01032 01497 01497 01497	No Yes Yes Yes Yes	No Yes Yes Yes Yes
Swol_1948 Swol_1949 Swol_1046	Swol_1045 Swol_1947		cobalt ion	K02008 K02006 K02006 K02006	00005 00005 00005 02361 02361	No No No No Yes	No No Yes No Yes
Swol_1951 Swol_1952	Swol_1950		cobalt ion	K02006 K02006 K02008	00005 00005 02361	No No No	No No Yes
Swol_2301 Swol_2302	Swol_2300		cobalt ion	K02006 K02006 K02008	00005 00005 02361	No No No	Yes Yes Yes
Swol_2430	Swol_2431	Swol_2432	D-methionine	K02071 K02072 K02073	00005 09383 00528 03180	NoNo Yes	NoYes No
		Swol_2012	dipeptide/oligopeptide	K02035	496	Yes	Yes
Swol_2457	Swol_2458		efflux (antimicrobial peptide)?	K02003 K02004	00005 02687	No No	Yes No
Swol_0941	Swol_0943		efflux (antimicrobial peptide?)	K02003 K02004	00005 02687	No Yes	No Yes
Swol_1683			efflux (antimicrobial peptide?)	K02004	5	No	No
Swol_1715	Swol_1714		efflux (antimicrobial peptide?)	K02003 K02004	00005 02687	No Yes	No Yes
Swol_2094			efflux (antimicrobial peptide?)	K02004	5	No	No
Swol_1737	Swol_1736	Swol_1738	glycine betaine/L-proline	K02000 K02001 K02002	00528 00005 04069	No No Yes	Yes No No
Swol_2478	Swol_2477	Swol_1685 Swol_2476	iron(III)	K02011 K02010 K02012	00005 00528 01547 01547	No Yes No Yes	No Yes No No
Swol_2481	Swol_2480	Swol_2479	iron(III)	K02011 K02010 K02012	00005 00528 01547	No No Yes	Yes No Yes
Swol_1890	Swol_1889	Swol_1891	manganese/zinc ion	K09816 K09817 K09815	00950 00005 01297	Yes No Yes	Yes No No

Swol_1554	Swol_1555	Swol_1556	molybdate	K02018 K02018 K02020	00005 00528 01547	No Yes Yes	No Yes No
Swol_0180	Swol_0181 Swol_0182		multidrug	K09687 K01990 K09686	00005 01061 01061	No Yes No	No Yes Yes
Swol_1367			multidrug	K09697	5	No	No
Swol_1383	Swol_1384		multidrug	K01990	5	No Yes	No Yes
Swol_1620			multidrug	K01990	5	No	No
Swol_1723	Swol_1722		multidrug	K09687 K09686	00005 01061	No Yes	No Yes
Swol_2038	Swol_2039		multidrug	K01990 K01992	5	No Yes	No Yes
Swol_2243	Swol_2242		multidrug	K09687 K09686	5	No Yes	Yes No
Swol_2447 Swol_2448	Swol_2449		multidrug	K09687 K01990 K09686	00005 00005 01061	No No Yes	No No Yes
Swol_0339	Swol_0340	Swol_0341	nitrate/sulfonate/taurine	K02049 K02050 K02051	00005 00528	No Yes Yes	No Yes Yes
	Swol_2228	Swol_2227	sugar	K02057	2653	Yes No	Yes No
Swol_0409	Swol_0403 Swol_0404	Swol_0405	sugar (glycerol-3-phosphate?)	K10112 K02026 K02025 K02027	00005 08402 00528 00528	No YesYes	No YesYes
Swol_0414	Swol_0415 Swol_0416		sugar (ribose?)	K02056	00005 02653 02653	No No Yes	No Yes Yes
Swol_0426	Swol_0424 Swol_0425	Swol_0423	sugar (ribose?)	K10441 K10440 K10440 K10555	00005 02653 02653 00532	No Yes Yes Yes	No Yes Yes No
	Swol_2230* Swol_2231*		toxin secretion	K06148 K11085	00005 00664 03412 00005	No No	Yes Yes
Swol_1631	Swol_1632	Swol_1630	tungsten	K02036	00005 00528 08239	Yes No Yes	Yes No Yes

The Arsenite-Antimonite (ArsAB) Efflux Family

Swol_0938	583	arsenite (ArsA)	K01551	2374	No	No
The H+- or Na+-translocating F-type V-type and A-type ATPase (F-ATPase) Superfamily						
Swol_2381	137	protons	K02114	2823	No	No
Swol_2382	476	protons	K02112	00006 00306 02874	No	No
Swol_2383	298	protons	K02115	231	No	No
Swol_2384	504	protons	K02111	00006 00306 09378	No	No
Swol_2385	182	protons	K02113	213	No	No
Swol_2386	173	protons	K02109	430	Yes	Yes
Swol_2387	72	protons	K02110	137	Yes	Yes
Swol_2388	227	protons	K02108	119	No	Yes
The H+-translocating Pyrophosphatase (H+-PPase) Family						
Swol_1064	820	proton-translocating pyrophosphatase	K01507	3030	Yes	Yes
The Type II (General) Secretory Pathway (IISP) Family						
Swol_0777	305	signal recognition particle-docking protein FtsY	K03110	00448 02881	No	No
Swol_1498	448	signal recognition particle protein Ffh/SRP54	K03106	00448 02881 02978	No	No
Swol_2313	421	preprotein translocase SecY	K03076	344	Yes	Yes
The P-type ATPase (P-ATPase) Superfamily						
Swol_0623	870	calcium ion	K01529	00122 00689 00690 00702	No	Yes
Swol_1240	903	calcium ion	K01529	00122 00689 00690 00702	No	Yes
Swol_1698	799	copper ion	K01533	00122 00403 00702	No	Yes

Swol_2086	735	calcium ion	K01529	00122 00403 00702	No	Yes
Ion Channels						
The Large Conductance Mechanosensitive Ion Channel (MscL) Family						
Swol_1671	150	large-conductance mechanosensitive ion channel	K03282	1741	Yes	Yes
The Small Conductance Mechanosensitive Ion Channel (MscS) Family						
Swol_1154	363	small-conductance mechanosensitive ion channel		924	No	Yes
The Voltage-gated Ion Channel (VIC) Superfamily						
Swol_0914	450	potassium ion channel	K03499	02080 02254	Yes	No
Secondary Transporter						
The Arsenical Resistance-3 (ACR3) Family						
Swol_0939	358	arsenite	K03325	1758	Yes	Yes
The Amino Acid-Polyamine-Organocation (APC) Family						
Swol_0074	365	spore germination protein (amino acid permease)		3845	Yes	Yes
Swol_0079	374	spore germination protein (amino acid permease)		3845	Yes	Yes
Swol_1192	366	spore germination protein (amino acid permease)		3845	Yes	Yes
The Ca2+:Cation Antiporter (CaCA) Family						
Swol_0654	336	sodium ion:calcium ion antiporter	K07301	1699	Yes	Yes
The Cation Diffusion Facilitator (CDF) Family						
Swol_1051	319	cation efflux		1545	No	Yes
The Monovalent Cation:Proton Antiporter-1 (CPA1) Family						
Swol_1590	498	sodium ion:proton antiporter	K11105	00999 02080	Yes	Yes
The Monovalent Cation:Proton Antiporter-2 (CPA2) Family						

Swol_1178	650	potassium ion efflux	K03455	00999 02080 02254	Yes	Yes
The Dicarboxylate/Amino Acid:Cation (Na+ or H+) Symporter (DAACS) Family						
Swol_0311	539	proton/sodium ion:glutamate/aspartate symporter	K11102	375	No	Yes
The Divalent Anion:Na+ Symporter (DASS) Family						
Swol_2091	423	sodium ion:anion symporter		3600	Yes	Yes
Swol_2166	423	sodium ion:anion symporter		3600	No	Yes
The Drug/Metabolite Transporter (DMT) Superfamily						
Swol_0129	151	multidrug efflux (SMR subfamily)		6695	Yes	Yes
Swol_0960	296	drug/metabolite?		892	No	Yes
Swol_1359	159	drug/metabolite?		892	Yes	Yes
Swol_2109	295	drug/metabolite?		892	Yes	Yes
The Formate-Nitrite Transporter (FNT) Family						
Swol_0091	293	formate/nitrite	K06212	1226	No	Yes
The Branched Chain Amino Acid Exporter (LIV-E) Family						
Swol_0922	229	branched-chain amino acid efflux (AzlD)		3591	Yes	Yes
The Major Facilitator Superfamily (MFS)						
Swol_1125	462	multidrug efflux (EmrB/QacA subfamily)		7690	Yes	Yes
Swol_1354	370	multidrug efflux (Bcr/CflA subfamily)	K08153	7690	No	Yes
Swol_1903	398	multidrug efflux			Yes	Yes
Swol_2172	401	multidrug efflux		7690	Yes	Yes
Swol_2240	411	D-galactonate?		7690	No	Yes
The Multidrug/Oligosaccharidyl-lipid/Polysaccharide (MOP) Flippase Superfamily						
Swol_0081	517	polysaccharide export	K06409	01943 03023	No	Yes
Swol_0122	496	virulence factor MviN	K03980	3023	Yes	Yes

Swol_0313	455	multidrug efflux		1554	Yes	Yes
Swol_0575	459	multidrug efflux		1554	No	Yes
Swol_0722	430	polysaccharide export		1554	Yes	Yes
Swol_1584	521	virulence factor MviN	K03980	3023	Yes	Yes
Swol_1820	461	multidrug efflux		1554	No	Yes
Swol_2061	560	multidrug efflux		1554	Yes	Yes
The Nucleobase:Cation Symporter-1 (NCS1) Family						
Swol_1416	189	cytosine/purines/uracil/thiamine/allantoin	K03457	9350	No	No
The Inorganic Phosphate Transporter (PiT) Family						
Swol_1646	329	phosphate	K03306	1384	Yes	Yes
The Resistance to Homoserine/Threonine (RhtB) Family						
Swol_2082	246	amino acid efflux		1810	Yes	Yes
The Resistance-Nodulation-Cell Division (RND) Superfamily						
Swol_0176	1034	multidrug/solvent efflux (HAE1 subfamily)	K03296	873	No	Yes
Swol_1118	1009	multidrug/solvent efflux (HAE1 subfamily)		873	Yes	Yes
Swol_1424	280	protein export (SecDF)	K03074	02355 07549	Yes	Yes
Swol_1425	403	protein export (SecDF)	K03072	02355 07549	Yes	Yes
The Twin Arginine Targeting (Tat) Family						
Swol_0681	283	protein export	K03118	902	Yes	Yes
Swol_0682	60	protein export	K03118	2416	Yes	Yes
Swol_1443	110	protein export	K03118	2416	Yes	Yes
The Tripartite ATP-independent Periplasmic Transporter (TRAP-T) Family						
Swol_0329	437	C4-dicarboxylate		6808	Yes	Yes
Swol_0330	163	C4-dicarboxylate		4290	No	Yes
Swol_0331	371	C4-dicarboxylate		3480	Yes	Yes
The K+ Transporter (Trk) Family						
Swol_0913	482	potassium ion uptake	K03498	2386	Yes	Yes

The Zinc (Zn2+)-Iron (Fe2+) Permease (ZIP) Family						
Swol_1139	237	zinc ion	K07238	2535	Yes	Yes
Unclassified						
The Ferrous Iron Uptake (FeoB) Family						
Swol_0661	601	ferrous ion	K04759	01926 07670	No	Yes
Swol_1325	441	ferrous ion	K03977	1926	Yes	No
Swol_1537	78	ferrous ion	K04759	4023	No	No
Swol_1538	259	ferrous ion	K04759	1926	No	No
Swol_1539	464	ferrous ion	K04759	02421 07664 07670	Yes	Yes
The Mg2+ Transporter-E (MgtE) Family						
Swol_1082	447	magnesium ion	K06213	00571 01769 03448	No	Yes

* contains both an ABC and a membrane domain as one polypeptide

Table 5S. List of sigma factor genes in *S. wolfei.*

Locus Tag	Product Name	AA Seq Length
Swol_0087	sigma-24 subunit, (FecI-like)	38
Swol_2058	sigma-24 subunit, RpoE	173
Swol_1791	sigma-24 subunit, RpoE	189
Swol_1212	sigma-24 subunit, RpoE	192
Swol_2019	sigma-24 subunit, RpoE	193
Swol_0132	sigma-24 subunit, RpoE	194
Swol_2523	sigma-24 subunit, RpoE	206
Swol_0517	sigma-27/28 subunit, RpsK/SigK	244
Swol_0501	sigma-28 subunit, (flagella/sporulation)	126
Swol_0615	sigma-28 subunit, RpoX/SigF	243
Swol_0878	sigma-28 subunit, SigD/FliA/WhiG	260
Swol_0835	sigma-29 subunit, SigE	240
Swol_2351	sigma-30 subunit, SigH	216
Swol_0944	sigma-54 factor, RpoN	259
Swol_0265	sigma-54 subunit, RpoN/SigL	461
Swol_1507	sigma-70 subunit, RpoD	358
Swol_0836	sigma-70 subunit, RpsG/SigG	234

Table 6S. List of genes involved in motility and chemotaxis in *S. wolfei.*

Locus Tag	Product Name	AA Seq Length	Signal Peptide	Trans-membrane Helices
Swol_0353	CheA signal transduction histidine kinase	1023	Yes	Yes
Swol_0874	CheA signal transduction histidine kinase	677	No	No
Swol_1332	CheA signal transduction histidine kinase	511	No	No
Swol_1455	CheA signal transduction histidine kinase	927	No	No
Swol_0873	CheB Protein-glutamate methylesterase	352	No	No
Swol_1329	CheB Protein-glutamate methylesterase	341	Yes	No
Swol_1449	CheB Protein-glutamate methylesterase	353	No	No
Swol_0335	CheC inhibitor of MCP methylation	214	No	No
Swol_0862	CheC inhibitor of MCP methylation	398	No	No
Swol_0876	CheC inhibitor of MCP methylation	208	No	No
Swol_0877	CheD	161	No	No
Swol_0695	CheR MCP methyltransferase	259	No	No
Swol_1330	CheR MCP methyltransferase	270	No	No
Swol_1457	CheR MCP methyltransferase	276	No	No
Swol_0875	CheW protein	154	No	No
Swol_1450	CheW protein	518	No	No
Swol_1886	CheW protein	159	No	No
Swol_1446	CheX protein	152	No	No
Swol_0864	CheY Chemotaxis protein	210	Yes	Yes
Swol_0613	Anti-anti-sigma regulatory factor	110	No	No
Swol_0614	Anti-sigma regulatory factor	148	No	No
Swol_0190	Anti-sigma-28 factor, FlgM	97	No	No
Swol_0857	Basal-body rod modification protein flgD	98	No	No
Swol_1447	Chemotaxis operon protein	158	No	No
Swol_0869	Flagella-associated protein	686	No	Yes

Swol_0847	Flagellar basal body rod protein	155	No	No
Swol_2373	Flagellar basal-body rod protein (flgG-2)	246	No	No
Swol_0846	Flagellar basal-body rod protein flgB	138	No	No
Swol_0947	Flagellar basal-body rod protein FlgG	261	Yes	No
Swol_1476	Flagellar biosynthesis	89	No	No
Swol_0870	Flagellar biosynthesis protein flhF	395	No	No
Swol_0868	Flagellar biosynthesis/type III secretory pathway protein	369	No	Yes
Swol_0851	Flagellar biosynthesis/type III secretory pathway protein	280	No	No
Swol_0865	Flagellar biosynthetic protein	240	Yes	Yes
Swol_0866	Flagellar biosynthetic protein fliQ	90	Yes	Yes
Swol_0867	Flagellar biosynthetic protein FliR	253	Yes	Yes
Swol_0197	Flagellar capping protein-like protein	893	No	No
Swol_0861	Flagellar fliL protein	328	Yes	No
Swol_0856	Flagellar hook capping protein-like protein	180	No	No
Swol_0858	Flagellar hook protein	475	No	No
Swol_0859	Flagellar hook protein flgE	73	Yes	No
Swol_0192	Flagellar hook-associated protein-like protein	838	Yes	No
Swol_0848	Flagellar hook-basal body protein	102	No	No
Swol_0855	Flagellar hook-length control protein-like protein	723	No	No
Swol_0849	Flagellar M-ring protein FliF	540	No	Yes
Swol_0853	Flagellar motor switch protein fliG	149	No	No
Swol_0189	Flagellar protein	139	No	No
Swol_0860	Flagellar protein (FliL)-like protein	159	No	Yes
Swol_0193	Flagellin and related hook-associated protein	870	No	No
Swol_0198	Flagellin and related hook-associated protein	936	No	No
Swol_0232	Flagellin-specific chaperone FliS-like	168	No	No

	protein			
Swol_0854	Flagellum-specific ATP synthase	200	Yes	Yes
Swol_0191	FlgN family protein	170	No	No
Swol_0872	Glycosyltransferase-like protein	219	No	No
Swol_0365	Methyl-accepting chemotaxis sensory transducer	548	Yes	Yes
Swol_0927	Methyl-accepting chemotaxis sensory transducer	572	Yes	Yes
Swol_1451	Methyl-accepting chemotaxis sensory transducer	648	No	No
Swol_1840	Methyl-accepting chemotaxis sensory transducer	415	No	No
Swol_2151	Methyl-accepting chemotaxis sensory transducer	656	Yes	Yes
Swol_2152	Methyl-accepting chemotaxis sensory transducer	655	Yes	Yes
Swol_2162	Methyl-accepting chemotaxis sensory transducer	665	Yes	Yes
Swol_0971	Methyl-accepting chemotaxis sensory transducer	777	Yes	Yes
Swol_1331	Methyl-accepting chemotaxis sensory transducer	370	No	No
Swol_0871	ParA protein	300	No	No
Swol_2362	Pili retraction protein PilT	366	Yes	Yes
Swol_0525	Pilin assembly protein	132	No	No
Swol_0226	PilT-like protein	145	No	No
Swol_1837	PilT-like protein	153	No	No
Swol_2474	PilT-like protein	141	No	No
Swol_1570	PilT-like protein	142	No	No
Swol_0863	Response regulator receiver protein	120	No	No
Swol_1448	Response regulator receiver protein	129	No	No
Swol_1456	Response regulator receiver protein	124	No	No
Swol_0517	RNA polymerase, sigma 27/28 subunit,	244	Yes	Yes

	RpsK/SigK			
Swol_0878	RNA polymerase, sigma 28 subunit, SigD/FliA/WhiG	260	No	No
Swol_0615	RNA polymerase, sigma subunit, RpoX/SigF	243	No	No
Swol_0501	Sigma 28 (flagella/sporulation)	126	Yes	Yes
Swol_0539	Tfp pilus assembly protein ATPase PilM-like protein	353	No	No
Swol_0538	Type 4 prepilin peptidase 1, Aspartic peptidase. MEROPS family A24A	250	Yes	Yes
Swol_0852	Type III secretion system ATPase, FliI/YscN	442	No	No

Table 7S. List of genes involved in sporulation in *S. wolfei.*

Locus Tag	JGI Annotation	Gene Description
Swol_0591	hypothetical protein	Stage 0 sporulation protein A
Swol_1795	anti-anti-sigma regulatory factor, SpoIIAA	Anti-anti-sigma regulatory factor, SpoIIAA
Swol_2062	anti-sigma F factor antagonist (stage II sporulation protein AA)	Stage II sporulation protein AA
Swol_2376	stage II sporulation protein D	Stage II sporulation protein D
Swol_1127	putative stage II sporulation protein P	Stage II sporulation protein P
Swol_0093	Phosphoprotein phosphatase	Stage II sporulation protein E
Swol_0605	uncharacterized membrane protein	Stage II sporulation protein M
Swol_1127	putative stage II sporulation protein P	Stage II sporulation protein P
Swol_1339	putative stage II sporulation protein P	Stage II sporulation protein P
Swol_1586	hypothetical protein	Stage II sporulation protein P
Swol_1885	phosphopantetheinyl transferase	Stage II sporulation protein P
Swol_0550	stage III sporulation protein spoIIIAA	Stage III sporulation protein AA
Swol_0551	hypothetical protein	Stage III sporulation protein AB
Swol_0552	hypothetical protein	Stage III sporulation protein AC
Swol_0553	putative sporulation protein	Stage III sporulation protein AD
Swol_0554	hypothetical protein	Stage III sporulation protein AE
Swol_0555	hypothetical protein	Stage III sporulation protein AG
Swol_2375	stage III sporulation protein D	Stage III sporulation protein D
Swol_1322	hypothetical protein	Stage IV sporulation protein A
Swol_0590	response regulator receiver protein	Stage IV sporulation protein B

Swol_1567	putative stage IV sporulation YqfD	Stage IV sporulation YqfD
Swol_0626	spore formation protein spoVAC	Stage V sporulation protein AC
Swol_0627	stage V sporulation AD	Stage V sporulation protein AD
Swol_0628	SpoVA protein	Stage V sporulation protein AE
Swol_0629	GerA spore germination protein	Stage V sporulation protein AF
Swol_0081	stage V sporulation protein B	Stage V sporulation protein B
Swol_0983	SpoVK	Stage V sporulation protein K
Swol_1250	stage V sporulation protein S	Stage V sporulation protein S
Swol_0080	transcriptional regulator, AbrB family	Stage V sporulation protein T
Swol_0086	hypothetical protein	Spore cortex biosynthesis protein
Swol_0201	hypothetical protein	Spore coat polysaccharide biosynthesis protein spsF
Swol_0212	glycosyltransferase	Spore coat polysaccharide biosynthesis protein spsG
Swol_0760	small acid-soluble spore protein	Small acid-soluble spore protein
Swol_2045	small acid-soluble spore protein	Small acid-soluble spore protein
Swol_1413	nucleoside recognition proteinn	Spore maturation protein A
Swol_1412	nucleoside recognition proteinn	Spore maturation protein B
Swol_1194	grkA; spore germination protein, GrkA	Spore germination protein KA
Swol_0078	germination protein	Spore germination protein KA
Swol_1192	hypothetical protein	Spore germination protein KB
Swol_0079	hypothetical protein	Spore germination protein KB
Swol_1193	hypothetical protein	Spore germination protein KC
Swol_0076	hypothetical protein	Spore germination protein KC
Swol_0077	hypothetical protein	Spore germination protein KC
Swol_0834	peptidase U4, sporulation	Sporulation sigma-E factor

	factor SpoIIGA	processing peptidase
Swol_0835	sporulation sigma factor SigE	RNA polymerase sigma-E factor
Swol_0836	RNA polymerase sigma-G factor	RNA polymerase sigma-G factor
Swol_0063	pro-sigma-E processing factor spoIIR	Pro-sigma-E processing factor spoIIR
Swol_0501	sigma 28 (flagella/sporulation)	Sigma 28 (flagella/sporulation)
Swol_0517	RNA polymerase, sigma 27/28 subunit, RpsK/SigK	RNA polymerase, sigma 27/28 subunit, RpsK/SigK
Swol_0615	sigma 28 (flagella/sporulation)	Sigma 28 (flagella/sporulation)
Swol_1609	spo0B-associated GTP-binding protein	spo0B-associated GTP-binding protein
Swol_1976	regulators of stationary/sporulation gene expression	Regulators of stationary/sporulation gene expression
Swol_2107	rRNA methylase (SpoU class)	rRNA methylase (SpoU class)
Swol_2108	sporulation protein and related proteins	Sporulation protein and related proteins
Swol_0761	GPR endopeptidase	Spore protease
Swol_1052	Spore germination protein-like protein	Sporulation kinase
Swol_1838	hypothetical protein	Spore photoproduct lyase
Swol_1871	glycosyl hydrolase-like protein	Spore peptidoglycan hydrolase (N-acetylglucosaminidase)
Swol_1976	regulators of stationary/sporulation gene expression	Regulators of stationary/sporulation gene expression

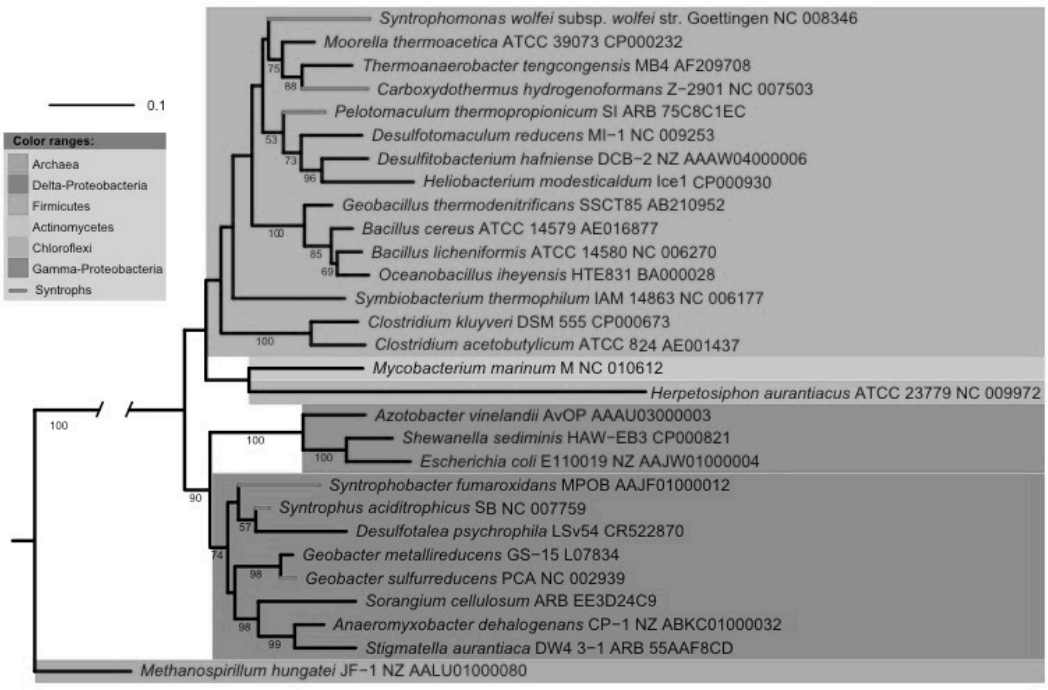


Figure 1S. Phylogeny of *S. wolfei*. A maximum likelihood dendrogram of syntrophic and non-syntrophic species was generated using near full length, aligned 16S rRNA genes downloaded from the Greengenes database (DeSantis et al., 2006). A bootstrapped (100 reps) maximum likelihood dendrogram was generated using the RAxML algorithm (Stamatakis et al., 2008) as implemented online by the CIPRES Portal (Miller et al., 2009).

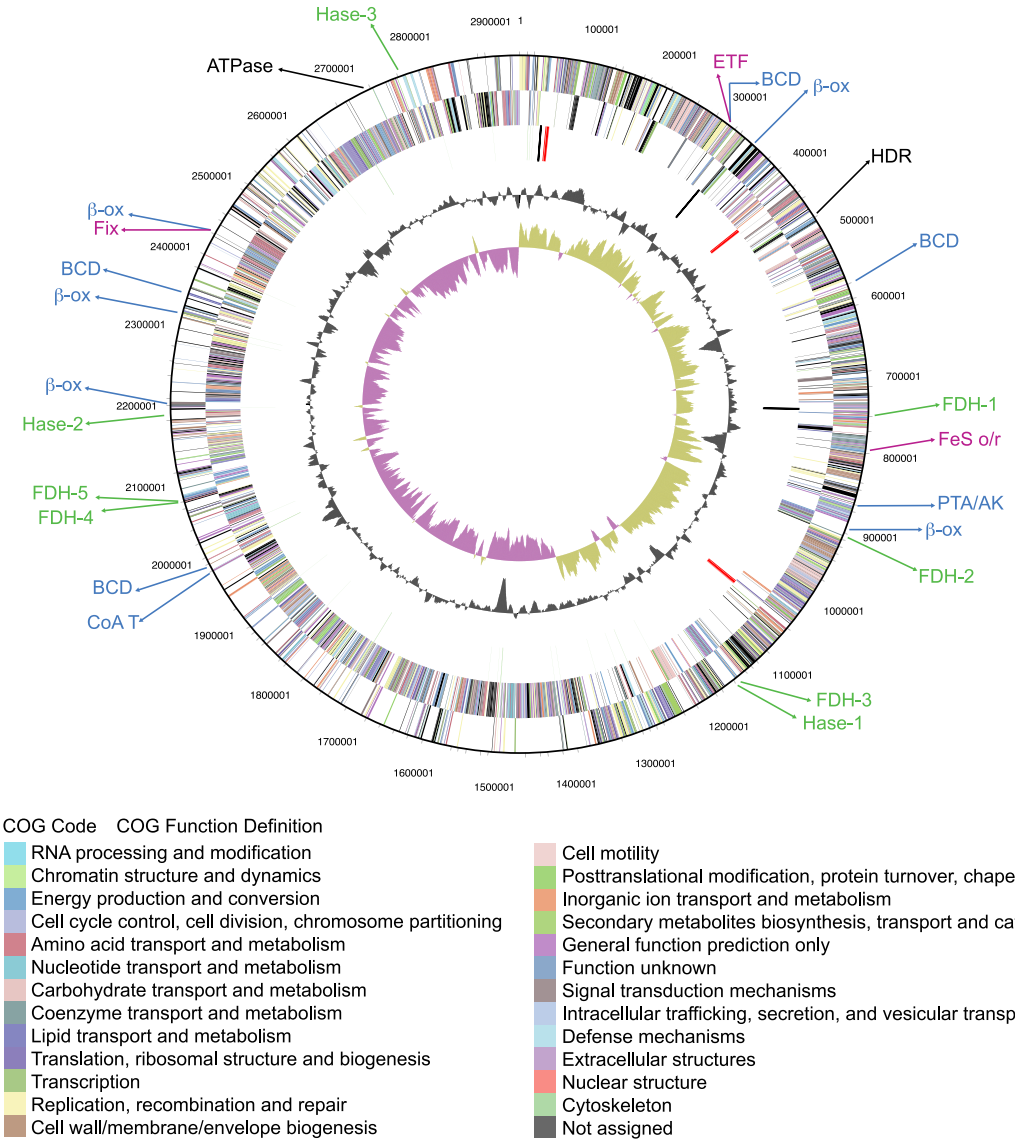


Figure 2S. Circular representation of the *S. wolfei* genome. The concentric circles (from outside to inside) indicate: ORFs on the forward (circle 1) and reverse (circle 2) strands (each colored by COG categories); RNA genes (tRNA genes in green, sRNA genes in red, and other RNA genes in black) (circle 3); G+C content (circle 4); and G + C skew (circle 5). Key genes are shown on the outside, Hydrogenases and Formate dehydrogenases in green, β-oxidation genes in blue, genes potentially involved in reverse electron transfer in pink, and ATPase and HDR in black.

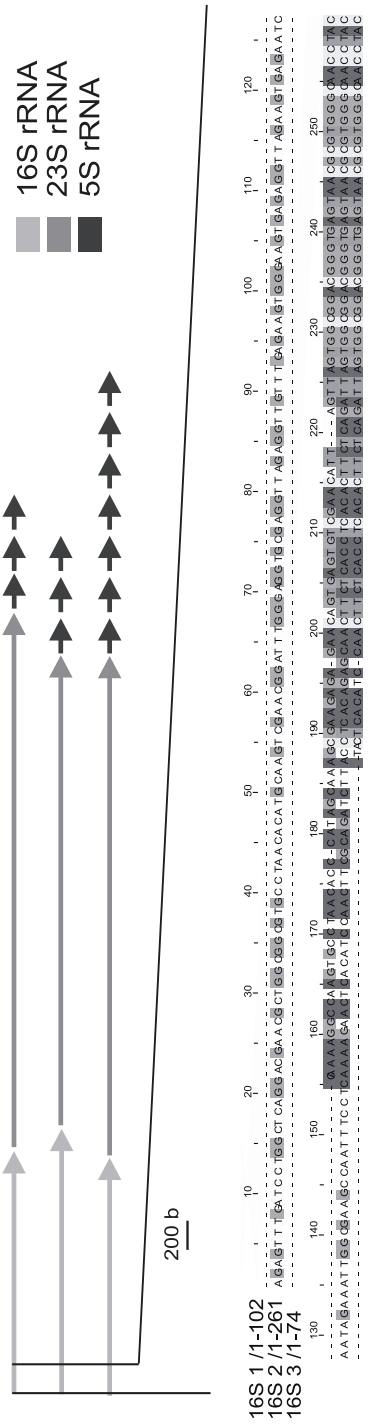


Figure 3S. Ribosomal RNA gene clusters of *S. wolfei*. The enlarged area shows the alignment of the initial portions of the three 16S rRNA genes.

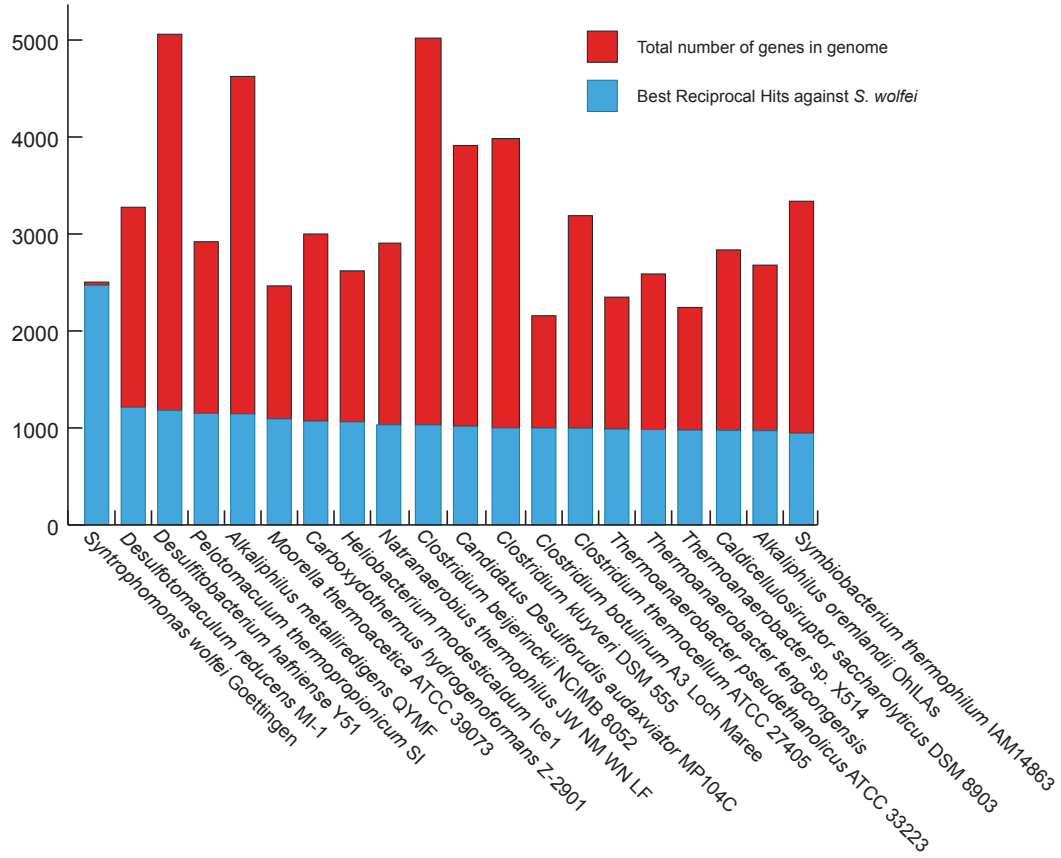


Figure 4S. Best reciprocal protein hits for *S. wolfei* ORFs with other genomes.

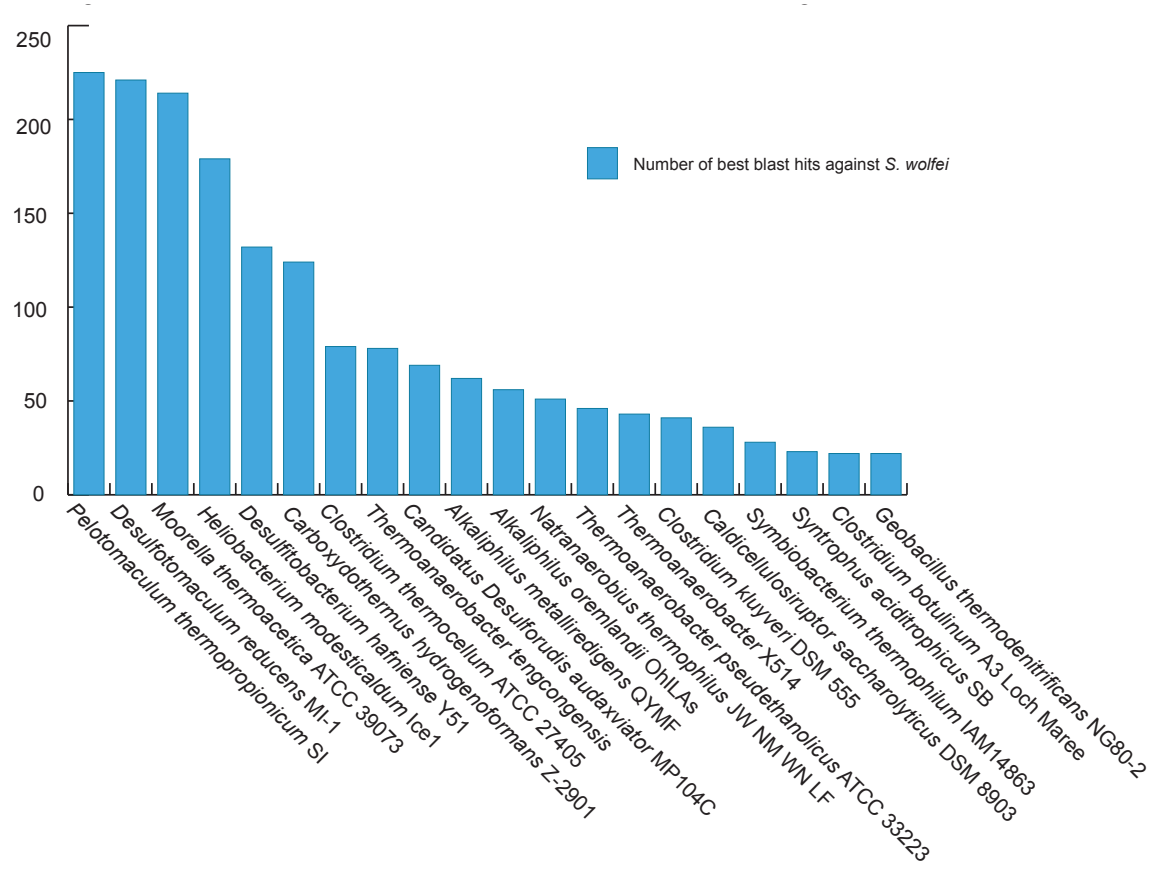


Figure 5S. Best Blast hit distribution of *S. wolfei* ORFs with other genomes.

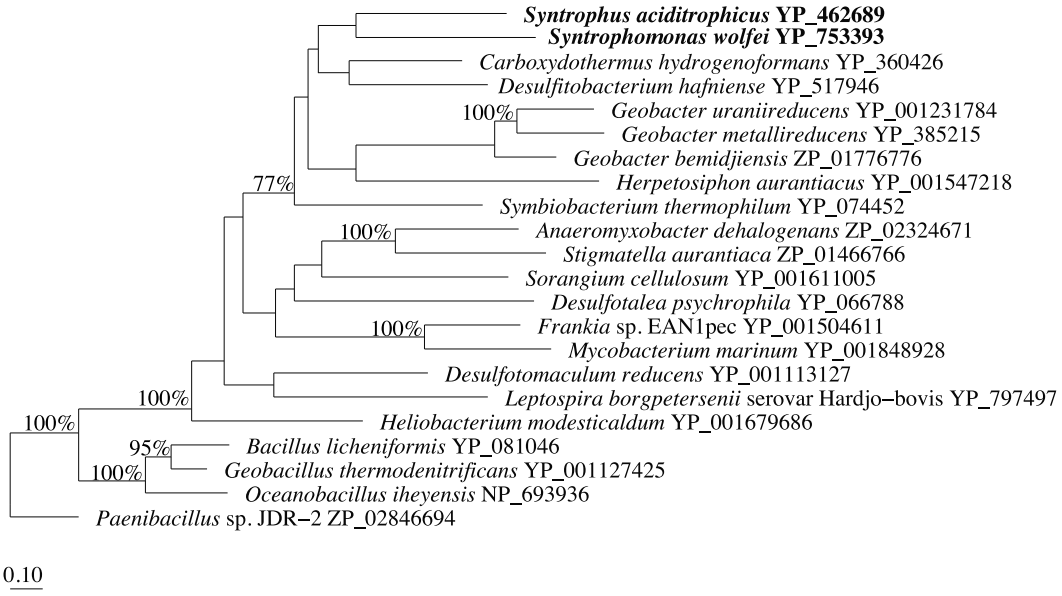


Figure 6S. Phylogenetic analysis of predicted coding sequences of the membrane-bound FeS oxidoreductase potentially involved in reverse electron transfer in *S. wolfei*. Similar protein coding genes of interest were identified, translated, and downloaded from the Integrated Microbial Genomes (IMG) database. Amino Acid sequences were aligned using ProbCons (Do et al., 2005) and databases were created using ARB (Ludwig et al., 2004). Sequences were exported and Maximum Likelihood trees were created (using the Jones-Taylor-Thornton probability model) and bootstrapped 100 times using the PHYLIP phylogenetic package (Felsenstein, 1989). Bootstrap values are given above each node only for values greater than 50%.

CHAPTER III

PROTEOMIC ANALYSIS OF THE SYNTROPHIC, FATTY ACID-OXIDIZING ORGANISM, *SYNTROPHOMONAS WOLFEI*

SUMMARY

Metabolic cooperation, termed syntrophy, is vital to the anaerobic carbon cycle. Multiple organisms interact to catalyze key degradative reactions such as fatty acid metabolism by exchanging interspecies electron carriers such as H_2 and formate at low concentrations. Syntrophic fatty acid degradation by *Syntrophomonas wolfei*, a fatty acid oxidizer, and *Methanospirillum hungatei*, a hydrogenotrophic methanogen, serves as a model for syntrophy in methanogenic ecosystems. The proteome of *S. wolfei* grown axenically on crotonate and syntrophically with *M. hungatei* with crotonate and butyrate was analyzed to determine proteins involved in key redox and energy conservation reactions necessary for syntrophy. Proteomic analysis identified a total of ~1090 polypeptides. Thirty-four polypeptides, including a zinc-dependent dehydrogenase with a GroES domain, were detected only in syntrophically grown *S. wolfei* (*e.g.* in coculture with *M. hungatei* on butyrate or crotonate). Multiple systems for interspecies electron transfer and reverse electron transfer including a confurcating hydrogenase, a putative membrane-bound hydrogenase, and a novel FeS oxidoreductase thought to serve as an electron transfer flavoprotein (ETF):quinone oxidoreductase were also detected. β-oxidation enzymes and ETF were detected in each growth condition. Under syntrophic conditions, the abundance of proteins involved in coenzyme and amino acid transport as well as metabolism increased while crotonate axenic conditions saw increased abundance in proteins involved in lipid transport and

metabolism. This work demonstrates that *S. wolfei* expresses multiple enzyme systems for fatty acid metabolism, interspecies electron transfer, and energy conservation under all growth conditions.

INTRODUCTION

Metabolic cooperation is an essential process in the flow of carbon in anaerobic ecosystems (Schink, 2006; McInerney et al., 2008). A very important metabolic interaction is syntrophy where multiple organisms must rely on each other to maintain pool sizes of exchanged metabolites at appropriate levels so that the catabolic reactions are thermodynamically favorable. Syntrophy is essential for the degradation of fatty and aromatic acid, hydrocarbons, alcohols, and some organic and amino acids in methanogenic ecosystems (McInerney et al., 2008; Stams and Plugge, 2009).

One of the most well defined syntrophic partnerships is that of *Syntrophomonas wolfei*, a short chain fatty acid oxidizer, and *Methanospirillum hungatei* JF1, a hydrogen/formate-utilizing methanogen. In this interaction, *M. hungatei* maintains the concentrations of hydrogen and formate at very low levels, which makes butyrate degradation to acetate, hydrogen and formate by *S. wolfei* thermodynamically favorable (McInerney et al., 1979).

Table 1. Thermodynamics of syntrophic butyrate metabolism

Reaction	**$\Delta G^{o,\,a}$**
$Butyrate^- + 2\ H_2O \rightarrow 2\ Acetate^- + H^+ + 2\ H_2$	+ 48.6 kJ/mol
$4\ H_2 + HCO_3^- + H^+ \rightarrow CH_4 + 3\ H_2O$	-135.6 kJ/mol

[a] Calculated from the data in (Thauer et al., 1977)

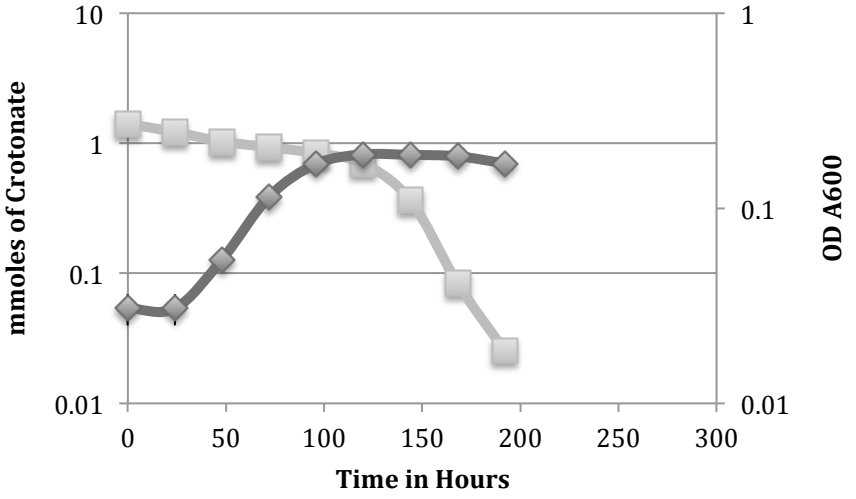
S. wolfei is a fermentative organism with a very limited substrate range. Unlike other organisms capable of syntrophy, *S. wolfei* does not use alternative electron acceptors such as sulfate like *Syntrophobacter fumaroxidans* (Harmsen et al., 1998) and various *Desulfovibrio* species, iron (III) like *Geobacter sulfurreducens* (Caccavo et al., 1994), or benzoate like *Syntrophus aciditrophicus* (Mouttaki et al., 2008). *S. wolfei* uses only C4-C8 unsaturated and saturated-fatty acids (McInerney et al., 1979; McInerney et al., 1981b). Saturated fatty acids like butyrate are degraded to acetate, hydrogen, and formate only during syntrophic growth with a H_2- and/or formate-using microorganism. *S. wolfei* can grow axenically with a few unsaturated fatty acids like crotonate, which are fermented to acetate and the corresponding saturated fatty acid (Beaty and McInerney, 1987; Amos and McInerney, 1990). Enzymatic analysis showed that *S. wolfei* uses the ß-oxidation pathway for fatty acid metabolism (Wofford et al., 1986) and requires an energized membrane for hydrogen production from butyrate (Wallrabenstein, 1994). However, little is known about the cellular machinery necessary for reverse electron transfer needed to drive hydrogen and formate production from electrons derived in β-

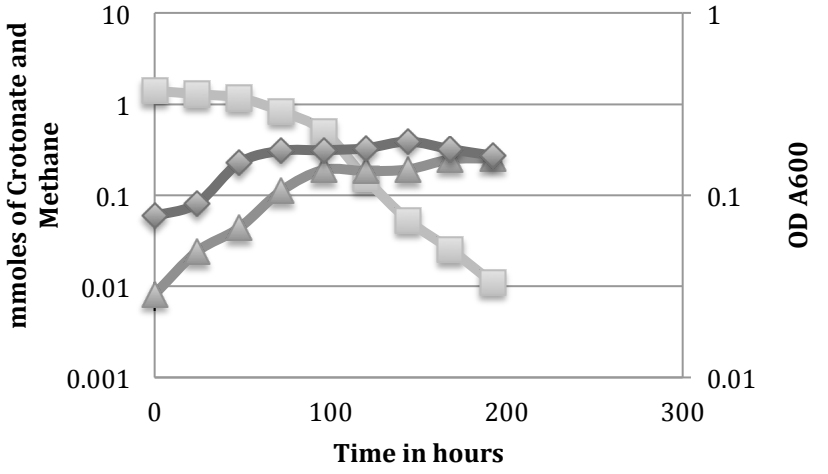
oxidation (Sieber et al., 2010b) and the mechanisms used by *S. wolfei* to initiate and maintain the syntrophic interaction with its partner.

The limited metabolic potential of *S. wolfei* makes it an ideal model organism for identifying the essential machinery of syntrophy, but makes it difficult to manipulate *S. wolfei* genetically. The genomes of *S. wolfei* (Sieber et al., 2010b) and *M. hungatei* (NCBI Reference Sequence: NC_007796) have been recently sequenced and annotated. Genomic analysis unveiled genetic systems for novel redox processes potentially important for syntrophy and opened the investigation of syntrophy to high-throughput analyses. To determine the enzyme systems used by *S. wolfei* for syntrophy, a parallel shotgun proteomic analysis of *S. wolfei* grown syntrophically with *M. hungatei* and *S. wolfei* grown axenically was conducted.

RESULTS AND DISCUSSION

For this proteomic study, *S. wolfei* was grown axenically (Fig. 1a) and syntrophically on crotonate (Fig. 1b) and syntrophically on butyrate (Fig 1c). Cells were harvested at 50% substrate loss, which was in the late exponential phase of growth as determined by change in absorbance for pure cultures and methane production for cocultures. Specific growth rate for *S. wolfei* pure culture was 0.024 h^{-1} and specific methane production rates for the *S. wolfei-M. hungatei* cocultures on crotonate and butyrate were 0.033 h^{-1} and 0.012 h^{-1}, respectively.


10
1
0.1
0.01
1
0.1
0.01
0
50
100
150
200
250
300
mmoles of Crotonate
OD A600
Time in Hours


10
1
0.1
0.01
0.001
1
0.1
0.01
0
100
200
300
mmoles of Crotonate and Methane
OD A600
Time in hours

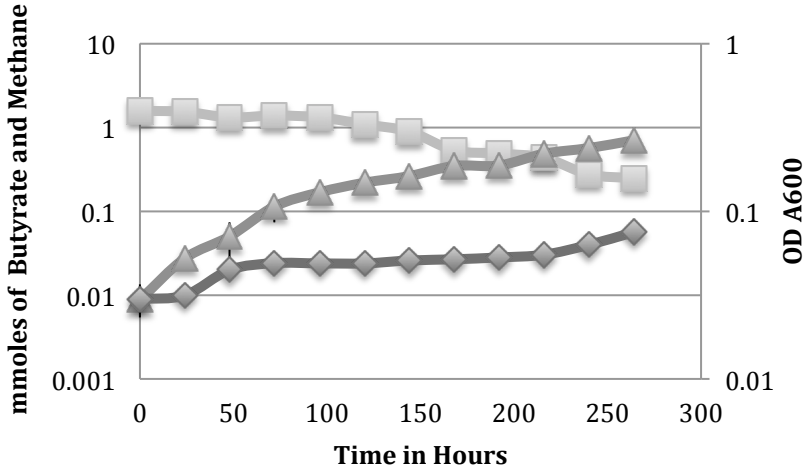

10
1
0.1
0.01
0.001
1
0.1
0.01
0
50
100
150
200
250
300
mmoles of Butyrate and Methane
OD A600
Time in Hours

Figure 1. Growth of *S. wolfei* in pure culture on crotonate (1a) and in coculture with *M. hungatei* on crotonate (1b) and butyrate (1c). squares indicate crotonate or butyrate; triangles are methane; and diamonds are absorbance. Means ± standard deviations of triplicate cultures; error bars are shown when the standard deviations were larger than width of the symbol.

The genome of *S. wolfei* contains 2574 protein encoding genes; the proteomic analysis detected 1090 unique proteins across the three conditions. Under axenic, crotonate-grown conditions, 912 proteins were detected of which 156 proteins were detected only under axenic conditions (Figure 2, Table 1S and Table 2S). When *S. wolfei* was grown on crotonate with *M. hungatei,* 656 proteins were detected of which 21 proteins were unique to this growth condition. Eight hundred and eighty-two proteins were detected in butyrate-grown cells with *M. hungatei* and 125 of those were only found in this growth condition. Five hundred and sixty-eight proteins were detected under all three conditions, of which 78 appear to be constitutively present (less than 0.5-fold change among all conditions). Only 34 proteins products were detected only during syntrophic growth regardless of substrate (Table 2). Three of the proteins detected only when the methanogen was present are predicted to contain transmembrane spanning helices: a ferrous iron transport gene (Swol_0661), a two-component response regulator (Swol_1041), and a formate dehydrogenase accessory protein (Swol_1030). Two proteins detected only when the methanogenic partner was present are predicted to contain signal peptides; one

with no known function (Swol_1906) and a protein involved in glycine cleavage (Swol_1982).

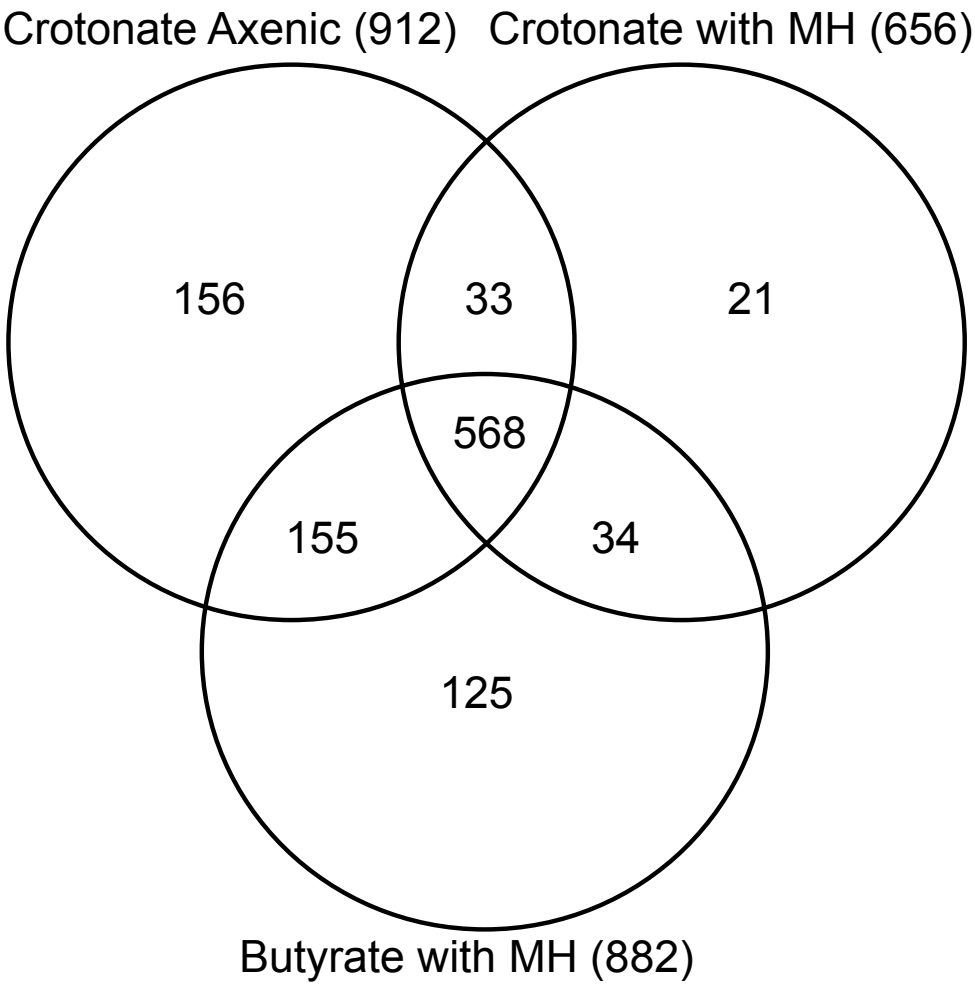


Figure 2. Number of proteins detected under each condition. Abbreviation: MH, *M. hungatei*.

Table 2. Abundance of proteins detected only during syntrophic growth with *M. hungatei* (JF1)

Locus Tag	Predicted Function	%NSAF Crotonate	%NSAF Butyrate
Swol_0001	Chromosomal replication initiator protein dnaA	0.016	0.029
Swol_0040	Thymidylate kinase	0.006	0.032
Swol_0393	DNA-damage-inducible protein J	0.015	0.017
Swol_0487	MaoC-like dehydratase	0.018	0.067
Swol_0488	Acyl-CoA dehydrogenase, short-chain specific	0.007	0.052
Swol_0660	Ferric uptake regulation protein	0.031	0.019
Swol_0661	Ferrous iron transport protein B	0.012	0.038
Swol_0715	Hypothetical protein	0.008	0.003
Swol_0746	Hypothetical protein	0.004	0.006
Swol_0780	L-fuculose phosphate aldolase	0.006	0.020
Swol_0819	S-adenosyl-methyltransferase mraW	0.008	0.005
Swol_0975	Hydantoinase/oxoprolinase family	0.034	0.035
Swol_1005	Hypothetical protein	0.015	0.017
Swol_1030	FdhD protein (fdsC)	0.030	0.068
Swol_1041	Two-component response regulator	0.007	0.014
Swol_1206	Transcriptional regulator, AsnC family	0.015	0.020
Swol_1241	Poly-β-hydroxyalkanoate polymerase subunit PhaC	0.027	0.020
Swol_1372	Hypothetical protein	0.027	0.055
Swol_1458	Site-specific recombinase	0.009	0.012
Swol_1528	Hypothetical protein	0.011	0.029
Swol_1647	Putative pit accessory protein	0.016	0.019
Swol_1727	Zn-dependent alcohol dehydrogenase	1.946	3.172
Swol_1760	Metal-dependent hydrolase	0.029	0.005
Swol_1857	Molybdopterin biosynthesis mog protein	0.011	0.024
Swol_1894	Metal-dependent phosphohydrolase	0.028	0.028
Swol_1906	Hypothetical protein	0.033	0.028
Swol_1935	3-hydroxybutyryl-CoA dehydrogenase	0.619	0.356
Swol_1936	3-hydroxybutyryl-CoA dehydratase	0.287	0.415
Swol_1938	Sensory transduction protein kinase	0.065	0.070
Swol_1982	Glycine cleavage system H protein	0.032	0.045
Swol_2174	Acetyltransferase, GNAT family	0.009	0.012
Swol_2364	Hypothetical protein	0.133	0.050
Swol_2365	Putative nucleic-acid-binding protein	0.005	0.006
Swol_2488	ATP-dependent endopeptidase Lon	0.002	0.003

To date attempts quantify the entire repertoire of genes/proteins for *S. wolfei* necessary for growth has not been attempted. Thus to visualize the similarity in global protein expression patterns under differing growth conditions, we chose to ordinate protein abundance patterns from the three growth conditions and their respective replicates using a nonmetric multidimensional scaling (NMDS) approach (Figure 3). NMDS has become a useful and highly used technique in ecological studies to help visualize abundance patterns of microbial communities. NMDS ordination showed that protein abundance from each growth condition was highly reproducible between the technical replicates from a single culture and between the biological replicates of a given growth condition. Despite the fact that all cultures shared a large proportion of the detected proteins (~50 %), the abundance patterns of proteins in each growth condition were very different from one another.

Bayesian Model Results

Models evaluated by baySeq revealed that much of the variance between growth conditions could be explained by a model that treated conditions independently (31%) and model that compared syntrophic growth on crotonate or butyrate to axenic growth on crotonate (29%). Interestingly these two models were able to explain nearly the same amount of variance within the dataset, suggesting that the expression profiles of genes under syntrophy are likely similar but different than axenic growth and that rare proteins expressed under specific syntrophic conditions are likely driving the variance detected

within the model. Much debate (Efron and Tibshirani, 2007; Efron, 2008) centers around whether large biological datasets, such as proteomes, follow traditional statistical assumption of a normal distribution. Thus utilization of a multiple T-Test method to extrapolate significance of differentially expressed proteins, which requires the assumption of a normal distribution and inflates type II statistical error, is potentially flawed. The empirical Bayesian method utilized by baySeq generates a distribution of genes/proteins within the dataset and seeks to find outliers "significant" genes from that distribution. Thus we feel that this method was robust and likely limits false discovery rate of significant proteins.

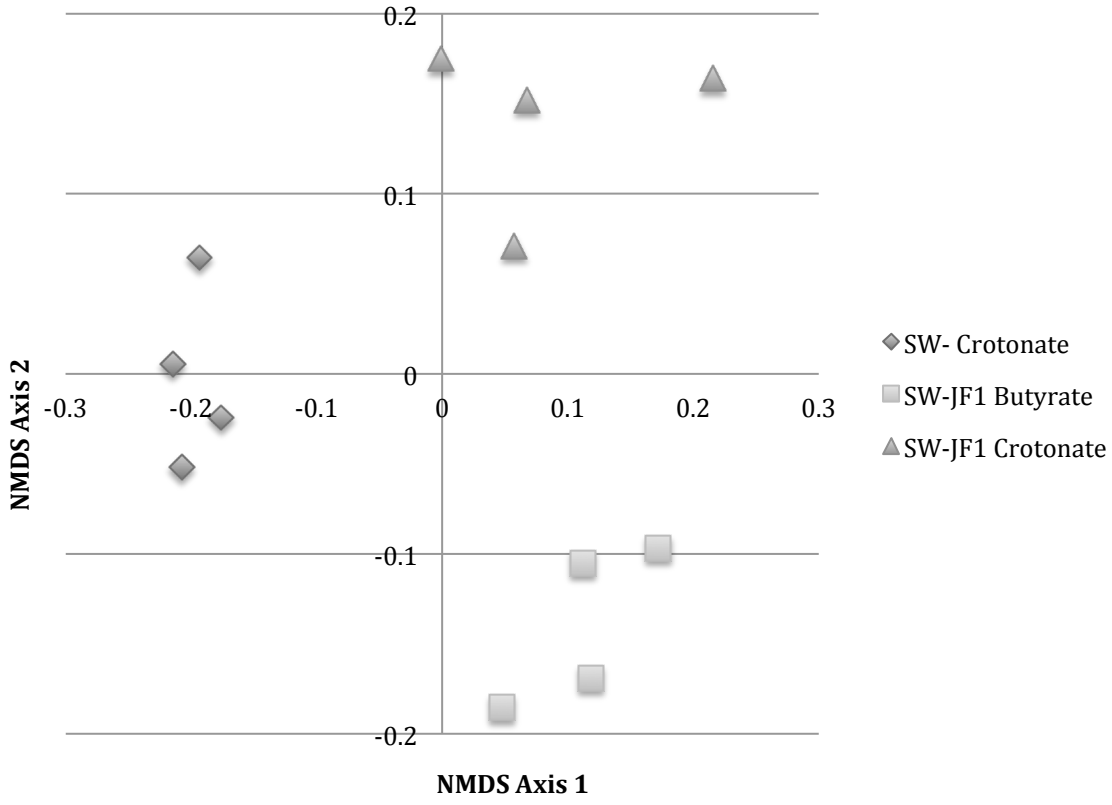
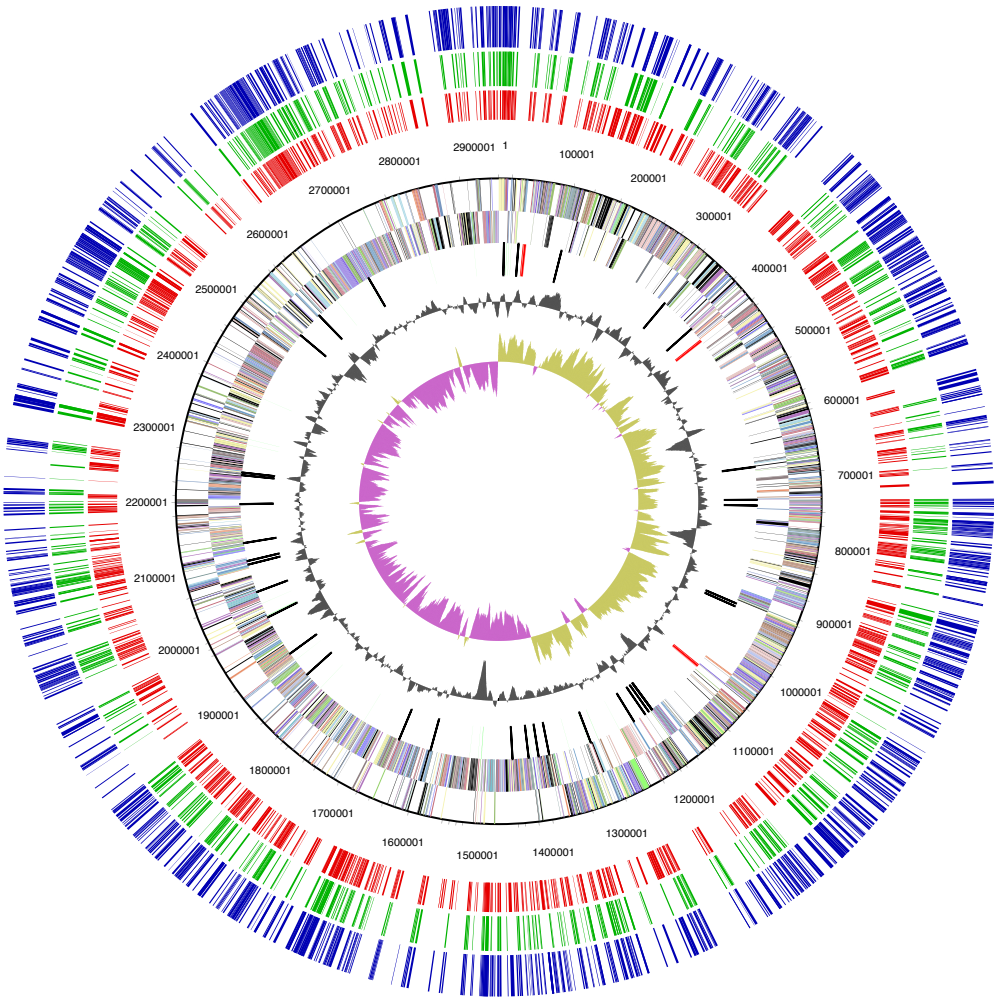


Figure 3. Nonmetric multidimentional scaling of the *S. wolfei* protein profiles obtained from each technical replicate for each duplicate culture grown under the three conditions: diamonds, *S. wolfei* pure culture on crotonate; triangles, *S. wolfei-M. hungatei* coculture on crotonate; squares, *S. wolfei-M. hungatei* coculture on butyrate.

Mapping the location of proteins identified in libraries of *S. wolfei* grown with *M. hungatei* did not reveal specific genomic regions or “islands” on the *S. wolfei* chromosome responsible for syntrophy (Figure 4). Rather, proteins specific to syntrophic growth appeared to be dispersed throughout the genome.



From outside to the center
Gene products detected during syntrophic growth on butyrate (blue)
Gene products detected during syntrophic growth on crotonate (green)
Gene products detected during axenic growth on crotonate (red)
Genes on forward strand (color by COG categories)
Genes on reverse strand (color by COG categories)
RNA genes (tRNAs green, rRNAs red, other RNAs black)
GC content
GC skew

Figure 4. Proteins detected under each growth condition mapped against the genome of *S. wolfei.* Proteins detected during syntrophic butyrate growth are in the outer blue ring, during syntrophic crotonate growth are in the green ring, and during axenic crotonate growth are in the red ring.

Abundant proteins

Proteins found to be highly abundant, typically represent the dominant pathways and processes within the cell. The most abundant proteins (% NSAF > 1%) in each condition are listed in Table 3. Ten proteins that had NSAF percentages greater than 1% under all three growth conditions were two chaperones (Swol_1855 and Swol_1856 gene products), an electron transfer flavoprotein complex (Swol_0696 and Swol_0697 gene products), a putative copper amine oxidase (Swol_0133 gene product), an acetyl-CoA acetyltransferase (Swol_2051 gene product), the B subunit of the ATP synthase (Swol_2386 gene product), a small heat shock protein (Swol_0588 gene product), a transcriptional regulator, AbrB family (Swol_0047 gene product) and the polyhydroxyalkanoate (PHA) synthesis regulator, PhaR, encoded by Swol_1244. When *S. wolfei* was grown with *M. hungatei* on crotonate or butyrate, a zinc-dependent dehydrogenase (Swol_1727 gene product), a DNA-binding protein (Swol_0648 gene product) and a protein without an annotated function (Swol_2296 gene product) had NSAF percentages > 1%. The high abundance of these proteins is surprising because they do not have an exact assigned function in *S. wolfei*. It would be expected that such highly abundant proteins would play an important role within the cell. The zinc-containing dehydrogenase also contains a chaperonin component, GroES, and is highly similar (BLAST E-value of 5e-104) to a gene found in another syntrophic organism, *Syntrophus aciditrophicus,* SYN_01269. This gene is also found in

other organisms capable of syntrophy that have been genome sequenced including *Syntrophobacter fumaroxidans, Pelotomaculum thermopropionicum, Syntrophothermus lipocalidus,* and *Syntrophobotulus glycolicus.* PhaR was significantly more abundant (at 99% cutoff) during growth with a methanogen. Two genes adjacent to PhaR, a poly-hydroxyalkanoic acid synthase encoded by Swol_1241 and an acyl-CoA dehydratase encoded by Swol_1242, are significantly more abundant (at 80% cutoff and 95% cutoff, respectively) during syntrophic growth. Two 3-hydroxybutyryl-CoA dehydrogenases (Swol_0435 and Swol_2030) were highly abundant in crotonate grown cells without a methanogen. The chaperonin, GroES encoded by Swol_1856, is significantly more abundant during axenic growth on crotonate. Other proteins significantly more abundant during axenic growth include: a transcription regulator AbrB/SpoV, acetyl-CoA acetyltransferase, 4-hydroxybutyrate coenzyme A transferase, a GTP-binding protein, an amino acid transporter, diaminopimelate decarboxylase, a ribosome recycling factor, and ribosomal proteins S9, S15P, S21P, and L14. During syntrophic butyrate growth, leucyl-tRNA synthetase, phenylalanyl-tRNA synthetase, isoleucyl-tRNA synthetase, seryl-tRNA synthetase, 3-deoxy-7-phosphoheptulonate synthase, 3-isopropylmalate dehydratase, phosphatidylserine decarboxylase, two ABC transporters, iron-sulfur cluster and nucleotide-binding protein, two hypothetical proteins, DNA-directed RNA polymerase, a putative flavoprotein, molybdopterin biosynthesis protein, and fructose-bisphosphate aldolase are significantly more abundant.

Table 3. The most abundant peptides detected in each condition.

Locus Tag	Gene Description	% NSAF of Peptides Detected		
		Crotonate	Crotonate with *M. hungatei*	Butyrate with *M. hungatei*
Swol_0047	Transcriptional regulator, AbrB family	1.05	1.16	1.28
Swol_0083	DNA-binding protein HU	0.77	1.17	0.82
Swol_0133	Copper amine oxidase	2.70	4.24	2.91
Swol_0435	3-hydroxybutyryl-CoA dehydrogenase	2.62	0.16	0.70
Swol_0436	Coenzyme A transferase	1.15	0.79	0.58
Swol_0588	Small heat shock protein	1.14	1.54	1.27
Swol_0648	DNA-binding protein HU	0.92	1.21	1.52
Swol_0670	Rubrerythrin	0.77	1.08	0.70
Swol_0696	Electron transfer flavoprotein β-subunit	2.20*	2.22*	1.19
Swol_0697	Electron transfer flavoprotein α-subunit	1.60*	2.18*	1.04
Swol_0767	Phosphate acetyltransferase	0.89	1.00	0.89
Swol_0768	Acetate kinase	0.67	1.37	0.93
Swol_1187	Iron(III) dicitrate-binding protein	0.71	1.11	0.80
Swol_1244	Polyhydroxyalkanoate synthesis regulator	1.14	2.80*	2.63*
Swol_1727	Zn-dependent dehydrogenase	ND	1.95	3.17
Swol_1855	60 kDa chaperonin GROEL	4.23	2.82	1.56
Swol_1856	10 kDa chaperonin GROES	4.95*	3.17	2.44
Swol_2030	3-hydroxybutyryl-CoA dehydrogenase	2.06	0.33	0.51
Swol_2051	Acetyl-CoA acetyltransferase	3.50*	1.00	1.08
Swol_2148	Branched-chain amino acid aminotransferase	0.38	0.59	1.01
Swol_2296	Hypothetical protein	0.47	1.24*	1.12*
Swol_2350	Translation elongation factor Tu	0.44	0.99	0.45
Swol_2382	Sodium-transporting two-sector ATPase	0.92	1.28	0.88
Swol_2386	F_0F_1-type ATP synthase subunit B	1.18	1.06	1.03

* indicates significantly differential abundance at a 90% cutoff

Further differences in cellular functions between the three growth conditions were detected when proteins were assigned to functional clusters of orthologous groups (COG). Of the 20 categories assigned, twelve remained unchanged in abundance of proteins between the three conditions (see Figure 5 and Table 3S). Axenic, crotonate grown *S. wolfei* cells had a significantly greater number of peptides ($P<0.05$) assigned to lipid metabolism and transport, posttranslational modification, protein turnover, chaperones, and translation. Energy production and conversion, ribosomal structure and biogenesis, ribosomal structure and biogenesis were also higher than in syntrophically grown cells, but the increase was not significant. Amino acid metabolism and transport proteins, proteins with unknown functions, and proteins involved in secondary metabolites biosynthesis, transport and catabolism were significantly less abundant than during syntrophic growth.

Syntrophically grown cells, on the other hand, had a significant increase in proteins assigned to amino acid metabolism and transport functions. Coenzyme metabolism and transport functions, secondary metabolites biosynthesis, transport and catabolism, and proteins with unknown functions were also significantly higher during syntrophic growth on butyrate. During growth on crotonate with a methanogen, energy production and conversion was significantly higher. The increase in peptides assigned to key biosynthetic functions under syntrophic conditions is unexpected as syntrophic cultures are marked by their slower growth rates when compared to axenic cultures of *S.*

wolfei. Similar shifts in amino acid synthesis have been shown in cocultures of termite gut spirochetes (Rosenthal et al., 2011) and syntrophically grown *P. thermopropionicum* (Kato et al., 2009) during transcriptional analysis. Isoleucine/ leucine/ valine transport, tryptophan/phenylalanine/ tyrosine biosynthesis, and methionine system and transport genes were all found to be more highly transcribed in *Treponema primitia* when cocultured with *Treponema azotonutricium* (Rosenthal et al., 2011). *P. thermopropionicum* is not capable of synthesizing many amino acids in pure culture, requiring yeast extract; yet in coculture, yeast extract is not necessary. Transcriptional analysis of *P. thermopropionicum* revealed that amino acid transport and metabolism genes were more expressed under syntrophic conditions; suggesting that the methanogen and syntrophic organism are transferring amino acids between the two of them (Kato et al., 2009). During syntrophic growth of *S. wolfei*, proteins for thiamine, threonine, glutamine, glutamate, and glycine synthesis were more abundant than during axenic growth. The tRNA synthetase proteins for leucine, phenylalanine, isoleucine, and serine were also more abundant during syntrophic growth on butyrate. While the tRNA synthetases for threonine and lysine were significantly more abundant during growth with a methanogen regardless of substrate.

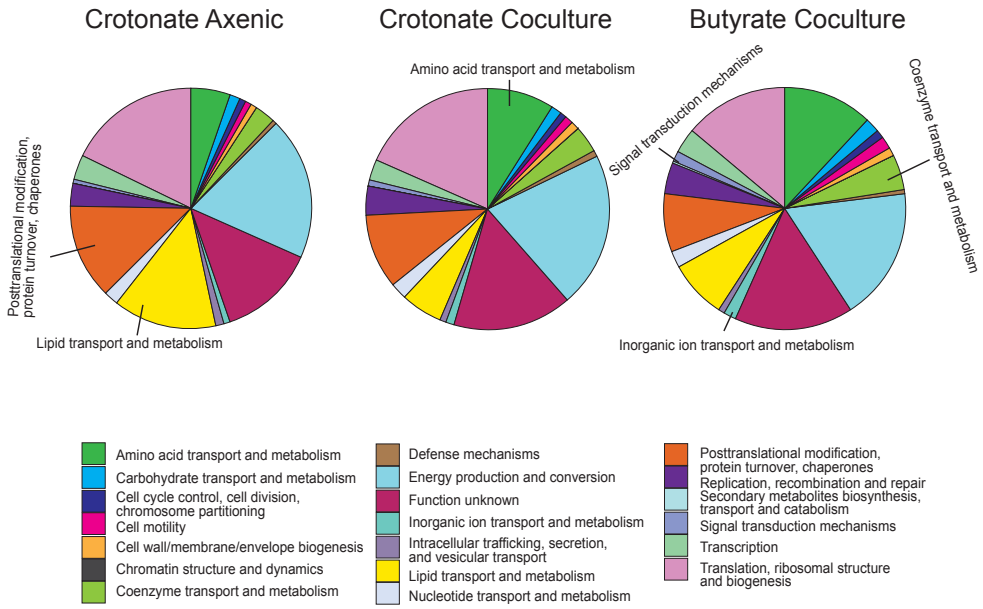


Figure 5. Representation of peptides detected in the *S. wolfei* proteome by assignment to major functional groups (COG).

Fatty Acid Metabolism

S. wolfei metabolizes short-chain saturated and unsaturated fatty acids by β-oxidation (Wofford et al., 1986). Sieber et al. 2010 identified multiple homologous genes for the β-oxidation enzymes within the genome of *S. wolfei*. The gene products of many of these homologs were detected in the proteome under all growth conditions (Figure 6). Eight of the nine butyryl-CoA dehydrogenases encoded on the genome were detected in the proteome. The most abundant butyryl-CoA dehydrogenase was that encoded by Swol_2052. Three other butyryl-CoA dehydrogenases, encoded by Swol_0268, Swol_0384, and Swol_2126, were equally abundant in cells grown syntrophically on butyrate (Figure 6). Butyryl-CoA dehydrogenases encoded by Swol_2052 and Swol_1933 were previously detected highly purified preparations of butyryl-CoA dehydrogenase activity from syntrophically grown cells (Müller et al., 2009). However, the Swol_1933 gene product was not the most abundant butyryl-CoA dehydrogenase in the proteome of our cells and was only detected during axenic growth on crotonate (Fig. 6). Interestingly, Swol_1933 is adjacent to other ß-oxidation genes on the *S. wolfei* chromosome including those for a CoA transferase (Swol_1932), an enoyl-CoA hydratase (Swol_1936), a 3-hydroxybutyryl-CoA dehydrogenase (Swol_1935), and an acetyl-CoA acetyltransferase (Swol_1934). All of the respective gene products were detected and differentially abundant when the methanogen was present (see Table 1S). Acetate kinases (Swol_0768 and Swol_1486 gene products) and

phosphotransacetylase (Swol_0767 gene product) were detected at similar abundances under all growth conditions, suggesting these proteins are constitutively present and part of the core metabolism. Interestingly, the proteins corresponding to one gene cluster (Swol_1483-1486), encoding for a butyryl-CoA dehydrogenase, an enoyl-CoA hydratase, a 3-hydroxybutyryl-CoA dehydrogenase, and an acetate kinase, were not detected in the proteome under any of the growth conditions. This gene cluster was the only set of β-oxidation genes whose gene products were not detected under any condition.

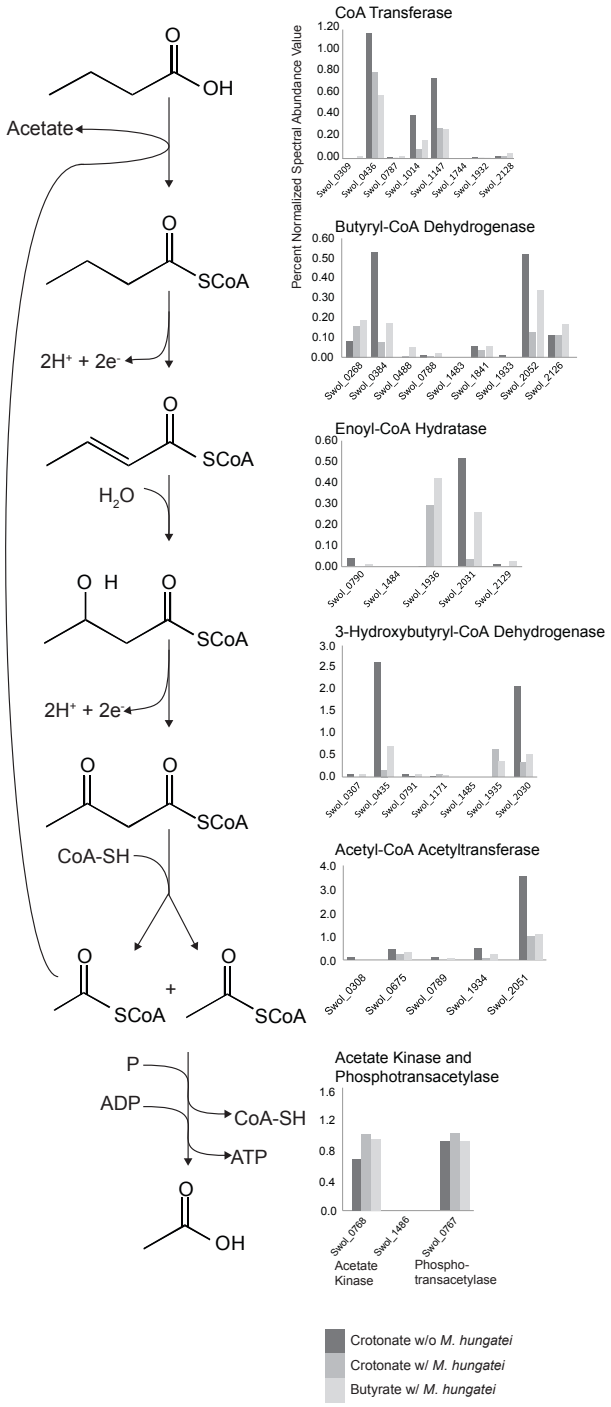


Figure 6. The β-oxidation pathway in *S. wolfei* and the abundance of the corresponding proteins detected in the proteome. Pathway was adapted from Wofford et al., 1986. Abundance of the proteins detected is shown in normalized spectral abundance values during axenic growth on crotonate (in dark grey), syntrophic growth on crotonate (in medium grey), and syntrophic growth on butyrate (in light grey).

Interspecies Electron Transfer

Interspecies electron transfer is the defining metabolic feature of syntrophic metabolism (Schink, 1997). Most obligate syntrophic organisms are known to utilize either hydrogen and/or formate as an electron shuttle to their syntrophic methanogen partner (Stams and Plugge, 2009; Sieber et al., 2010a). The genome of *S. wolfei* contains three hydrogenase gene clusters (see Figure 7a) and six formate dehydrogenase gene clusters (see Figure 8a).

All three hydrogenases encoded in the genome were detected in the proteome under all growth conditions (see Figure 7b). Thus, there are multiple routes to produce hydrogen, potentially including receiving electrons from NADH and ferredoxin by a bifurcation mechanism (Hyd I), ferredoxin only (Hyd III), and possibly from the quinone pool by a membrane-bound hydrogenase (Hyd II), although the cytochrome subunit was not detected. Hyd III is significantly more abundant under crotonate growth conditions.

A signal transduction histidine kinase, encoded by Swol_1040, which contains domains similar to those of Fe-only hydrogenases and ferredoxins, was only detected during syntrophic butyrate metabolism. This protein may be part of a two-component system involved in the regulation of hydrogen production.

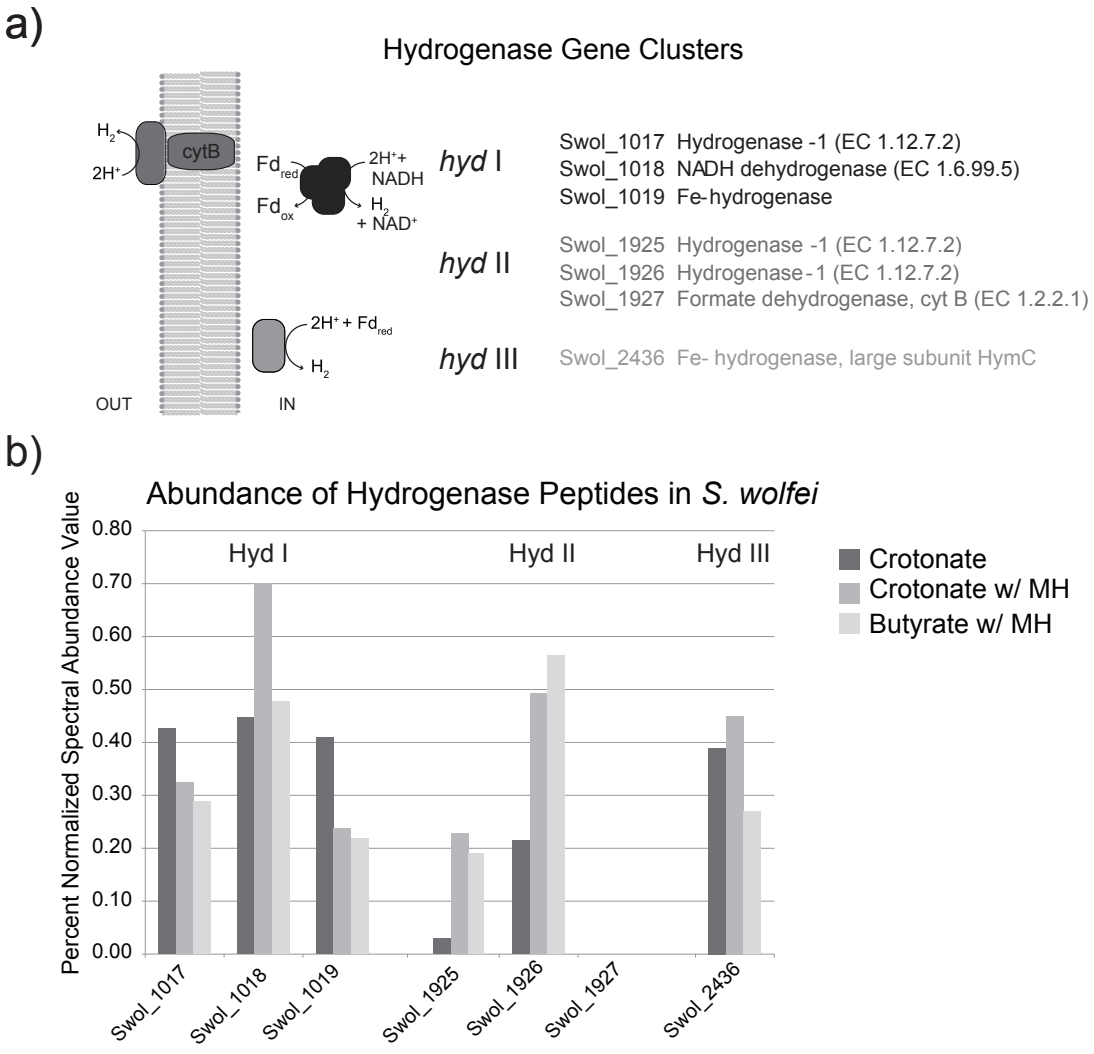
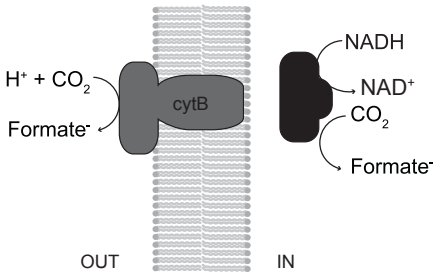


Figure 7. Potential routes for interspecies hydrogen transfer. a) Illustration of the predicted function and location of hydrogenases and their corresponding genes, color-coded to match the illustrated function. b) The graph shows the normalized spectral abundance value of the hydrogenase peptides detected in the proteome during axenic growth on crotonate (in dark grey), syntrophic growth on crotonate (in medium grey), and syntrophic growth on butyrate (in light grey).

Many subunits of the formate dehydrogenases were detected, but were found in lower abundance than the hydrogenases under all growth conditions (see Figure 8b), and not all of the subunits of any of the six formate dehydrogenase were detected. Abundance levels of five of the six formate dehydrogenases were either more abundant or in some cases only detected in cells of *S. wolfei* axenically-grown on crotonate (Figure 8b). A small number of formate dehydrogenase subunits were detected under all conditions; these included subunits of FDH I, FDH IV, and FDH VI, encoded by Swol_0658, Swol_1024, and Swol_1833. Formate dehydrogenase systems II and III were present primarily during axenic growth on crotonate. None of the corresponding peptides for the Fdh V were detected in any of the conditions tested.

a) Formate Dehydrogenase Gene Clusters



fdh I
Swol_0656 NADH-quinone oxidoreductase chain E
Swol_0657 NADH-quinone oxidoreductase chain F
Swol_0658 NADP- dependent formate dehydrogenase b

fdh II
Swol_0783 NADH dehydrogenase I chain E
Swol_0784 NADH dehydrogenase subunit F
Swol_0785 NADH dehydrogenase I chain G
Swol_0786 Formate dehydrogenase alpha subunit

fdh III
Swol_0797 Formate dehydrogenase, cyt B556 subunit
Swol_0798 Formate dehydrogenase (cyt b) iron-sulfur subunit
Swol_0799 Formate dehydrogenase (cyt b) major subunit
Swol_0800 Formate dehydrogenase (cyt b) major subunit

fdh IV
Swol_1024 NADH-quinone oxidoreductase chain F
Swol_1025 NADH-quinone oxidoreductase chain E
Swol_1028 Formate dehydrogenase alpha subunit
Swol_1029 NADH-ubiquinone oxidoreductase 75kDa subunit

fdh V
Swol_1823 Formate dehydrogenase, cyt B556 subunit
Swol_1824 Formate dehydrogenase (cyt b) iron-sulfur subunit
Swol_1825 Formate dehydrogenase (cyt b) major subunit
Swol_1826 Formate dehydrogenase (cyt b) major subunit

fdh VI
Swol_1828 NADH- quinone oxidoreductase chain F
Swol_1829 NADH- quinone oxidoreductase chain E
Swol_1830 Formate dehydrogenase alpha subunit
Swol_1831 NADH-ubiquinone oxidoreductase 75kDa subunit
Swol_1832 Ferredoxin
Swol_1833 NADH dehydrogenase
Swol_1834 Ferredoxin

b) Abundance of Formate Dehydrogenase Peptides in *S. wolfei*

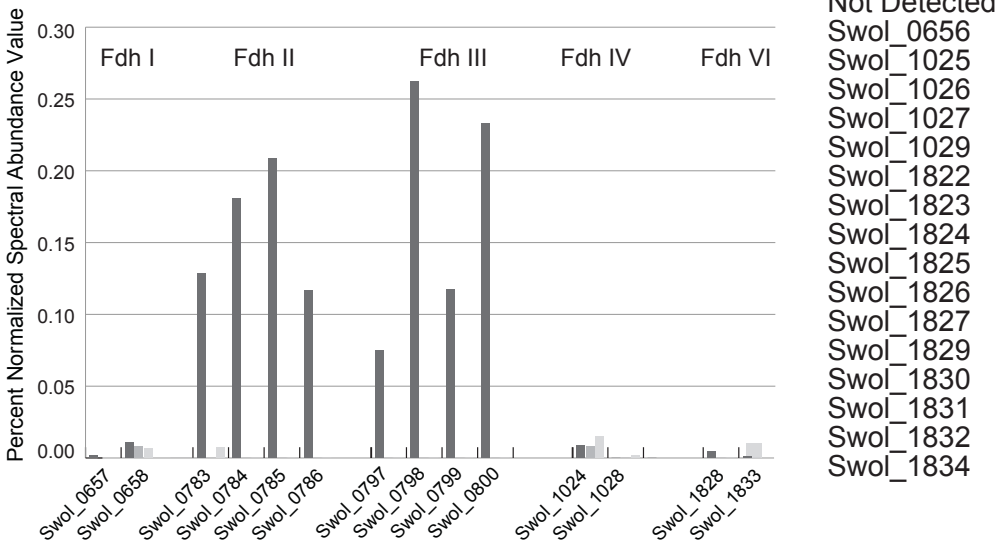


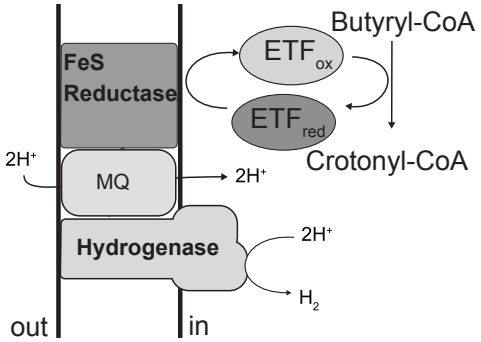
Figure 8. Potential routes for interspecies formate transfer. a) Illustration of the function and location of formate dehydrogenases and their corresponding genes color-coded to match the illustration. b) The graph shows the normalized spectral abundance value of the formate dehydrogenase peptides detected in the proteome during axenic growth on crotonate (in dark grey), syntrophic growth on crotonate (in medium grey), and syntrophic growth on butyrate (in light grey).

Metals are essential co-factors needed within the active sites of hydrogenase and formate dehydrogenase. The *S. wolfei* genome encodes for several hydrogenases that require iron while formate dehydrogenases require tungsten or molybdenum in addition to iron for the redox active iron-sulfur clusters. Multiple peptides were detected for Fe^{2+} or potentially Zn^{2+} transporters under conditions when the methanogen was present, including an iron transporter encoded by Swol_0661-662 although the protein encoded by Swol_0662 was also found under axenic growth on crotonate. The iron transporter encoded by Swol_0661-662 may be regulated by the ferric uptake regulation protein encoded by Swol_0660, which was detected only when a methanogen was present (see Table 1S). A molybdate-binding protein was in 2-fold higher abundance in cells syntrophically grown on butyrate than in those grown on crotonate. Multiple zinc-dependent dehydrogenases were present only when the methanogen was present. Noteworthy here is the Swol_1727 gene product, which accounted for more than 2% of detected peptides when *M. hungatei* was present and was not detected when *S. wolfei* was grown axenically. However, the role of the zinc-dependent dehydrogenases in *S. wolfei* is unknown.

Reverse electron transfer

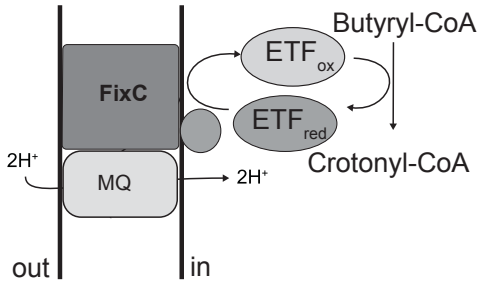
Multiple routes for reverse electron transfer from butyryl-CoA oxidation were proposed from genomic analysis (Sieber et al.). These included a novel FeS oxidoreductase, the Fix system, and electron bifurcation by a butyryl-CoA

dehydrogenase/electron transfer flavoprotein (ETF) complex (see Chapter 2). All three sets of ETF genes were detected during the axenic and syntrophic growth (see Figure 9). The ETF, encoded by Swol_0696 and Swol_0697, whose genes are adjacent to that of a predicted membrane-bound, FeS oxidoreductase (Swol_0698), was more abundant than all other ETF subunits. ETF encoded by Swol_0696-97 was more abundant in crotonate (both syntrophic and axenic) grown cells than in butyrate-grown cells. The FeS oxidoreductase was constitutively detected in cells under all growth conditions and has been implicated in reverse electron transfer during syntrophic metabolism (Müller et al., 2009). However, Muller et al. (2009) did not detect the associated ETF (Swol_0696-97 gene products). The Fix complex, comprised of an ETF (Swol_2121 and Swol_2122), ferredoxin (Swol_2123), and ETF:Quinone oxidoreductase (Swol_2124), whose genes are associated with a butyryl-CoA dehydrogenase gene (Swol_2126), appear to be constitutively co-present (see Figure 9). The Fix complex is ten-fold less abundant than the FeS oxidoreductase and its associated ETF under all conditions, suggesting a biosynthetic rather than a major catabolic role for Fix (see Figure 9).



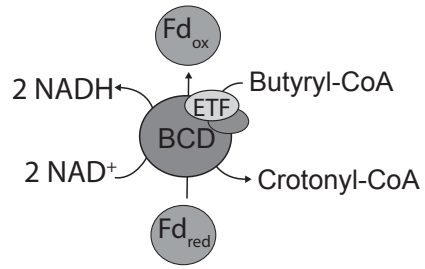
Abundance of Peptides Detected in % NSAF

		Crotonate	Crotonate +Mh	Butyrate +Mh
FeS reductase linked to ETF				
ETF, beta subunit	Swol_0696	2.20	2.23	1.19
ETF, alpha subunit	Swol_0697	1.60	2.18	1.04
FeS reductase	Swol_0698	0.51	0.45	0.52
Membrane Bound Hydrogenase				
Fe-only H_2ase	Swol_1925	0.03	0.23	0.19
Fe-only H_2ase	Swol_1926	0.21	0.49	0.56
Cytochrome B	Swol_1927	ND	ND	ND



Abundance of Peptides Detected in % NSAF

		Crotonate	Crotonate +Mh	Butyrate +Mh
ETF:Quinone Oxidoreductase				
ETF, beta subunit	Swol_2121	0.13	0.08	0.17
ETF, alpha subunit	Swol_2122	0.18	0.16	0.19
Ferredoxin	Swol_2123	0.08	0.01	0.05
FixC	Swol_2124	0.03	0.05	0.14
Butyryl-CoA DH	Swol_2126	0.11	0.11	0.17



Abundance of Peptides Detected in % NSAF

		Crotonate	Crotonate +Mh	Butyrate +Mh
Butyryl-CoA DH linked to ETF				
ETF, beta subunit	Swol_0266	0.01	0.00	0.02
ETF, alpha subunit	Swol_0267	0.05	0.04	0.03
Butyryl-CoA DH	Swol_0268	0.08	0.16	0.19

Figure 9. Abundance of peptides potentially involved in reverse electron transfer. Illustration of the potential roles for electron transfer flavoproteins and their associated proteins, either a membrane-bound oxidoreductase, Fix proteins, or butyryl-CoA dehydrogenase. The tables show the abundance of the corresponding proteins based on normalized spectral abundance values. +MH denoted growth with the methanogen, *M. hungatei*.

Syntrophy

One hundred and twenty five proteins were detected exclusively during syntrophic butyrate growth (see Table 4) including multiple transcriptional regulators, encoded by Swol_0177, Swol_0456, Swol_0792, Swol_0952, Swol_1040, Swol_1052, Swol_1793, Swol_2106, Swol_2130, and Swol_2424. Many of these transcriptional regulators have not been shown to regulate any specific functions with the *S. wolfei* cell. These regulators could play an important role in energy conservation via reverse electron transfer or hydrogen/formate transfer, or in response to the presence of the methanogen. Swol_0456 and Swol_0792 contain a large amount of sequence similarity to each other. Both have no assigned regulatory function, but do have PAS, AAA-type ATPase, and DNA-binding domains. Swol_2525-2528 gene products, which are encoded by adjacent genes on the genome and have no predicted functions, were detected only in butyrate-grown cells. Gene products of nearby genes, Swol_2524 and Swol_2529, were detected under multiple growth conditions. Genes Swol_2524-2529 are adjacent to a CRISPR region (Regions known to give resistance to encountered viruses) (Sorek et al., 2008; Horvath et al., 2009; Sieber et al., 2010b). In total, 25 gene products without predicted function were detected only under syntrophic butyrate growth.

Table 4. Proteins detected only during syntrophic growth on butyrate

Locus TAG	Predicted Function	% Normalized spectral abundance factor
Swol_0027	ATPase	0.0025
Swol_0029	Protein of unknown function DUF182	0.0154
Swol_0073	Transcription-repair coupling factor	0.0008
Swol_0094	tRNA(Ile)-lysidine synthetase TilS	0.0125
Swol_0174	Hypothetical protein	0.0028
Swol_0177	Transcriptional regulator, TetR family	0.0140
Swol_0217	Hypothetical protein	0.0208
Swol_0224	Hypothetical protein	0.0810
Swol_0228	dTDP-glucose 4,6-dehydratase	0.0220
Swol_0231	Flagellar protein fliS	0.0394
Swol_0262	Glucose-6-phosphate isomerase	0.0073
Swol_0275	Phosphoglycerate mutase	0.0020
Swol_0279	HDIG domain protein	0.0059
Swol_0339	ABC transporter ATP-binding protein	0.0047
Swol_0343	Adenylate cyclase	0.0026
Swol_0353	Serine/threonine protein kinase	0.0011
Swol_0355	Chemotaxis protein cheY	0.0089
Swol_0368	DNA helicase II	0.0033
Swol_0386	Rod shape-determining protein	0.0031
Swol_0387	Hypothetical protein	0.0051
Swol_0408	Nitrogenase iron protein	0.0042
Swol_0414	Sugar transport ATP-binding protein	0.0031
Swol_0456	Signal-transduction protein	0.0172
Swol_0469	Hypothetical protein	0.0298
Swol_0475	ATP-dependent RNA helicase	0.0093
Swol_0476	Hypothetical protein	0.0131
Swol_0516	Type I restriction-modification subunit	0.0011
Swol_0519	Pyruvate carboxylase	0.0093
Swol_0524	Shikimate 5-dehydrogenase	0.0096
Swol_0532	Pili retraction protein pilT	0.0363
Swol_0569	Dimethylallyltransferase	0.0074
Swol_0663	Iron-sulfur cluster assembly/repair	0.0089
Swol_0669	Agmatinase	0.0169
Swol_0699	Phosphopantetheine adenylyltransferase	0.0100
Swol_0703	Nucleotide-sugar aminotransferase	0.0116
Swol_0712	Amino acid transport ATP-binding protein	0.0090
Swol_0740	Putative integrase	0.0034
Swol_0744	Cobyrinic acid a,c-diamide synthase	0.0051
Swol_0765	Hypothetical membrane spanning protein	0.0127
Swol_0766	Serine protease	0.0039
Swol_0776	Chromosome partition protein smc	0.0008
Swol_0792	Signal-transduction and transcriptional-control protein	0.0017
Swol_0805	Single-stranded-DNA-specific exonuclease recJ	0.0048
Swol_0838	Site-specific DNA-methyltransferase	0.0150
Swol_0843	ATP-dependent endopeptidase	0.0183
Swol_0901	Ribosome-binding factor A	0.0132
Swol_0904	Riboflavin kinase	0.0034
Swol_0910	Peptidase, M16 family	0.0057
Swol_0914	Trk system potassium uptake protein trkA	0.0074
Swol_0929	Cinnamoyl ester hydrolase	0.0152

Swol_0952	Two-component sensor kinase yycG	0.0102
Swol_0966	UDP-N-acetylmuramoylalanyl-D-glutamate--2,6-diaminopimelate ligase	0.0096
Swol_0974	DNA mismatch repair protein mutS	0.0011
Swol_0984	Hypothetical ATPase	0.0153
Swol_0998	Hypothetical protein	0.0101
Swol_0999	ATP-dependent endopeptidase Lon	0.0017
Swol_1028	Formate dehydrogenase alpha subunit	0.0019
Swol_1040	Two component system histidine kinase	0.0082
Swol_1048	Formate acetyltransferase	0.0031
Swol_1050	Fatty acid-binding protein, DegV family	0.0039
Swol_1052	Sensory transduction protein kinase	0.0118
Swol_1158	Hypothetical cytosolic protein	0.0264
Swol_1188	Hypothetical protein	0.0062
Swol_1214	Protein Translation Elongation Factor G	0.0017
Swol_1222	Diaminohydroxyphosphoribosylaminopyrimidine deaminase	0.0121
Swol_1237	Guanylate kinase	0.0081
Swol_1246	Hypothetical protein	0.0329
Swol_1275	RNA-binding protein-like protein	0.0056
Swol_1280	Dihydroorotate dehydrogenase electron transfer subunit	0.0234
Swol_1293	Hypothetical protein	0.0059
Swol_1356	3-hydroxybutyryl-CoA dehydratase	0.0080
Swol_1469	2-polyprenylphenol 6-hydroxylase accessory protein ubiB	0.0014
Swol_1480	Glutaconate CoA-transferase subunit B	0.0425
Swol_1487	Sigma-54-dependent transcriptional activator	0.0039
Swol_1509	Deoxyguanosinetriphosphate triphosphohydrolase	0.0031
Swol_1550	ATP-dependent helicase hepA	0.0011
Swol_1595	COME operon protein 3	0.0014
Swol_1620	ABC transporter ATP-binding protein	0.0096
Swol_1625	Hypothetical protein	0.0074
Swol_1645	Redox-sensitive transcriptional regulator Rex	0.0470
Swol_1675	Biotin synthase	0.0028
Swol_1701	NADH-quinone oxidoreductase chain F	0.0017
Swol_1704	Ferredoxin	0.0201
Swol_1764	Phosphoribosyl-AMP cyclohydrolase	0.0100
Swol_1767	Imidazoleglycerol-phosphate dehydratase	0.0432
Swol_1779	Adenylosuccinate lyase	0.0303
Swol_1793	Sigma factor sigB regulation protein rsbU	0.0028
Swol_1806	Hypothetical cytosolic protein	0.0087
Swol_1826	Formate dehydrogenase (cyt b) major subunit	0.0017
Swol_1847	(3R)-hydroxyacyl-[acyl carrier protein] dehydratase	0.0146
Swol_1849	Enoyl-[acyl-carrier protein] reductase	0.1769
Swol_1929	Hypothetical protein	0.0062
Swol_2008	Hypothetical protein	0.0060
Swol_2069	Hypothetical protein	0.0020
Swol_2085	Exodeoxyribonuclease V alpha chain	0.0023
Swol_2089	Hypothetical protein	0.0232
Swol_2092	Arsenical pump membrane protein	0.0040
Swol_2102	Hypothetical protein	0.0037
Swol_2106	Sensory transduction protein kinase	0.0033
Swol_2130	Two-component response regulator	0.0322
Swol_2150	Metal-dependent phosphohydrolase	0.0045
Swol_2191	Hypothetical cytosolic protein	0.0505
Swol_2207	Hypothetical protein	0.0017

Swol_2288	Acetylornithine aminotransferase	0.0062
Swol_2299	Pseudouridylate synthase	0.0081
Swol_2353	Thymidylate synthase complementing protein	0.0320
Swol_2368	ATP:guanido phosphotransferase	0.0063
Swol_2391	Putative ComE operon protein 2	0.0216
Swol_2393	Tyrosine phosphatase	0.0563
Swol_2415	Signal peptide peptidase sppA	0.0110
Swol_2424	Two-component response regulator	0.0031
Swol_2486	Iron(III) dicitrate-binding protein	0.0090
Swol_2495	Hypothetical protein	0.0056
Swol_2516	CRISPR-associated protein	0.0034
Swol_2519	CRISPR-associated protein	0.0236
Swol_2521	CRISPR-associated protein	0.0073
Swol_2525	CRISPR-associated protein	0.0250
Swol_2526	Hypothetical protein	0.0022
Swol_2527	Hypothetical protein	0.0014
Swol_2528	Hypothetical protein	0.0019
Swol_2542	Selenide,water dikinase	0.0248
Swol_2552	Branched-chain amino acid transport ATP-binding protein	0.0191
Swol_2557	Activator of D-2-hydroxyacyl-CoA dehydratase	0.0008
Swol_2568	Chromosome partitioning protein parA	0.0042
Swol_2572	GTPase	0.0138

Two chemotaxis regulators, which transmit chemoreceptor signals to the flagellar motor component, CheY, were differentially expressed in response to syntrophic growth conditions. The CheY peptide encoded by Swol_0863 was significantly less abundant during syntrophic growth than during axenic crotonate growth, while the peptide encoded by Swol_1448 is significantly more abundant during syntrophic growth. Flagella and chemotaxis have been shown to play important roles in some syntrophic relationships; including recognition of partner methanogens (Shimoyama et al., 2009) and aiding in co-aggregation to facilitate hydrogen transfer (Ishii et al., 2005).

Proteins without predicted function

In the *S. wolfei* proteome, 180 proteins with no predicted function were detected. Of these proteins, seven were found to be significantly differentially more abundant during syntrophic growth (at 80% cutoff). *S. wolfei* has such a simple metabolism, that it is unexpected to find these proteins encoded by hypothetical genes, particularly those that are differentially abundant or high in abundance. The protein encoded by Swol_2296, is both highly abundant and is significantly differentially abundant during syntrophic growth, yet has no assigned function. Swol_2296 is adjacent to and in the opposite transcriptional direction to many small and large ribosomal subunit proteins and transport genes. This gene contains multiple membrane occupation and recognition nexus (MORN) motifs, which are thought to be involved in regulation, although it is not yet clear how. Many of these ribosomal subunit proteins were found to be

significantly more abundant during growth on crotonate (Swol_2303, Swol_2305, Swol_2314, Swol_2326, Swol_2327, Swol_2329, and Swol_2337 at 80% cutoff) suggesting this protein could be acting as a transcriptional repressor for this set of ribosomal subunit proteins, during syntrophic growth.

CONCLUSIONS

Syntrophic metabolism has been long characterized as a meager lifestyle that approaches the theoretical thermodynamic limit of life (Jackson and McInerney, 2002). Thus, mechanisms of electron flow and energy use in *S. wolfei* are essential to understanding syntrophy. Only a relatively small number of proteins, 34 in total, were unique to the syntrophic lifestyle, many of which are functionally uncharacterized. *S. wolfei* proteome contained multiple enzyme systems for fatty acid metabolism. Hydrogenases were more highly abundant than formate dehydrogenases during syntrophic butyrate growth, suggesting they are the dominant interspecies electron transfer mechanism. Fdh II and Hyd I were previously detected as part of a NADH:quinone oxidoreductase complex, under syntrophic conditions (Müller et al., 2009). This NADH oxidoreductase complex is predicted to be important for energy conservation during growth on butyrate. An FeS oxidoreductase predicted to function as an ETF:quinone oxidoreductase was prevalent under all growth conditions and was in much higher abundance than Fix components. The FeS oxidoreductase may be the

major membrane input complex for electrons derived from butyryl-CoA oxidation. Multiple proteins involved in amino acid synthesis were found to be significantly abundant during syntrophic growth.

The proteome of *S. wolfei* grown syntrophically on either butyrate or crotonate and axenically on crotonate demonstrates that *S. wolfei* responds differently to the substrate available. Moreover the changes found in the protein profiles of *S. wolfei* when grown syntrophically shows that *S. wolfei* responds to the presence of a partner methanogen.

MATERIALS AND METHODS

Organisms and Growth Conditions

Pure cultures of *Syntrophomonas wolfei* (DSM 2245B) (McInerney et al., 1981b) and cocultures of *S. wolfei* with *Methanospirillum hungatei* strain JF1 (ATCC 27890) were grown anaerobically as described previously (McInerney et al., 1979). *S. wolfei* pure cultures were grown in medium with 20 mM crotonate. *S. wolfei-M. hungatei* cocultures were grown in medium with 20 mM crotonate or 20 mM butyrate. Media were prepared using a modified Balch technique (Balch and Wolfe, 1976). All cultures were grown in 75 ml volumes in 160 ml serum bottles in triplicate. The headspace was pressurized to 27.5 kPa with N_2/CO_2 (80:20 v/v). All cultures were incubated at 37°C without shaking. Culture

purity was checked daily by microscopic examination and inoculation of a thioglycolate medium.

Growth was monitored by measuring optical density at 600 nm. One ml samples were taken daily to measure substrate depletion and product formation. Methane formation by cocultures was measured by daily headspace analysis. The concentrations of crotonate, butyrate, and acetate were determined by high performance liquid chromatography with a Prevail Organic acid column (250 by 4.6 mm; particle size 5 µm; Alltech Inc, Deerfield, Ill.) at a flow rate of 1 ml/min. The isocratic mobile phase consisted of 25 mM KH_2PO_4 (pH 2.5) to measure acetate concentrations. A mobile phase of 60% (v/v) KH_2PO_4 (25 mM, pH 2.5):40% (v/v) acetonitrile was used to quantify crotonate and butyrate. The UV absorbance detector was set at 210 nm to detect acetate and butyrate, and 254 nm for crotonate.

Methane was measured by gas chromatography with a flame ionization detection equipped with Poropak Q, 80/100 column (6 feet x 1/8 inch) (Supelco, Bellefonte, PA). The injector temperature was set at 100°C, the column at 100°C and the detector at 125°C. Helium was used as a carrier gas.

Sample Preparation

Cells from duplicate cultures for each of the three growth conditions, e.g., *S. wolfei* pure culture grown on crotonate, *S. wolfei-M. hungatei* coculture grown on crotonate and *S. wolfei-M. hungatei* coculture grown on butyrate, were harvested at 50% substrate loss by centrifugation (14,300 x G, 20min, 4°C) and

processed separately shotgun proteomics analysis. Cell pellet wet weights were 90 mg and 73 mg for *S. wolfei* pure cultures, 105 mg and 79 mg for *S. wolfei-M. hungatei* cocultures grown on crotonate, and 61 mg and 67 mg for *S. wolfei-M. hungatei* coculture grown on butyrate. Cell pellets were processed by generally following a protocol optimized for measurements of small bacterial samples (Thompson et al., 2008). Cell pellets were lysed and proteins denatured by incubating each cell pellet overnight at 37°C in 250-400 mL of 6 M guanidine and 10 mM dithiothreitol (DTT) (larger volumes used for larger cell pellets). Lysates were cooled to ambient temperature, and diluted with 50 mM Tris with 10mM $CaCl_2$ to decrease the guanidine concentration to ~1 M. Ten mg of trypsin (sequencing grade, Promega, Madison WI) was added to each lysate, followed by a 5-hour incubation at 37°C. An additional 10 mg trypsin was added, followed by a further overnight incubation at 37°C. Remaining disulfide bonds were reduced by adding additional DTT to a final concentration of 10 mM and incubation for 1 hour at 37°C. Desalting was performed using reverse-phase solid-phase extraction cartridges (Sep-Pak Lite C18, Waters, Milford MA), with final elution using 0.1% formic acid in acetonitrile. Solvent transfer to aqueous 0.1% formic acid was performed by vacuum centrifugation, with final volume adjusted to 150 ml. Particulates and remaining cellular debris were removed by centrifugation through 0.45 μm pore filters (Ultrafree-MC, Millipore, Billerica MA). Samples were frozen at -80°C until further use.

LC-MS-MS Analysis

Tryptic peptide mixtures were analyzed by two-dimensional liquid chromatography/tandem mass spectrometry (2D LC-MS-MS), using the MudPIT approach (Washburn et al., 2001; Wolters et al., 2001) implemented as previously described in further detail (Hervey IV et al.). Two LC-MS-MS analyses were performed on the tryptic digest from each cell pellet. Thus, for each growth condition, two technical replicates were analyzed for each of the two biological replicates. Aliquots (50 ml) were loaded via a pressure cell (New Objective, Woburn MA) onto a "back" column fabricated from 150 mm internal diameter (ID) fused silica tubing (Polymicro Technologies, Phoenix AZ) packed with a ~4 cm long bed of reverse-phase chromatographic phase (Jupiter C18, 3 mm particle size, Phenomenex, Torrance CA) upstream of a ~4 cm bed of strong cation exchange material (5 mm particle size SCX, Phenomenex).

After sample loading, the back column was attached via a filter union (Upchurch Scientific, Oak Harbor WA) to a "front" analytical column fabricated from a 100 mm ID PicoTip Emitter (New Objective), packed with a ~14 cm bed of reverse-phase material (Jupiter C18, 3mm particle size, Phenomenex). Two-dimensional LC was performed via twelve step gradients of increasing salt (ammonium acetate) concentration, with the eluted peptides from each strong cation exchange step subsequently resolved via a separate reverse-phase gradient (Ultimate HPLC, LCPackings/Dionex, Sunnyvale CA). The LC eluent was interfaced via a nanospray source (Proxeon, Odense, Denmark) with a linear-geometry quadrupole ion trap mass spectrometer (LTQ, ThermoFinnigan,

San Jose CA). Data acquisition was performed in data-dependent mode under the control of XCalibur software. Up to 5 tandem mass spectra were acquired from the most abundant parent ions in full-scan mass spectra; dynamic exclusion was enabled with a repeat count of 1 and duration of 60 seconds.

Proteomics Data Analysis

Peptide identifications were obtained from tandem mass spectra using Sequest software (version 27) (Eng et al., 1994), and protein identifications were compiled from peptide identifications using DTASelect (version 1.9) (Tabb et al., 2002). A multiple-species protein FASTA file was constructed from individual FASTA files for *S. wolfei* subspecies *wolfei* Göttingen and *M. hungatei* JF-1, downloaded from the DOE Joint Genome Institute website. The sequence-reversed analog of each protein sequence was appended to the FASTA file to allow estimation of the false discovery rate of peptide identification (Moore et al., 2002; Elias and Gygi, 2007). Sequences of 36 common contaminant proteins were also appended to the FASTA file. Peptide identifications were retained for XCorr ≥1.8 (z=1), ≥2.5 (z=2), or ≥3.5 (z=3), with DeltaCN ≥0.08. Protein identifications required identification of two peptides. The false discovery rate for peptides was generally ≤1%. Estimates of protein abundance were calculated using normalized spectral abundance factors (Zybailov et al., 2006).

Nonmetric multidimensional scaling was performed using Bray-Curtis dissimilarities of normalized spectral abundance factors from different growth conditions. Bray-Curtis utilizes a shared presence absence matrix to score similarity, which is why it has been well used in ecology to assess the similarity of two communities. Rare or missing proteins were included within the analysis as these may have biological significance, with the caveat that if they only occur in a single treatment rare peptides will be detected by the Bray-Curtis algorithm and left out. NMDS was calculated using the vegan package (Oksanen et al., 2011) as implemented in R (RDevelopmentCoreTeam, 2011). To assess whether growth conditions significantly influenced the abundance patterns of the proteins detected, a Bayesian model was built with the baySeq package (Hardcastle and Kelly, 2010) in the Bioconductor software (Gentleman et al., 2004) implemented in R. An empirical Bayesian approach was chosen over a traditional multiple t-test approach to alleviate type II statistical error (Efron and Tibshirani, 2007; Efron, 2008). The baySeq program generates a prior distribution from the data using user defined models based on the experimental design then calculates posterior probabilities of proteins from the prior distribution. BaySeq is unique in that is allows the user to build models based on the experimental design and to incorporate replicate data within treatments. Due to the experimental design, four models were tested within the baySeq program in order to determine the amount of variance each condition contributed. Variance was calculated by using 100 bootstraps using 500

randomly selected proteins from each model per bootstrap iteration. First model was a total data model (control model) incorporating *S. wolfei* only on crotonate (axenic), crotonate with methanogen, and butyrate with methanogen. Second model tested the difference between both syntrophy conditions and axenic growth. Third condition addressed the difference between crotonate growth (both axenic and syntrophic growth) and butyrate syntrophy. The final model separated all growth conditions to address whether substrate and the presence or absence of a methanogen affected the protein distribution. Posterior probabilities of each protein were generated for each model and several stringency cutoffs were evaluated (high >90%, medium >80%, and low 70%) depending on the probability were designated to assess whether a protein was significantly expressed.

SUPPLEMENTAL MATERIALS

Table 1S. Probability of differential abundance during syntrophic growth. Proteins in grey are positively differentially abundant during growth with a methanogen.

		% Normalized Spectral Abundance Factor			
Locus Tag	**Function**	**Crotonate**	**Crotonate with *M. hungatei***	**Butyrate with *M. hungatei***	**Likelihood of differential abundance**
Swol_1244	Polyhydroxyalkanoate synthesis regulator	1.143	2.796	2.628	0.999
Swol_2051	Acetyl-CoA acetyltransferase	3.504	0.999	1.081	0.996
Swol_1856	10 kDa chaperonin GROES	4.948	3.171	2.439	0.993
Swol_2296	Hypothetical protein	0.467	1.243	1.120	0.991
Swol_1147	4-hydroxybutyrate coenzyme A transferase	0.733	0.271	0.260	0.990
Swol_1242	3-hydroxybutyryl-CoA dehydratase	0.129	0.347	0.350	0.989
Swol_0916	Inosine-5'-monophosphate dehydrogenase	0.142	0.247	0.250	0.983
Swol_0671	Hypothetical protein	0.091	0.378	0.388	0.980
Swol_0639	Thiamin-phosphate pyrophosphorylase	0.033	0.146	0.149	0.978
Swol_1089	Threonyl-tRNA synthetase	0.042	0.107	0.095	0.972
Swol_2334	Ribosomal protein S10	0.180	0.354	0.037	0.963
Swol_0905	SSU ribosomal protein S15P	0.298	0.096	0.030	0.962
Swol_2323	Ribosomal protein L14	0.069	0.031	0.031	0.959
Swol_1268	Zn-dependent hydrolase	0.018	0.078	0.072	0.953
Swol_1019	NADH-quinone oxidoreductase chain E	0.409	0.238	0.218	0.952
Swol_1938	Sensory transduction protein kinase	0.000	0.065	0.070	0.952
Swol_1980	Glycine dehydrogenase	0.035	0.116	0.093	0.948
Swol_2235	Pyruvate synthase alpha chain	0.081	0.208	0.173	0.944
Swol_2520	Hypothetical protein	0.020	0.101	0.102	0.941
Swol_2054	Rubredoxin-oxygen oxidoreductase	0.026	0.085	0.104	0.935
Swol_0870	Flagellar biosynthesis protein flhF	0.003	0.000	0.024	0.934
Swol_1490	GTP-binding protein	0.055	0.029	0.040	0.929
Swol_2297	Ribosomal protein S9	0.124	0.068	0.070	0.921
Swol_1573	SSU ribosomal protein S21P	0.183	0.069	0.113	0.920
Swol_1981	Glycine dehydrogenase	0.026	0.070	0.060	0.916
Swol_0378	Isocitrate dehydrogenase	0.110	0.287	0.233	0.915
Swol_0004	Hypothetical protein	0.063	0.078	0.139	0.915
Swol_1976	Transcription regulator AbrB/SpoV	0.076	0.029	0.024	0.914
Swol_1775	IMP cyclohydrolase	0.041	0.096	0.112	0.914
Swol_1578	Chaperone protein dnaK	0.447	0.484	0.543	0.913
Swol_0116	Lysyl-tRNA synthetase	0.039	0.078	0.094	0.912
Swol_1070	ABC transporter amino acid-binding protein	0.077	0.009	0.011	0.908
Swol_2170	NAD-specific glutamate dehydrogenase	0.038	0.128	0.083	0.906
Swol_2459	Glutaminyl-tRNA synthetase	0.075	0.158	0.125	0.906
Swol_1232	Peptide deformylase	0.104	0.092	0.032	0.904
Swol_1422	Diaminopimelate decarboxylase	0.013	0.003	0.004	0.903
Swol_0885	Ribosome recycling factor	0.136	0.117	0.085	0.901

Table 2S. Probability of differential abundance during growth on crotonate regardless of the presence of a methanogen. Proteins in grey are positively differentially abundant during growth on crotonate.

Locus Tag	Function	% Normalized Spectral Abundance			Likelihood of differential abundance
		Crotonate	Factor Crotonate with *M. hungatei*	Butyrate with *M. hungatei*	
Swol_1348	3-deoxy-7-phosphoheptulonate synthase	0.320	0.326	0.511	0.986
Swol_2327	30S ribosomal protein S3	0.337	0.353	0.144	0.980
Swol_2141	3-isopropylmalate dehydratase	0.150	0.154	0.321	0.980
Swol_0697	Electron transfer flavoprotein alpha-subunit	1.602	2.177	1.043	0.976
Swol_0696	Electron transfer flavoprotein beta-subunit	2.199	2.225	1.189	0.975
Swol_1651	Phosphatidylserine decarboxylase	0.032	0.030	0.076	0.974
Swol_2314	Ribosomal protein L15	0.260	0.274	0.144	0.971
Swol_0341	ABC transporter substrate-binding protein	0.064	0.060	0.145	0.963
Swol_1599	Leucyl-tRNA synthetase	0.040	0.046	0.104	0.956
Swol_1529	Iron-sulfur cluster and nucleotide-binding protein	0.077	0.074	0.194	0.955
Swol_0010	Seryl-tRNA synthetase	0.058	0.057	0.134	0.946
Swol_2337	30S ribosomal protein S7	0.482	0.455	0.187	0.946
Swol_1907	Deoxyuridine 5'-triphosphate nucleotidohydrolase	0.088	0.107	0.054	0.946
Swol_1424	Protein translocase subunit secF	0.028	0.034	0.024	0.940
Swol_1002	Hypothetical protein	0.008	0.020	0.272	0.927
Swol_2436	Hydrogenase-1	0.389	0.448	0.269	0.925
Swol_2464	Hypothetical protein	0.147	0.093	0.494	0.925
Swol_2340	DNA-directed RNA polymerase	0.058	0.057	0.090	0.923
Swol_2363	Putative flavoprotein	0.024	0.025	0.099	0.921
Swol_0801	Molybdopterin biosynthesis MoeA protein	0.012	0.013	0.016	0.915
Swol_2411	Fructose-bisphosphate aldolase	0.081	0.102	0.205	0.913
Swol_1094	Phenylalanyl-tRNA synthetase alpha chain	0.055	0.069	0.133	0.913
Swol_0962	Isoleucyl-tRNA synthetase	0.026	0.030	0.056	0.911
Swol_2432	ABC transporter ATP-binding protein	0.332	0.323	0.500	0.910

Table 3S. Abundance of proteins assigned to COG categories.

Clusters of Orthologous Groups	**Crotonate Axenic**	**Crotonate w/ *M. hungatei***	**Butyrate w/ *M. hungatei***
Amino acid transport and metabolism	5.49[b]	9.13	11.97[a]
Carbohydrate transport and metabolism	1.27	1.31	1.94
Cell cycle control, cell division, chromosome partitioning	0.71	0.73	1.24
Cell motility	0.87	0.96	1.44
Cell wall/membrane/envelope biogenesis	0.98	1.12	1.20
Chromatin structure and dynamics	0.02	0.05	0.06
Coenzyme transport and metabolism	1.99	2.52	3.91 [a]
Defense mechanisms	0.55	0.75	0.58
Energy production and conversion	19.18	20.77 [a]	17.66[b]
Function unknown	12.66 [b]	15.82	15.91 [a]
Inorganic ion transport and metabolism	1.65	2.05	2.24
Intracellular trafficking, secretion, and vesicular transport	0.95	0.95	0.89
Lipid transport and metabolism	13.83 [a]	5.54 [b]	7.65
Nucleotide transport and metabolism	2.19	2.26	2.21
Posttranslational modification, protein turnover, chaperones	12.79 [a]	9.91	7.91 [b]
Replication, recombination and repair	3.07	4.09	4.46
Secondary metabolites biosynthesis, transport and catabolism	0.07[b]	0.15	0.34
Signal Transduction	0.67	0.73	1.24
Transcription	3.27	2.81	3.38
Translation, ribosomal structure and biogenesis	17.78	18.35 [a]	13.76 [b]

[a] indicates P<0.05 and significantly more expressed as determined by ANOVA.

[b] indicates P<0.05 and significantly less expressed as determined by ANOVA.

CHAPTER IV

INTERSPECIES ELECTRON TRANSFER DURING SYNTROPHIC FATTY ACID- AND AROMATIC ACID METABOLISM

SUMMARY

Syntrophic degradation of aromatic, alicyclic and fatty acids by obligate syntrophs requires a partner organism to maintain extremely low concentrations of H_2 and/or formate so that the degradation of the initial substrate is thermodynamically favorable. However, recent evidence that syntrophic ethanol metabolism involves direct electron transfer through nanowires raised doubt about the importance of interspecies hydrogen and/or formate transfer. A combination of genomic analysis, gene expression, and enzymatic analyses along with inhibitor-based approaches were used to test whether syntrophic benzoate and cyclohexane carboxylate metabolism by *Syntrophus aciditrophicus* and syntrophic butyrate oxidation by *Syntrophomonas wolfei* involves transfer of H_2 and/or formate or direct electron transfer. The genomes of organisms contain multiple hydrogenase (Hase) and formate dehydrogenase (FDH) genes, but neither genome contains genes for the pilus or cytochrome system implicated in direct electron transfer by nanowires. Syntrophically grown cells and cell-free extracts of *S. aciditrophicus* and *S. wolfei*, separated from their syntrophic partner by Percoll density gradient centrifugation had high hydrogenase and formate dehydrogenase activity. Syntrophic benzoate oxidation and CH_4 production by washed cell suspensions of *S. aciditrophicus* and *M. hungatei* were inhibited by a formate analog, hypophosphite, but not by the Hase inhibitors, cyanide and carbon monoxide. All three inhibitors were equally effective in halting syntrophic cyclohexane carboxylate oxidation. Butyrate metabolism and CH_4 production by washed cell suspensions of *S.*

wolfei and *M. hungatei* were inhibited by Hase inhibitors, but not by the FDH inhibitor. *hydI* and *hydII* were significantly more abundant when *S. wolfei* was grown syntrophically with butyrate than with crotonate, while the FDH were more abundant during syntrophic crotonate metabolism by *S. wolfei*. *fdhII* was highly up-regulated during syntrophic growth on benzoate, while *hydII, fdhI,* and *fdhIII* were up-requlated during benzoate and cyclohexane carboxylate growth, but with less than 2x change over crotonate axenic growth. These results demonstrate the importance of hydrogen transfer for syntrophic butyrate metabolism by *S. wolfei*, formate transfer for syntrophic benzoate metabolism by *S. aciditrophicus* and hydrogen and formate transfer for syntrophic cyclohexane carboxylate metabolism by *S. aciditrophicus*. Thus, the importance of H_2 versus formate transfer depends on the substrate and organism involved.

INTRODUCTION

Syntrophy is a tightly coupled mutualistic interaction among microorganisms that is essential for the global cycling of carbon in essentially all anaerobic environments(Schink, 2006; McInerney et al., 2008). Our basic understanding of the biochemical processes involved in syntrophy is currently limited, and this impacts the modeling of biomass turnover in natural habitats, the control of waste degradation, and the conversion of renewable resources to the energy-rich fuel, methane. In syntrophy, the microbial partners exchange metabolites and the concentrations of these metabolites must be kept very low for syntrophy to proceed. In methanogenic environments, syntrophy involves

the exchange of hydrogen and formate between fermentative syntrophic metabolizers and methanogenic archaea. The syntrophic partner produces hydrogen and formate during the metabolism of the various substrates (e.g., propionate, butyrate, and benzoate) used as their energy source (McInerney et al., 2008; Stams and Plugge, 2009). In return, the methanogen consumes these products, keeping them at the low concentrations necessary to support the degradative reactions catalyzed by the syntrophic metabolizer. For example, the syntrophic degradation of butyrate to acetate and H_2 under standard conditions of one atmosphere (101 kPa) for gases and one molar concentration for soluble compounds at pH 7 is thermodynamically unfavorable with a Gibbs free energy change of +48.6 kJ per mole of butyrate (eq. 1) (McInerney et al., 2009).

$$Butyrate^- + 2\ H_2O \rightarrow 2\ Acetate^- + H^+ + 2\ H_2 \qquad \text{eq. 1}$$

When hydrogen and formate concentrations are kept low by methanogens or other hydrogen/formate users, the degradation of butyrate is energetically favorable with a Gibbs free energy change of -39.2 kJ per mole butyrate (calculated using a H_2 partial pressure of 1 Pa and butyrate and acetate concentrations of 0.1 mM each).

Initial concepts of syntrophic metabolism were based on interspecies hydrogen transfer among the syntrohophic partners as the first syntrophic

consortium contained the ethanol degrader, S organism, and a methanogen that used only hydrogen, *Methanobacterium bryantii* MoH (Bryant et al., 1967). Other syntrophic associations with a methanogen only capable of hydrogen transfer include butyrate-degrading *Syntrophomonas wolfei*, (McInerney et al., 1979; McInerney et al., 1981b), glycolate-degrading *Syntrophobotulus glycolicus* (Friedrich et al., 1996), glucose-degrading *Syntrophococcus sucromutans* (Krumholz and Bryant, 1986), and the thermophilic, acetate-oxidizing strain AOR (Lee and Zinder, 1988). However, others have argued that diffusion of hydrogen is too slow to account for syntrophic metabolism (Conrad et al., 1985; Boone et al., 1989). High levels of activity and protein of formate dehydrogenases in cell extracts, the up-regulation of their genes during syntrophic propionate metabolism, and the inability to establish consortia with methanogens that used only hydrogen indicated that formate rather than hydrogen was the dominant interspecies electron carrier in *Syntrophobacter fumaroxidans* (de Bok et al., 2002a; de Bok et al., 2002b; de Bok et al., 2003; Worm et al., 2011). The transfer of formate during syntrophic metabolism has also been shown to be an important in upflow anaerobic sludge blanket reactor (UASB) (Thiele and Zeikus, 1988). However, in many cases, the argument to rule out hydrogen transfer in these systems, and support for formate transfer is mathematical rather than experimental (Boone et al., 1989).

Other possibilities exist for exchange of reducing equivalents among syntrophic partners such cysteine exchange (Kaden et al., 2002) and direct

electron transfer by nanowires (Reguera et al., 2005, Summers, 2010 #3297). Direct electron transfer via nanowires rather than hydrogen transfer has been proposed for adapted cocultures of *Geobacter metallireducens* and *Geobacter sulfurreducens* that syntrophically degrade ethanol (Summers et al., 2010). The aggregates were electron conductive and syntrophic ethanol metabolism was not affected when a hydrogenase mutant of *G. sulfurreducens* was used. Syntrophic degradation of ethanol is not as sensitive to hydrogen concentrations as syntrophic fatty acid oxidation (Seitz et al., 1988; Seitz et al., 1990; Schink, 1997). Direct electron transfer by nanowires is thought to occur by conductive pili (Reguera et al., 2005; Gorby et al., 2006) and an extensive extracellular cytochrome *c* network, which included cytochromes bound to the pili and in the outer membrane (Leang et al., 2010). So far, evidence for direct electron transfer has only been obtained with a limited set of microorganisms; specifically metal-reducing microorganisms in the genera *Geobacter* and *Shewanella* (Gorby et al., 2006). The limited number of microorganisms involved in direct electron transfer may indicate that this is a specialize type of syntrophic metabolism and not used by most fatty and aromatic acid degrading syntrophic metabolizers.

To determine the importance of hydrogen and formate transfer in syntrophic fatty and aromatic acid metabolism, the enzymes and genes involved in syntrophic butyrate metabolism by *S. wolfei* (McInerney et al., 1981b; Sieber et al., 2010b) and syntrophic benzoate and cyclohexane carboxylate by

Syntrophus aciditrophicus (Jackson et al., 1999; McInerney et al., 2007) were studied. Both of these organisms maintain an obligate syntrophic partnership with the methanogen, *Methanospirillum hungatei*, when degrading the above compounds. Their relationship is considered obligate, because metabolism of the above compounds requires the activity of the methanogen to maintain low pool sizes of hydrogen and/or formate (Stams and Plugge, 2009). Both can grow axenically on crotonate (Beaty and McInerney, 1987; Jackson et al., 1999).

RESULTS

Whole cell enzyme activity of hydrogenase and formate dehydrogenase

The specific activities of hydrogenase and formate dehydrogenase in washed cell suspensions of *S. wolfei* grown axenically on crotonate and in coculture with *M. hungatei* on crotonate and on butyrate were determined (Table 1). Because hydrogenases and formate dehydrogenases are often internally or externally oriented, two redox sensitive dyes, a membrane impermeable dye, methyl viologen, and a membrane permeable dye, benzyl viologen, where used to detect the activity. Washed cell suspensions of *S. wolfei* contained both hydrogenase and formate dehydrogenase activities under all growth conditions (Table 1). The specific activities for formate dehydrogenase were two to five-fold higher when *S. wolfei* was grown on crotonate either axenically or syntrophically than when grown syntrophically on butyrate. The specific activities for formate dehydrogenase were higher than

hydrogenase specific activities for all conditions. Formate dehydrogenase activity with benzyl viologen was 19-fold higher during syntrophic butyrate or crotonate growth and 3-fold higher during axenic growth on crotonate than hydrogenase activity. Formate dehydrogenase activity was higher with benzyl viologen than with methyl viologen as the acceptor, suggesting that most of the activity was internal. The hydrogenase activity was higher with benzyl viologen than methyl viologen in crotonate-grown cells, indicating a dominant internal hydrogenase. In butyrate-grown cells, hydrogenase activities with benzyl viologen and methyl viologen were comparable, suggesting that the activity was externally oriented. Localization of activity using these dyes can be problematic if the integrity of cell membrane has been compromised. To address this issue, the cells were broken and the membrane was separated from the soluble fraction by centrifugation.

Table 1. Specific activities for hydrogenase and formate dehydrogenase in whole cells of *S. wolfei.*

	Hydrogenase	Formate Dehydrogenase
Butyrate with *M. hungatei*		
Methyl Viologen	0.15 ± 0.05[a]	0.63 ± 0.23
Benzyl Viologen	0.22 ± 0.07	4.22 ± 0.65
Crotonate with *M. hungatei*		
Methyl Viologen	0.18 ± 0.074	3.17 ± 1.01
Benzyl Viologen	0.77 ± 0.22	15.39 ± 2.79
Crotonate axenic		
Methyl Viologen	0.72 ± 0.19	2.14 ± 0.60
Benzyl Viologen	2.42 ± 0.19	7.14 ±0.96

[a] Mean ± standard deviation of whole cell specific activities expressed as $\mu mol \cdot min^{-1} \cdot mg^{-1}$ of protein.

Hydrogenase activity was found in both the membrane and the soluble fractions in *S. wolfei* cells under all conditions (Table 2). In crotonate-grown cells, most of the hydrogenase activity was found in the membrane. In butyrate-grown cells, the activity in the soluble fraction (0.297 ± 0.067 μmol•min^{-1}•mg^{-1} of protein) was approximately twice as active as that found in the membrane fraction (0.165 ± 0.03 μmol•min^{-1}•mg^{-1} of protein). These data suggest that at least two hydrogenases are active in *S. wolfei*. Formate dehydrogenase was predominately detected in the soluble fraction of the cell. Little formate dehydrogenase activity was detected in the membrane fraction. In butyrate-grown cells, the activity found in the soluble and membrane fractions was lower than in the crude extract, suggesting that some of the activity was lost upon cell breakage.

Table 2. Localization of hydrogenase and formate dehydrogenase activity in *S. wolfei* by cell fractionation

	Hydrogenase	Formate Dehydrogenase
Butyrate with *M. hungatei*		
Crude Extract	0.52 ± 0.04	0.51 ± 0.03
Soluble Fraction	0.30 ± 0.07	0.24 ± 0.08
Membrane Fraction	0.17 ± 0.03	0.003 ± 0.00
Crotonate with *M. hungatei*		
Crude Extract	1.12 ± 0.13	0.22 ± 0.06
Soluble Fraction	0.61 ± 0.18	0.29 ± 0.07
Membrane Fraction	1.15 ± 0.27	0.002 ± 0.00
Crotonate axenic		
Crude Extract	0.48 ± 0.07	0.34 ± 0.09
Soluble Fraction	0.15 ± 0.04	0.12 ± 0.03
Membrane Fraction	0.33 ± 0.01	0.01 ± 0.02

[a] Mean ± standard deviation of specific activities expressed as $\mu mol \cdot min^{-1} \cdot mg^{-1}$ of protein.

Similar experiments were conducted with *S. aciditrophicus* grown axenically on crotonoate and syntrophically on benzoate and cyclohexane-1-carboxylate (Tables 3 and 4). Washed cell suspensions of *S. aciditrophicus* contained both hydrogenase and formate dehydrogenase activities under all growth conditions (Table 3). Activities of each enzyme varied with growth condition. Formate dehydrogenase activity with benzyl viologen was higher than hydrogenase activity when *S. aciditrophicus* was grown syntrophically on benzoate and cyclohexane carboxylate and axenically on crotonate (Table 3). Levels of formate dehydrogenase were much lower in syntrophically grown cells on crotonate compared to other growth conditions. Hydrogenase and formate dehydrogenase activity with benzyl viologen was at least three fold higher during syntrophic growth on cyclohexane carboxylate than during syntrophic growth on benzoate or crotonate. Formate dehydrogenase activity was higher with benzyl viologen than methyl viologen under all conditions tested, implicating the presence of internally and externally oriented enzymes. Hydrogenase activity with benzyl viologen was higher with methyl viologen only in crotonate-grown cells. For all other growth conditions, an externally oriented hydrogenase appears to be dominant (Table 3). When the cells were exposed to $CuCl_2$, 90% of the formate dehydrogenase activity and 99.9% of the hydrogenase activity were inhibited (data not shown), which provides additional evidence for externally oriented enzymes.

Table 3. Specific activities for hydrogenase and formate dehydrogenase in whole cells of *S. aciditrophicus*

	Hydrogenase	Formate Dehydrogenase
Benzoate w/ *M. hungatei*		
Methyl Viologen	0.41 ± 0.10	0.35 ± 0.09
Benzyl Viologen	0.25 ± 0.08	0.86 ± 0.17
Cyclohexane Carboxylate w/ *M. hungatei*		
Methyl Viologen	0.27 ± 0.07	2.29 ± 0.63
Benzyl Viologen	1.21 ± 0.20	3.12 ± 0.29
Crotonate w/ *M. hungatei*		
Methyl Viologen	0.31 ± 0.07	0.09 ± 0.02
Benzyl Viologen	0.22 ± 0.09	0.14 ± 0.02
Crotonate		
Methyl Viologen	1.19 ± 0.40	0.46 ± 0.07
Benzyl Viologen	0.55 ± 0.06	1.59 ± 0.03

[a] Mean ± standard deviation of whole cell specific activities expressed as $\mu mol \cdot min^{-1} \cdot mg^{-1}$ of protein.

Fractionation of *S. aciditrophicus* cells confirmed the presence of both soluble and membrane-bound hydrogenases although the membrane-bound activity was low in crotonate-grown cells (Table 4). Most of the hydrogenase activity was found in the membrane fraction in cells grown syntrophically on benzoate and on crotonate. Conversely, most of the hydrogenase activity was found in the soluble fraction in cells grown on cyclohexane carboxylate. Formate dehydrogenase activity was primarily found in the soluble fraction. Very little membrane-bound formate dehydrogenase activity was detected under any growth condition. The specific activities found in cell extracts were much lower than the corresponding specific activity detected in whole cells, indicating that some of the activity was lost upon breakage.

Table 4. Localization of hydrogenase and formate dehydrogenase activity in *S. aciditrophicus* by cell fractionation

	Hydrogenase	Formate dehydrogenase
Benzoate w/ *M. hungatei*		
Crude Extract	0.34 ± 0.04	0.11 ± 0.01
Soluble Fraction	0.12 ± 0.01	0.10 ± 0.00
Membrane Fraction	0.28 ± 0.04	0.04 ± 0.01
Cyclohexane Carboxylate w/ *M. hungatei*		
Crude Extract	0.56 ± 0.07	0.28 ± 0.05
Soluble Fraction	0.40 ±0.05	0.31 ± 0.05
Membrane Fraction	0.20 ± 0.07	0.01 ± 0.00
Crotonate w/ *M. hungatei*		
Crude Extract	0.26 ± 0.00	0.11 ± 0.01
Soluble Fraction	0.04 ± 0.01	0.08 ± 0.01
Membrane Fraction	0.20 ± 0.03	0.02 ± 0.00
Crotonate		
Crude Extract	0.22 ± 0.03	0.21 ± 0.04
Soluble Fraction	0.05 ± 0.00	0.11 ± 0.02
Membrane Fraction	0.11 ± 0.01	ND

[a] Mean ± standard deviation of specific activities expressed as $\mu mol \cdot min^{-1} \cdot mg^{-1}$ of protein.

Inhibition of hydrogenase and formate dehydrogenase in washed cell suspensions

To assess the need for interspecies hydrogen and formate transfer, the effect of three inhibitors on syntrophic metabolism was determined. Hypophosphite is a formate analog (Takamiya, 1953) while cyanide and carbon monoxide are both hydrogenase inhibitors (Hoberman and Rittenberg, 1943; Farkas and Fischer, 1947). Carbon monoxide is a more specific inhibitor than cyanide, but mass-transfer limitations from gas to liquid requires the cultures to be shaken. A caveat to using carbon monoxide is that shaking syntrophic cultures will often cause uncoupling of the syntrophic association, either due to the increase dispersion of metabolites and disaggregation of the cells. Cells of cocultures of *S. aciditrophicus* and *M. hungatei* and *S. wolfei* and *M. hungatei* as well as pure cultures of *S. aciditrophicus* and *S. wolfei* grown on respective substrates were resuspended in medium with 100 µM substrate and the inhibitor in the range 250 µM to 1 mM for hypophosphite and cyanide and 5 to 15% of the gas phase for CO. These concentrations of inhibitors were chosen after being found to inhibit methane production by pure cultures of *M. hungatei* (Table 5), but did not to inhibit crotonate fermentation by *S. aciditrophicus* (Table 6) or *S. wolfei* (Table 7).

Table 5. Inhibition of washed cell suspensions of *M. hungatei* with hydrogen, formate, or formate and hydrogen as electron donors for methane production.

% Inhibition of Methane Production	Hypophosphite 0.25mM	Cyanide 1mM	15% Carbon Monoxide
Hydrogen	0%	95%	100%
Formate	100%	0%	9%
Formate and Hydrogen	34%	90%	47%

All data presented as percentage of the inhibition of methane produced as compared to the respective positive control.

For *S. aciditrophicus* cocultures grown on benzoate, hypophosphite completely inhibited benzoate oxidation and methane production (Table 6). Cyanide and carbon monoxide did not inhibit benzoate utilization or methane production significantly. These results indicated that formate transfer is essential for syntrophic benzoate utilization by *S. aciditrophicus*. For the cocultures on cyclohexane carboxylate, all three inhibitors were equally effective (see Table 6). No methane was produced in any of the inhibited cultures and less than 20% of the initial amount of cyclohexane carboxylate was utilized. These data indicate that both hydrogen and formate transfer are important for syntrophic cyclohexane carboxylate metabolism.

Table 6. Summary of *S. aciditrophicus* and *M. hungatei* washed cell suspension inhibition experiments.

	S. aciditrophicus/ *M. hungatei*		*S. aciditrophicus*/ *M. hungatei*		*S. aciditrophicus*
Treatment	Benzoate Loss (in µmoles)	Methane Production (in µmoles)	Cyclohexane Carboxylate Loss (in µmoles)	Methane Production (in µmoles)	Crotonate Loss (in µmoles)
Positive Control	2.17±0.13	2.63±0.05	1.61±0.26	0.56±0.05	2.00±0.10
1 mM NaCl	2.16±0.18	1.60±0.26	1.72±0.04	0.83±0.11	1.92±0.07
0.25 mM $H_2PO_2^-$	0.47±0.07	BDL	0.36±0.05	BDL	1.66±0.33
0.5 mM $H_2PO_2^-$	0.49±0.04	BDL	0.29±0.09	BDL	2.03±0.23
1.0 mM $H_2PO_2^-$	0.44±0.16	BDL	0.10±0.03	BDL	2.14±0.19
0.25 mM CN	1.41±0.10	2.64±0.24	0.15±0.15	BDL	1.83±0.06
0.5 mM CN	1.41±0.09	1.41±0.26	0.08±0.02	BDL	2.50±0.25
1.0 mM CN	1.70±0.07	1.42±0.35	0.16±0.03	BDL	1.64±0.12
Shaking	1.94±0.22	2.50±0.20	1.16±0.79	0.26±0.08	2.18±0.19
5% CO	1.94±0.23	1.74±0.04	0.30±0.08	BDL	1.23±0.20
10% CO	2.05±0.01	1.76±0.10	0.32±0.10	BDL	1.84±0.26
15% CO	1.95±0.04	1.66±0.10	0.25±0.05	BDL	2.00±0.23

BDL stands for below detection limit.

Cyanide and CO syntrophic butyrate metabolism and methane production by washed cell suspensions of cocultures of *S. wolfei* and *M. hungatei* but not crotonate metabolism by axenically or coculture grown cells (Table 7). Cyanide also inhibited crotonate metabolism and methane production by *S. wolfei-M. hungatei* coculture cells, but had little effect on crotonate metabolism by cells of axenically grown *S. wolfei*. Hypophosphite was not an effective inhibitor syntrophic butyrate or crotonate metabolism. These results indicate that hydrogen, but not formate, transfer is essential for electron carrier during syntrophic metabolism by *S. wolfei*. The inhibition of methane production but not crotonate use in cocultures of *S. wolfei* and *S. aciditrophicus* in the presence of inhibitors is expected because both organisms can ferment crotonate without interspecies hydrogen or formate transfer.

Table 7. Inhibition of washed cell suspensions of *S. wolfei* and *M. hungatei* with butyrate or crotonate. BDL stands for below detection limit.

	S. wolfei/ M. hungatei		*S. wolfei/ M. hungatei*		*S. wolfei*
Treatment	**Butyrate loss (in µmoles)**	**CH_4 Produced (in µmoles)**	**Crotonate loss (in µmoles)**	**CH_4 Produced (in µmoles)**	**Crotonate loss (in µmoles)**
Positive Control	16.2±1.65	20.8±7.81	23.8±0.50	13.4±0.28	17.8±1.59
1 mM NaCl	15.2±2.84	19.7±3.52	23.4±0.64	10.9±0.94	18.6±0.87
0.25 mM $H_2PO_2^-$	16.8±1.48	24.3±11.4	23.4±0.60	10.7±0.58	15.2±0.41
0.5 mM $H_2PO_2^-$	19.8±4.78	39.2±0.62	23.4±1.26	11.0±1.54	15.8±0.53
1.0 mM $H_2PO_2^-$	21.4±3.12	33.6±1.80	23.2±0.50	7.62±3.88	14.8±0.76
0.25 mM CN	1.66±0.22	0.48±0.28	24.0±0.28	5.56±0.68	16.0±0.63
0.5 mM CN	3.82±1.55	0.26±0.04	22.6±0.26	2.8±1.14	15.9±1.33
1.0 mM CN	4.22±1.65	0.26±0.14	23.6±0.40	1.52±1.32	15.4±1.36
Positive control-shaking	10.6±0.80	22.7±1.36	23.6±0.24	10.9±0.08	15.0±0.49
5% CO-shaking	7.17±3.65	2.62±0.64	23.8±0.52	0.28±0.12	15.1±0.79
10% CO-shaking	5.87±0.14	1.14±0.92	23.4±0.70	BDL	13.8±0.66
15% CO-shaking	1.45±1.31	0.18±0.02	22.8±1.34	BDL	12.1±0.74

BDL stands for below detection limit.

Expression of hydrogenases and formate dehydrogenases

To determine which hydrogenases and formate dehydrogenases were the most abundant in the cells of *S. wolfei* and *S. aciditrophicus* under different growth conditions, quantitative-reverse transcriptase pcr (Q-RT-PCR) was used. Primers for *S. wolfei* genes (Table 8) were designed using NCBI-Primer BLAST, which selected primer sequences with specificity to *S. wolfei* while excluding primers that bind to *M. hungatei* DNA or RNA. The gene for the major subunit of each hydrogenase or formate dehydrogenase was targeted for Q-RT-PCR. The list of hydrogenase or formate dehydrogenase genes, their predicted functions, and their respective primers can be found in Table 8. There are six predicted formate dehydrogenase genes. Four formate dehydrogenases are predicted to be soluble systems and NADH dependent. Two formate dehydrogenases are predicted to be membrane-bound and interactive with menaquinone. Three hydrogenase gene clusters are found in the genome of *S. wolfei* (Sieber et al., 2010b), two of which are predicted to be soluble and one is predicted to be membrane-bound.

Table 8. Primers for Q-RT-PCR analysis of the hydrogenases and formate dehydrogenases of *S. wolfei*.

Gene	Locus Tag	Localization	Function	Primer Sequence (5'-3')
gyrB	Swol_0006	cytoplasm	DNA gyrase	TGAAGGACAGACCAAAACCA
				AATATAGCCTGGTAGGTGCG
hyd-1	Swol_1017	cytoplasm	NADH + Fd_{red} ↔ H_2 +NAD^+ +Fd_{ox}	CAGAGTGGCTATTGCTGAAG
				TCAATACCCATCTTCTCGGC
hyd-2	Swol_1925	membrane	MQ ↔ H_2	TATGCGGAGGACAACTACCC
				CTGAGGATTTCATAGGCGGT
hyd-3	Swol_2436	cytoplasm	Fd_{red} ↔ H_2	ATTTCACTGCCGATCTCACC
				AGTAGGCACCTCCCATTCTA
fdh-1	Swol_0658	cytoplasm	Formate ↔ NADH	AAGGCGGTTGCGTAGTTTTG
				AATCCCCCATTCCCATTCGG
fdh-2	Swol_0786	membrane	Formate ↔ MQ	CATAGAAGCCAACCGGGAAA
				CCCTTCTCTCGGTGTTGGTA
fdh-3	Swol_0800	cytoplasm	Formate ↔ NADH	CAGCATCAGCAGCAAAAGAG
				CTTCCCACTTGTCACTACCA
fdh-4	Swol_1028	cytoplasm	Formate ↔ NADH	GAATACCCGTTCCTGCTTTC
				GCTTAACCGCACAGACCTTG
fdh-5	Swol_1825	membrane	Formate ↔ MQ	CCAAGAACAACCCAGCAAAT
				GGGGTTTTAATGCCACTTCC
fdh-6	Swol_1830	cytoplasm	Formate ↔ NADH	TGGAACCAATCCTACCGAAG
				TACAGGTCATCCACCGAGA

mRNA of *S. wolfei* and *M. hungatei* was purified from axenically and syntrophically grown cultures on crotonate and syntrophically grown cultures on butyrate. In order to make quantitative comparisons among the different growth conditions, the expression level of each hydrogenase or formate dehydrogenase gene was compared to that of a DNA gyrase subunit, whose expression is needed under all growth conditions. Transcripts from all three hydrogenases and six formate dehydrogenases were detected in all three, growth conditions (Figure 1). Five of the formate dehydrogenases (*fdhII, fdhIII, fdhIV, fdhV* and *fdhVI*) were more highly expressed in cells grown syntrophically on crotonate or butyrate compared to axenically grown cells on crotonate. Also, expression levels of *fdhII, fdhIII, fdhIV, fdhV* and *fdhVI* were higher in syntrophically grown cells on crotonate than on butyrate. *fdhII*, *fdhIV*, and *fdhVI* encode for NADH-dependent, formate dehydrogenase while *fdhIII* and *fdhV* encoding for a membrane-bound formate dehydrogenases. *hydI*, encoding the putative confurcating hydrogenase, and *hydII*, the membrane-bound hydrogenase, were 100-fold more abundant under syntrophic growth on butyrate than axenic growth on crotonate (Figure 1). These two hydrogenases were about 50-fold more abundant under syntrophic growth on crotonate as compared to axenic growth on crotonate. *hydI* and *hydII* were significantly more abundant grown syntrophically with butyrate than during axenic crotonate. *hydIII*, encoding for a Fe-only hydrogenase, is more highly expressed in syntrophically grown cells with crotonate than with butyrate, although not to the extent of *hydI*

or *hydII*. The expression of formate dehydrogenase genes was much lower in butyrate versus crotonate grown cells compared to that for *hydI* and *hydII*. The up-regulation of *hydI* and *hydII* in butyrate-grown cells argues for the importance of hydrogen transfer during syntrophic butyrate metabolism. Two to the formate dehydrogenases, *fdhIII* and *fdhVI*, were significantly up-regulated during syntrophic growth on crotonate in comparison to axenic crotonate growth and syntrophic growth on butyrate.

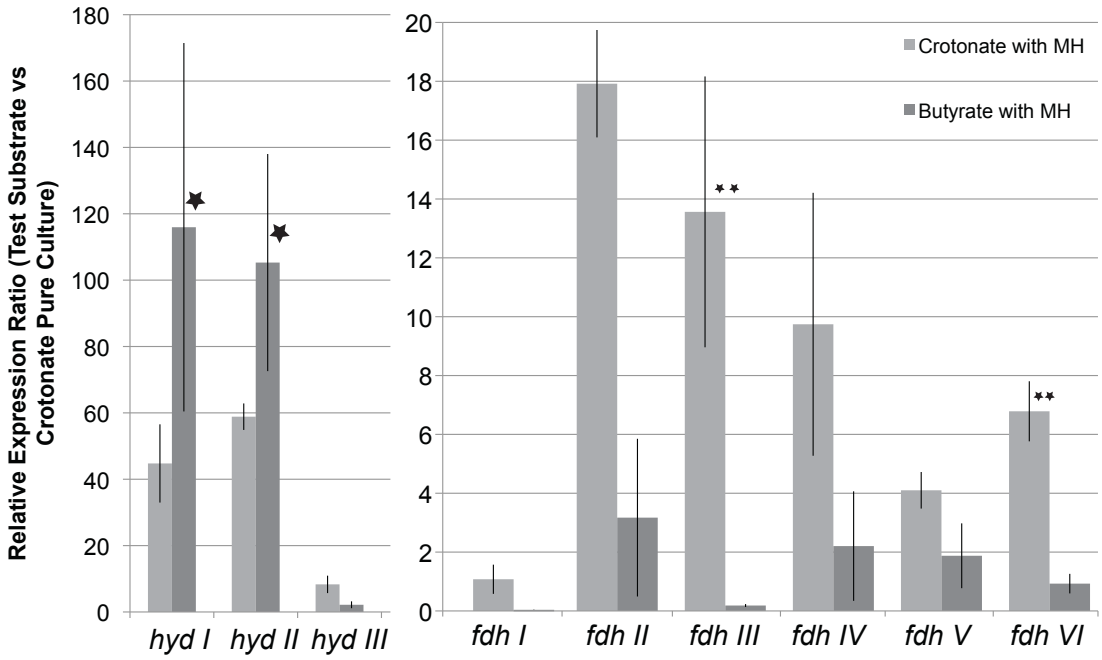


Figure 1. Response of hydrogenases and formate dehydrogenases gene expression to growth condition of *S. wolfei.* MH is *M. hungatei* * indicates P<0.05 and significantly more expressed during syntrophic versus axenic crotonate growth as determined by ANOVA. ** indicates P<0.05 and significantly more expressed during syntrophic crotonate versus butyrate growth and syntrophic crotonate versus axenic crotonate growth as determined by ANOVA.

Primers for *S. aciditrophicus* hydrogenase and formate dehydrogenase genes were designed the same way as the primers for *S. wolfei* (Table 9). *S. aciditrophicus* contains genes encoding a cytoplasmic Fe-only hydrogenase, *hydI* (SYN1370) and a cytoplasmic Ni-Fe-type hydrogenase, *hydII* (SYN2219 to SYN2222) (McInerney et al., 2007). There are also two cytoplasmic, *fdhI* and *fdhII*, and two periplasmic formate dehydrogenases, *fdhII* and *fdhIII*. Thus, like *S. wolfei, S. aciditrophicus* has the genetic potential to use both hydrogen and formate.

Table 9. Primers for Q-RT-PCR analysis of the hydrogenases and formate dehydrogenases of *S. aciditrophicus*.

Gene	Locus Tag	Localization	Function	Primer Sequence (5'-3')
gyrB	SYN_02049	cytoplasm	DNA gyrase	TGTGGACGGTTCTCATATCC TCCTGAATGGTGAAAGAGGG
hydI	SYN_01370	cytoplasm	NADH + Fd_{red} ↔ H_2 +NAD^+ +Fd_{ox}	AATCACCCCAGCAGATGTTC GCTCTTCTCCGGTAACGAC
hydII	SYN_02222	cytoplasm	Fd_{red} ↔ H_2	CCGAAGAACTGGGTTTGAAG CGAACCAGCATTTCCATCTT
fdhI	SYN_00603	membrane	Formate ↔ MQ	GGGACTTACGGATGGGAAAT GAATGATGCACATGGTACGG
fdhII	SYN_00629	cytoplasm	Formate ↔ NADH	CCACGGAAAAGGAATCTTCA TGAGCAATGCCAAGTTTCTG
fdhII-2	SYN_00634	membrane	Formate ↔ MQ	ATCTGGACAGCAAAGGACAT GAGTTTGCGTTTGGGATTGT
fdhIII	SYN_01672	cytoplasm	Formate ↔ NADH	ATCTATACGACGCCGCATTC GCCGCTCTTTGAGTTGGATA
fdhIV	SYN_02138	cytoplasm	Formate ↔ NADH	ACGGTCACACCCTCTTATGC TTTCCGATATTTTCGCCTTG

Response ratios of the expression of the catalytic units of the hydrogenase and formate dehydrogenase genes show that only *fdhII* was differentially expressed (greater than 2-fold change in expression ratio) under any of the tested growth conditions (Figure 2). *fdhII* was up-regulated during syntrophic benzoate growth, which is consistent with the inhibition studies that found formate transfer to be essential for syntrophic benzoate metabolism. *fdhII* may be part of an operon containing both internal and external subunits (McInerney et al., 2007). None of the *hyd* or *fdh* were found to be significantly differentially expressed by ANOVA.

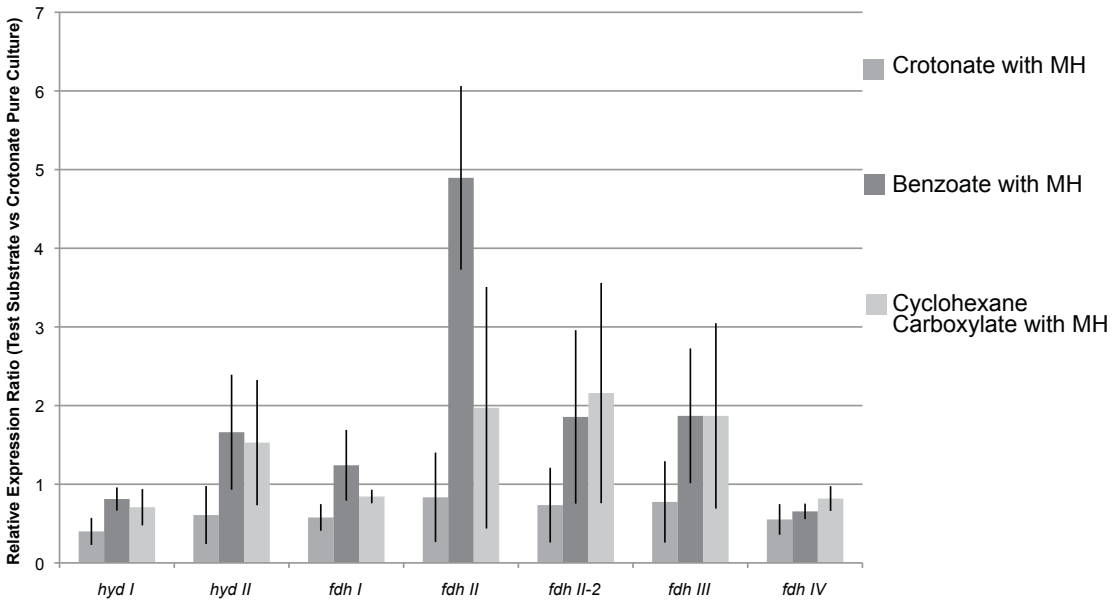


Figure 2. Response of hydrogenases and formate dehydrogenases gene expression to growth condition of *S. aciditrophicus.* MH is *M. hungatei.*

DISCUSSION

The discovery of electron conductive pili in propionate-degrading coculture of *Pelotomaculum thermopropionicum* with its methanogenic partner (Ishii et al., 2005; Gorby et al., 2006) and the fact the deletion of the gene for hydrogenase in *Geobacter sulfurreducens* did not affect syntrophic ethanol metabolism by *Geobacter metallireducens* and *Geobacter sulfurreducens* coculture (Summers et al., 2010) has raised doubts about the importance of hydrogen and formate in syntrophic metabolism. In addition, kinetic analyses suggested that hydrogen turnover was too slow to account for methane production in aquatic sediments (Conrad et al., 1985). Some studies pointed to aggregation of cells in cocultures as evidence of direct electron transfer (Gorby et al., 2006). However, I found that disruption of aggregates of *S. aciditrophicus* or *S. wolfei* with *M. hungatei* by shaking did not greatly effect substrate utilization or methane production (see Tables 6 and 7). Decreasing the distance between the partners by aggregation would be expected to enhance the rates of syntrophic metabolism by decreasing the diffusion distance for metabolite transfer (Ishii et al., 2005; Ishii et al., 2006). Genome analysis revealed neither *S. aciditrophicus* or *S. wolfei* have the multiheme *c*-type cytochrome system that has been shown to be necessary for direct electron transfer (Leang et al., 2003; Leang et al., 2010). Also, both organisms lack homologues to the pili gene found in *Geobacter sulfurreducens* that has also been implicated in direct electron transfer. Interestingly cocultures of *Geobacter metallireducens* and *G.*

sulfurreducens use direct electron transfer only when other electron shuttles, like cysteine, are excluded (Summers et al., 2010).

We found that *S. wolfei* and *S. aciditrophicus* contain genes for both hydrogenases and formate dehydrogenases and expressed these genes under most growth conditions tested. In *S. wolfei*, *hydI* and *hydII* were highly up-regulated (50-100-fold) when *S. wolfei* was grown syntrophically with butyrate or crotonate, implicating their function in syntrophic metabolism (Fig. 1). In *S. aciditrophicus*, *fdhII* was up-regulated in syntrophically grown cells with benzoate (Fig. 2). The effect of hydrogenase and formate dehydrogenase inhibitors provides additional support for the importance of hydrogen and formate transfer during syntrophic metabolism by *S. wolfei* and *S. aciditrophicus*. The inhibition of syntrophic methane production and butyrate metabolism by carbon monoxide and cyanide, but not by hypophosphite (Table 7), implicates that hydrogen transfer is essential for syntrophic butyrate metabolism by *S. wolfei*. Inhibition of syntrophic methane production and benzoate metabolism by hypophosphite, but not by carbon monoxide or cyanide, and inhibition of syntrophic methane production and cyclohexane carboxylate metabolism by all three inhibitors implicates the importance of formate transfer for syntrophic benzoate metabolism and both formate and hydrogen transfer for syntrophic cyclohexane carboxylate metabolism. My results along with those for *S. fumaroxidans,* which primarily uses formate as an electron carrier (Dong and Stams, 1995b; Stams and Dong, 1995; de Bok et al., 2002a; de Bok et al.,

2002b; de Bok et al., 2003; Worm et al., 2011) and *P. thermopropionicum,* which uses hydrogen as an electron carrier (Ishii et al., 2005), show that many obligately syntrophic communities rely on hydrogen and formate transfer between partners.

A second question is whether interspecies electron transfer actually involves hydrogen at all (Thiele and Zeikus, 1988; Boone et al., 1989; de Bok et al., 2002a). Based on pool size measurements and diffusion rates, these authors argued that the rate of hydrogen flux would be too slow to account for the observed methane production rates. Instead, the syntrophic partners must have exchanged formate. My work shows that both interspecies hydrogen and formate transfer are possible although inhibitor studies implicate that the transfer of one or both of these molecules is essential depending on the substrate and organism involved. Enzyme analyses of *S. wolfei* (Tables 1 and 2) and *S. aciditrophicus* grown axenically and syntrophically (Tables 3 and 4) show that hydrogenase and formate dehydrogenase activity is present in both organisms under all growth conditions tested. Thus, they have the enzymatic machinery for hydrogen and formate production. Formate dehydrogenase activities were much higher than hydrogenase activities in *S. wolfei* under almost all growth conditions, which implicates a more important role for formate transfer in *S. wolfei* than previously thought (McInerney et al., 1981b). However, inhibition and gene expression studies argue that hydrogen transfer is essential during syntrophic butyrate metabolism by *S. wolfei* (Table 7; Fig. 1). It may be

that there is some essential redox reaction in *S. wolfei* that is coupled exclusively to hydrogen production. Other redox reactions could funnel reducing equivalents to either hydrogen or formate production. This scenario would explain the need for hydrogen production but also why *S. wolfei* contains both hydrogenase and formate dehydrogenase activities. Alternatively, formate may play a role in energy conservation, similar to the hydrogen cycling mechanisms found in most sulfate reducers (Heidelberg et al., 2004).

Inhibitor and gene expression studies argue that *S. aciditrophicus* relies on formate transfer during syntrophically benzoate metabolism (Table 6 and Fig. 2). The important formate dehydrogenase gene appears to be *fdhII*, based on gene expression work. This formate dehydrogenase is predicted to be soluble and may account for the observed formate dehydrogenase activity. *S. aciditrophicus* appears to rely on both hydrogen and formate transfer for syntrophic cyclohexane carboxylate metabolism as both hydrogenase and formate dehydrogenase inhibitors inhibited syntrophic cyclohexane carboxylate metabolism (Table 6). *hydII*, *fdhII*, *fdhII-2*, and *fdhIII* were expressed during growth on cyclohexane carboxylate. Genomic analysis did not predict that *S. aciditrophicus* contains membrane-bound hydrogenase (McInerney et al., 2007), although studies with whole cells (Table 3) and cell fractions (Table 4) showed that much of the hydrogenase activity appeared to be localized to the membrane.

In *S wolfei*, two hydrogenase genes, *hydI and hydII*, were highly expressed during syntrophic growth (Fig. 1). *hydI* has three contiguous genes, Swol_1017-1019, which are predicted to encode a confurcating Fe-only hydrogenase based on sequence homology and the presence of a NADH dehydrogenase gene (Swol_1018) (Schut and Adams, 2009; Sieber et al., 2010b). *hydII* also has three contiguous genes, Swol_1925-1927, and is predicted to encode a membrane-bound, cytochrome *b*-linked hydrogenase (Sieber et al., 2010b). Hydrogenase activity was found in both the soluble and membrane portions of the cell, which correlates with the predicted placement of HydI and HydII. Moreover, inhibition of hydrogen transfer between *S. wolfei* and *M. hungatei* halted both methane production and butyrate metabolism during syntrophic growth (Table 7), signifying the essential role of hydrogen transfer. The high expression levels of *hydI and hydII* during syntrophic growth argue for the importance of the genes in interspecies hydrogen transfer and syntrophic metabolism.

This work on the interspecies electron transfer mechanisms of *S. wolfei* and *S. aciditrophicus* coupled with previous studies of *S. fumaroxidans* (de Bok et al., 2002a; de Bok et al., 2002b; de Bok et al., 2003; Worm et al., 2011), *S. bryantii,* (Dong and Stams, 1995b, a; Stams and Dong, 1995) and *P. thermopropionicum*, (Ishii et al., 2005; Kato et al., 2009; Shimoyama et al., 2009) show that hydrogen and/or formate are the important metabolites for obligate interspecies electron transfer.

METHODS

Pure cultures of *Syntrophus aciditrophicus* strain SB (ATCC 700169), *Syntrophomonas wolfei* (DSM 2245B), and *Methanospirillum hungatei* (ATCC 27890) were grown anaerobically as described previously (McInerney et al., 1979). The media were prepared using a modified Balch technique (Balch and Wolfe, 1976). The headspace was pressurized to 27.5 kPa with N_2/CO_2 (80:20 v/v). Cultures were incubated at 37°C without shaking, except *M. hungatei* which was shaken at 125 rpm with a headspace pressurized with 172 kPa of H_2/CO_2 (80:20 v/v). The culture purity was checked daily by microscopic examination and inoculation of a thioglycolate medium. Cells were harvested at mid-log phase of growth by centrifugation (14,300 x G, 20min, 4°C). *S. aciditrophicus* was grown in pure culture on 20 mM crotonate on a minimal medium, in coculture with *M. hungatei* on 20 mM crotonate, 12 mM benzoate, or 12 mM cyclohexane carboxylate. *S. wolfei* was grown in pure culture on 20 mM crotonate (Beaty and McInerney, 1987), in coculture with *M. hungatei* on 20 mM crotonate or 20mM butyrate.

Cultures for enzyme assays were grown 2 liter sealed anaerobic bottles, with 1.6 liters of culture and harvested during late log phase growth. Cultures for Q-RT-PCR were grown in 500 ml sealed anaerobic bottles, with 350 ml of culture, all substrate concentrations are the same as listed above. These cultures were harvested at 50% substrate loss.

One ml samples were taken daily to measure substrate depletion and product formation. Methane formation by cocultures was measured by daily headspace analysis.

Analytical procedures

Growth was monitored by measuring optical density at 600 nm. The concentrations of crotonate, cyclohexane carboxylate, benzoate, cyclohex-1-ene carboxylate, and acetate were determined by high performance liquid chromatography with a Prevail Organic acid column (250 by 4.6 mm; particle size 5 µm; Alltech Inc., Deerfield, Ill.) at a flow rate of 1 ml/min. The isocratic mobile phase consisted of 25 mM KH_2PO_4 (pH 2.5) to measure acetate concentrations. A mobile phase of 60% (v/v) KH_2PO_4 (25 mM, pH 2.5):40% (v/v) acetonitrile was used to quantify crotonate, cyclohexane carboxylate, and benzoate. The UV absorbance detector was set at 210 nm to detect acetate and cyclohexane carboxylate, and 254 nm for crotonate and benzoate.

Hydrogen was quantified by gas chromatography equipped with a mercury vapor detector (RGA3 Reduction Gas Analyzer, Trace Analytical, Menlo Park, CA). Methane was measured by gas chromatography with a flame ionization detection equipped with Poropak Q, 80/100 column (6 feet x 1/8 inch) (Supelco, Bellefonte, PA). The injector temperature was set at 100°C, the column at 100°C and the detector at 125°C. Helium was used as a carrier gas.

Acetate was analyzed with a gas chromatography apparatus equipped with a flame ionization detector and a glass column (2 m x 2 mm) packed with

80/120 Carbopack B-DA/ 4 % Carbowax 20M. The carrier gas was nitrogen with a flow rate set at 24 ml/min. The isothermal column temperature was 155°C. The injector and the detector temperatures were 200°C. Each sample contained 30 mM oxalic acid.

Protein concentrations were determined by the method of Bradford (Bradford, 1976) using the protocol and reagent from Pierce (Rockford, Il.) with bovine serum albumin as the standard.

Percoll Separation

The cells of the syntrophic partners were harvested anaerobically by centrifugation, washed twice and resuspended with 50 mM potassium phosphate buffer and separated from each other by using density gradient centrifugation in Percoll (Beaty et al., 1987). The concentrations of the Percoll solution were configured based on the following cell densities; *S. wolfei*, 1.075 g/ml; *S. aciditrophicus,* 1.115 g/ml; and *M. hungatei,* 1.140 g/ml. The Percoll solution was mixed 10:1 with 500 mM potassium phosphate buffer before gradients were made. Ratios of Percoll to cells suspended in 50 mM potassium phosphate buffer were 5 ml percoll to 4 ml buffer for separating *S. wolfei* and *M. hungatei* and 7 ml percoll to 2 ml buffer for separating for *S. aciditrophicus* and *M. hungatei*. Density gradients were created by centrifugation at 20,000 x G for 20 min. Fractions were extracted by puncturing the tube, and isolating bands of cells with a syringe.

Cell Fractionation

Percoll separated cells were suspended in 50 mM potassium phosphate (KPi) buffer at pH 7.4 and the cells were broken by French press cell. All the procedures were performed in an anaerobic chamber (Coy, Ann Arbor, Michigan, USA) under a gas phase of 95% N_2 and 5% H_2. Centrifugation was performed in sealed 8-ml tubes to maintain an anaerobic environment. Cell debris was removed by centrifugation at 10, 000 × g for 20 min at 4°C. Then the crude extract was centrifuged at 120,000 × g for 1h. The soluble fraction of the cell was collected and the membrane extract were resuspended and washed twice with 50 mM KPi (pH 7.4) by centrifuging at 120,000 × g for 30 minutes and resuspending the pellet in 50 mM KPi. The washed membranes were solubilized and homogenized with 40 mM dodecyl maltoside. The detergent-treated membrane preparation was centrifuged at 120,000 × g for 30 minutes to remove particulates. The supernatant after centrifugation was collected as the solubilized membrane extract.

Enzyme Assays

Formate dehydrogenase and hydrogenase were assayed for using whole cells of *S. aciditrophicus* grown with either *M. hungatei* JF1 with benzoate or crotonate, or grown axenically on crotonate. Similar enzyme assays were performed on whole cells of *S. wolfei* after syntrophic growth on butyrate or crotonate, or axenically on crotonate. Cells of the *S. wolfei* and *S. aciditrophicus* were separated from their syntrophic partner by Percoll centrifugation prior to analysis. Two viologen dyes were used to help determine the location of the

enzyme's activity, externally oriented or inside of the cell. Methyl viologen is a membrane impermeable dye and benzyl viologen is a membrane permeable dye. The use of the latter would detect internal and externally oriented enzymes. Enzyme assays were performed anaerobically contained 50 mM HEPES, 1 mM methyl viologen or benzyl viologen, and 1 mM formate, or 70 kPa H_2. Dye reduction was measured at 600 nm.

Enzyme assays with the soluble fraction of the cell and the membrane fraction were assayed as described above with methyl viologen. Formate dehydrogenase assays were carried out in a 96-well plate reader, while hydrogenase assays were done in 3-ml sealed cuvettes containing a 2-ml headspace of H_2.

Controls for the formate dehydrogenase assay were without formate, with 1 mM NaCl, and with heat killed cells or cell fractions. For hydrogenase assays, the controls were 70 kPa N_2 and with heat killed cells or cell fractions. Concentrations of cellular protein was varied to ensure the rate of activity was proportional to the amount of enzyme.

Inhibition studies

The effect of hydrogenase and formate dehydrogenase inhibitors was assayed for in washed cell suspensions of *S. wolfei* and *S. aciditrophicus* pure cultures and cocultures harvested during mid-log phase of growth. *S. aciditrophicus* was grown in pure culture on 20 mM crotonate on a minimal medium, in coculture with *M. hungatei* on 12 mM benzoate, or 12 mM

cyclohexane carboxylate. *S. wolfei* was grown in pure culture on 20 mM crotonate (Beaty and McInerney, 1987), in coculture with *M. hungatei* on 20 mM crotonate or 20 mM butyrate.

The three inhibitors used in this experiment were sodium hypophosphite, sodium cyanide, and carbon monoxide. Hypophosphite is a formate analog, which will inhibit formate dehydrogenases. Cyanide and carbon monoxide are both hydrogenase inhibitors. The cells were grown in three 2-liter volumes for each substrate, then anaerobically centrifuged and washed with sterile, anaerobic medium without vitamins twice by centrifugation at 5,000 x G for 15 minutes and resuspending the pellet in medium. The final cell pellet was resuspended 30 ml of medium without vitamins and headspace was exchanged to N_2:CO_2. Washed cell suspensions consisted of 1 ml of resuspended cells in 40 ml medium without vitamins with 100 µM of the substrate and the inhibitor, cyanide or hypophosphite, in the range 250 µM to 1 mM. CO as added to the gas phase to give 5, 10 and 15%. Cultures exposed to carbon monoxide were shaken at 100 rpm with the bottles lying on their sides. Substrate loss, hydrogen accumulation, and methane production was monitored every 2 hours after methane production began in the uninhibited washed cell suspensions. Controls included washed cell suspensions with no substrate, NaCl instead of sodium cyanide or sodium hypophosphite to control for sodium inhibition, and addition of N_2 instead of carbon monoxide.

RNA extraction and quantitative reverse transcriptase polymerase chain reaction (Q-RT-PCR)

After 50% substrate loss, which corresponded to mid-exponential phase of growth, cells from each growth condition were harvested by rapid cooling in a dry ice-ethanol bath, centrifuged at 8,000 x G for 15 min, and resuspended in RNAlater (Applied Biosystems/Ambion, Austin, TX). Total RNA was obtained by using a RNeasy Mini Kit (Qiagen Inc., Valencia, CA). DNA was removed by using on-column DNA digestion with RNAse-free DNAse Set (Qiagen Inc., Valencia, CA). The primers used for *S. wolfei* are listed in Table 8 and primers for in *S. aciditrophicus* are listed in Table 9. RNA was verified to be free of DNA contamination by PCR without reverse transcriptase. Q-RT-PCR was performed using the MyIQ real-time PCR system (Bio-Rad, Hercules, CA) and the iScriptT One-Step RT-PCR Kit with SYBR Green. Each reaction mixture (25-µl total volume) consisted of 12.5 µl IQ SYBR Green Supermix (Bio-Rad, Hercules, CA), 8 µl of nuclease-free water, 1.5 µl (10 µM) of each primer, 0.5 µl of reverse transcriptase and 1.0 µl of RNA. Q-RT-PCR generally followed a standard one-step protocol consisting of 10 min at 50°C, 5 min at 95°C, followed by 45 cycles of 95°C for 30 s, 56°C for 30 s, and 72°C for 30 s. No primer dimers were observed in all primer sets as determined by melting curve analysis of Q-RT-PCR amplicons. Amplification efficiency was determined by testing the primers against decreasing concentrations of DNA. The expression level of the target gene was normalized to the expression level of a reference gene, the DNA

gyrase gene (Pfaffl, 2001), using the following equation: $R=(E_{test}\text{^}(Ct^{control}-Ct^{treatment}))/(Efficency_{reference}\text{^}(Ct^{control}-Ct^{treatment}))$

Etest is efficiency of PCR amplification for the target gene, Ereference is efficiency of PCR amplification for the reference gene, and CTcontrol is Cycle Threshold for the control condition which is crotonate axenic and CTtreatment is Cycle Threshold is the coculture being tested.

REFERENCES

Amos, D.A., and McInerney, M.J. (1989) Poly-β-hydroxyalkanoate in *Syntrophomonas wolfe*i. *Arch Microbiol* **152**: 172-177.

Amos, D.A., and McInerney, M.J. (1990) Growth of *Syntrophomonas wolfei* on short-chain unsaturated fatty acids. *Arch Microbiol* **154**: 31-36.

Amos, D.A., and McInerney, M.J. (1993) Formation of d-3-hydroxybutyryl-coenzyme A by an acetoacetyl-coenzyme A reductase in *Syntrophomonas wolfei* subsp. wolfei. *Arch Microbiol* **159**: 16-20.

Anderson, A.J., Haywood, G.W., and Dawes, E.A. (1990) Biosynthesis and composition of bacterial poly(hydroxyalkanoates). *Int J Biol Macromol* **12**: 102-105.

Balch, W., and Wolfe, R. (1976) New approach to the cultivation of methanogenic bacteria: 2-mercaptoethanesulfonic acid (HS-CoM)-dependent growth of *Methanobacterium ruminantium* in a pressurized atmosphere. *Appl Environ Microbiol* **32**: 781.

Beatrix, B., Bendrat, K., Rospert, S., and Buckel, W. (1990) The biotin-dependent sodium ion pump glutaconyl-CoA decarboxylase from *Fusobacterium nucleatum* (subsp. nucleatum). Comparison with the glutaconyl-CoA decarboxylases from gram-positive bacteria. *Arch Microbiol* **154**: 362-369.

Beaty, P.S., and McInerney, M.J. (1987) Growth of *Syntrophomonas wolfei* in pure culture on crotonate. *Arch Microbiol* **147**: 389-393.

Beaty, P.S., and McInerney, M.J. (1989) Effects of organic acid anions on the growth and metabolism of *Syntrophomonas wolfei* in pure culture and in defined consortia. *Appl Environ Microbiol* **55**: 977-983.

Beaty, P.S., and McInerney, M.J. (1990) Nutritional Features of *Syntrophomonas wolfei*. *Appl Environ Microbiol* **56**: 3223-3224.

Beaty, P.S., Wofford, N.Q., and McInerney, M.J. (1987) Separation of *Syntrophomonas wolfei* from *Methanospirillum hungatei* in syntrophic cocultures by using percoll gradients. *Appl Environ Microbiol* **53**: 1183-1185.

Beckmann, J.D., and Frerman, F.E. (1985a) Reaction of electron-transfer flavoprotein with electron-transfer flavoprotein-ubiquinone oxidoreductase. *Biochemistry* **24**: 3922-3925.

Beckmann, J.D., and Frerman, F.E. (1985b) Electron-transfer flavoprotein-ubiquinone oxidoreductase from pig liver: purification and molecular, redox, and catalytic properties. *Biochemistry* **24**: 3913-3921.

Boetius, A., Ravenschlag, K., Schubert, C.J., Rickert, D., Widdel, F., Gieseke, A. et al. (2000) A marine microbial consortium apparently mediating anaerobic oxidation of methane. *Nature* **407**: 623-626.

Boll, M., and Fuchs, G. (1998) Identification and characterization of the natural electron donor ferredoxin and of FAD as a possible prosthetic group of benzoyl-CoA reductase (dearomatizing), a key enzyme of anaerobic aromatic metabolism. *Eur J Biochem* **251**: 946-954.

Boll, M., Albracht, S.S., and Fuchs, G. (1997) Benzoyl-CoA reductase (dearomatizing), a key enzyme of anaerobic aromatic metabolism. A study of

adenosinetriphosphatase activity, ATP stoichiometry of the reaction and EPR properties of the enzyme. *Eur J Biochem* **244**: 840-851.

Boll, M., Fuchs, G., Tilley, G., Armstrong, F.A., and Lowe, D.J. (2000) Unusual spectroscopic and electrochemical properties of the 2[4Fe-4S] ferredoxin of *Thauera aromatica*. *Biochemistry* **39**: 4929-4938.

Boone, D.R., Johnson, R.L., and Liu, Y. (1989) Diffusion of the interspecies electron carriers H_2 and formate in methanogenic ecosystems and its implications in the measurement of K_m for H_2 or formate uptake. *Appl Environ Microbiol* **55**: 1735-1741.

Bradford, M.M. (1976) A rapid and sensitive method for the quantitation of microgram quantities of protein utilizing the principle of protein-dye binding. *Analytical biochemistry* **72**: 248-254.

Breese, K., and Fuchs, G. (1998) 4-Hydroxybenzoyl-CoA reductase (dehydroxylating) from the denitrifying bacterium *Thauera aromatica*--prosthetic groups, electron donor, and genes of a member of the molybdenum-flavin-iron-sulfur proteins. *Eur J Biochem* **251**: 916-923.

Bryant, M.P., Wolin, E.A., Wolin, M.J., and Wolfe, R.S. (1967) *Methanobacillus omelianskii*, a symbiotic association of two species of bacteria. *Arch Microbiol* **59**: 20-31.

Caccavo, F., Lonergan, D., Lovley, D., Davis, M., Stolz, J., and McInerney, M. (1994) *Geobacter sulfurreducens* sp. nov., a hydrogen-and acetate-oxidizing dissimilatory metal-reducing microorganism. *Appl Environ Microbiol* **60**: 3752-3759.

Colwell, F.S., Boyd, S., Delwiche, M.E., Reed, D.W., Phelps, T.J., and Newby, D.T. (2008) Estimates of biogenic methane production rates in deep marine sediments at Hydrate Ridge, Cascadia margin. *Appl Environ Microbiol* **74**: 3444-3452.

Conrad, R., Phelps, T., and Zeikus, J. (1985) Gas metabolism evidence in support of the juxtaposition of hydrogen-producing and methanogenic bacteria in sewage sludge and lake sediments. *Appl Environ Microbiol* **50**: 595-601.

de Bok, F.A., Luijten, M.L., and Stams, A.J. (2002a) Biochemical evidence for formate transfer in syntrophic propionate-oxidizing cocultures of *Syntrophobacter fumaroxidans* and *Methanospirillum hungatei*. *Appl Environ Microbiol* **68**: 4247-4252.

de Bok, F.A., Roze, E.H., and Stams, A.J. (2002b) Hydrogenases and formate dehydrogenases of *Syntrophobacter fumaroxidans*. *Antonie Van Leeuwenhoek* **81**: 283-291.

de Bok, F.A., Hagedoorn, P.L., Silva, P.J., Hagen, W.R., Schiltz, E., Fritsche, K., and Stams, A.J. (2003) Two W-containing formate dehydrogenases (CO_2-reductases) involved in syntrophic propionate oxidation by *Syntrophobacter fumaroxidans*. *Eur J Biochem* **270**: 2476-2485.

Delcher, A.L., Harmon, D., Kasif, S., White, O., and Salzberg, S.L. (1999a) Improved microbial gene identification with GLIMMER. *Nucleic Acids Res* **27**: 4636-4641.

Delcher, A.L., Kasif, S., Fleischmann, R.D., Peterson, J., White, O., and Salzberg, S.L. (1999b) Alignment of whole genomes. *Nucleic Acids Res* **27**: 2369-2376.

DeSantis, T.Z., Hugenholtz, P., Larsen, N., Rojas, M., Brodie, E.L., and Keller, K. (2006) Greengenes, a chimera-checked 16S rRNA gene database and workbench compatible with ARB. *Appl Environ Microbiol* **72**: 5069-5072.

Do, C.B., Mahabhashyam, M.S., Brudno, M., and Batzoglou, S. (2005) ProbCons: Probabilistic consistency-based multiple sequence alignment. *Genome Res* **15**: 330-340.

Dong, X., and Stams, A.J. (1995a) Localization of the enzymes involved in H_2 and formate metabolism in *Syntrophospora bryantii*. *Antonie Van Leeuwenhoek* **67**: 345-350.

Dong, X., and Stams, A.J. (1995b) Evidence for H_2 and formate formation during syntrophic butyrate and propionate degradation. *Anaerobe* **1**: 35-39.

Dong, X., Cheng, G., and Stams, A.J.M. (1994a) Butyrate oxidation by *Syntrophospora bryantii* in co-culture with different methanogens and in pure culture with pentenoate as electron acceptor. *Appl Microbiol Biotechnol* **42**: 647-652.

Dong, X., Plugge, C.M., and Stams, A.J. (1994b) Anaerobic degradation of propionate by a mesophilic acetogenic bacterium in coculture and triculture with different methanogens. *Appl Environ Microbiol* **60**: 2834-2838.

Dwyer, D.F., Weeg-Aerssens, E., Shelton, D.R., and Tiedje, J.M. (1988) Bioenergetic conditions of butyrate metabolism by a syntrophic, anaerobic bacterium in coculture with hydrogen-oxidizing methanogenic and sulfidogenic bacteria. *Appl Environ Microbiol* **54**: 1354-1359.

Earl, C.D., Ronson, C.W., and Ausubel, F.M. (1987) Genetic and structural analysis of the *Rhizobium meliloti* fixA, fixB, fixC, and fixX genes. *J Bacteriol* **169**: 1127-1136.

Edgren, T., and Nordlund, S. (2004) The fixABCX genes in *Rhodospirillum rubrum* encode a putative membrane complex participating in electron transfer to nitrogenase. *J Bacteriol* **186**: 2052-2060.

Efron, B. (2008) Microarrays, empirical Bayes and the two-groups model. *Statistical Science* **23**: 1-22.

Efron, B., and Tibshirani, R. (2007) On testing the significance of sets of genes. *The Annals of Applied Statistics* **1**: 107-129.

Ehhalt, D., Prather, M., Dentener, F., Derwent, R., Dlugokencky, E., Holland, E. et al. (2001) Atmospheric chemistry and greenhouse gases. In *Climate Change 2001: The Scientific Basis*. Houghton, J.T., Ding, Y., Griggs, D.J., Noguer, M., Van der Linden, P.J., Dai, X. et al. (eds). Cambridge: Cambridge University Press, pp. 239-287.

Eichler, K., Buchet, A., Bourgis, F., Kleber, H.P., and Mandrand-Berthelot, M.A. (1995) The fix *Escherichia coli* region contains four genes related to carnitine metabolism. *J Basic Microbiol* **35**: 217-227.

Elias, J., and Gygi, S. (2007) Target-decoy search strategy for increased confidence in large-scale protein identifications by mass spectrometry. *Nat methods* **4**: 207-214.

Elshahed, M.S., Bhupathiraju, V.K., Wofford, N.Q., Nanny, M.A., and McInerney, M.J. (2001) Metabolism of benzoate, cyclohex-1-ene carboxylate, and cyclohexane carboxylate by *Syntrophus aciditrophicus* strain SB in syntrophic

association with H_2-using microorganisms. *Appl Environ Microbiol* **67**: 1728-1738.

Eng, J.K., McCormack, A.L., and Yates Iii, J.R. (1994) An approach to correlate tandem mass spectral data of peptides with amino acid sequences in a protein database. *J Am Soc Mass Spectrom* **5**: 976-989.

Ewing, B., and Green, P. (1998) Base-calling of automated sequencer traces using phred. II. Error probabilities. *Genome Res* **8**: 186-194.

Ewing, B., Hillier, L., Wendl, M.C., and Green, P. (1998) Base-calling of automated sequencer traces using phred. I. Accuracy assessment. *Genome Res* **8**: 175-185.

Farkas, L., and Fischer, E. (1947) On the activation of molecular hydrogen by *Proteus vulgaris*. *J Biol Chem* **167**: 787-805.

Felsenstein, J. (1989) PHYLIP - Phylogeny Inference Package (Version 3.2). *Cladistics* **5**: 164-166.

Ferry, J.G., and Wolfe, R.S. (1976) Anaerobic degradation of benzoate to methane by a microbial consortium. *Arch Microbiol* **107**: 33-40.

Fisher, N., and Rich, P.R. (2000) A motif for quinone binding sites in respiratory and photosynthetic systems. *J Mol Biol* **296**: 1153-1162.

Friedrich, M., and Schink, B. (1993) Hydrogen formation from glycolate driven by reversed electron transport in membrane vesicles of a syntrophic glycolate-oxidizing bacterium. *Eur J Biochem* **217**: 233-240.

Friedrich, M., and Schink, B. (1995) Electron transport phosphorylation driven by glyoxylate respiration with hydrogen as electron donor in membrane vesicles of a glyoxylate-fermenting bacterium. *Arch Microbiol* **163**: 268-275.

Friedrich, M., Springer, N., Ludwig, W., and Schink, B. (1996) Phylogenetic positions of *Desulfofustis glycolicus* gen. nov., sp. nov., and *Syntrophobotulus glycolicus* gen. nov., sp. nov., two new strict anaerobes growing with glycolic acid. *Int J Syst Bacteriol* **46**: 1065-1069.

Gallert, C., and Winter, J. (1994) Anaerobic degradation of 4-hydroxybenzoate: Reductive dehydroxylation of 4-hydroxybenzoyl-CoA and ATP formation during 4-hydroxybenzoate decarboxylation by the phenol-metabolizing bacteria of a stable, strictly anaerobic consortium. *Appl Microbiol Biotechnol* **42**: 408-414.

Gentleman, R., Carey, V., Bates, D., Bolstad, B., Dettling, M., Dudoit, S. et al. (2004) Bioconductor: open software development for computational biology and bioinformatics. *Genome Biology* **5**: R80.

Gibson, J., Dispensa, M., and Harwood, C.S. (1997) 4-hydroxybenzoyl coenzyme A reductase (dehydroxylating) is required for anaerobic degradation of 4-hydroxybenzoate by *Rhodopseudomonas palustri*s and shares features with molybdenum-containing hydroxylases. *J Bacteriol* **179**: 634-642.

Gibson, J., Dispensa, M., Fogg, G.C., Evans, D.T., and Harwood, C.S. (1994) 4-Hydroxybenzoate-coenzyme A ligase from *Rhodopseudomonas palustris*: purification, gene sequence, and role in anaerobic degradation. *J Bacteriol* **176**: 634-641.

Gorby, Y.A., Yanina, S., McLean, J.S., Rosso, K.M., Moyles, D., Dohnalkova, A. et al. (2006) Electrically conductive bacterial nanowires produced by

Shewanella oneidensis strain MR-1 and other microorganisms. *Proc Natl Acad Sci USA* **103**: 11358-11363

Gordon, D., Abajian, C., and Green, P. (1998) Consed: a graphical tool for sequence finishing. *Genome Res* **8**: 195-202.

Greene, E.A., Hubert, C., Nemati, M., Jenneman, G.E., and Voordouw, G. (2003) Nitrite reductase activity of sulphate-reducing bacteria prevents their inhibition by nitrate-reducing, sulphide-oxidizing bacteria. *Environ Microbiol* **5**: 607-617.

Hardcastle, T., and Kelly, K. (2010) baySeq: Empirical Bayesian methods for identifying differential expression in sequence count data. *BMC Bioinformatics* **11**: 422.

Harmsen, H.J., Van Kuijk, B.L., Plugge, C.M., Akkermans, A.D., De Vos, W.M., and Stams, A.J. (1998) *Syntrophobacter fumaroxidans* sp. nov., a syntrophic propionate-degrading sulfate-reducing bacterium. *Int J Syst Bacteriol* **48**: 1383-1387.

Harwood, C.S., Burchhardt, G., Herrmann, H., and Fuchs, G. (1998) Anaerobic metabolism of aromatic compounds via the benzoyl-CoA pathway. *FEMS Microbiol Rev* **22**: 439-458.

Hedderich, R., and Whitman, W. (2006) Physiology and biochemistry of the methane-producing Archaea. In *The Prokaryotes: an evolving electronic resource for the microbiological community*. Dworkin, M., Falkow, S., Rosenberg, E., Schleifer, K.H., and Stackebrandt, E. (eds). New York: Springer-Verlag, pp. 1050–1079.

Heidelberg, J.F., Seshadri, R., Haveman, S.A., Hemme, C.L., Paulsen, I.T., Kolonay, J.F. et al. (2004) The genome sequence of the anaerobic, sulfate-reducing bacterium *Desulfovibrio vulgaris* Hildenborough. *Nat Biotechnol* **22**: 554-559.

Heider, J., and Fuchs, G. (1997a) Anaerobic metabolism of aromatic compounds. *Eur J Biochem* **243**: 577-596.

Heider, J., and Fuchs, G. (1997b) Microbial anaerobic aromatic metabolism. *Anaerobe* **3**: 1-22.

Herrmann, G., Jayamani, E., Mai, G., and Buckel, W. (2008) Energy conservation via electron-transferring flavoprotein in anaerobic bacteria. *J Bacteriol* **190**: 784-791.

Hervey IV, W., Strader, M., and Hurst, G. (2007) Comparison of digestion protocols for microgram quantities of enriched protein samples. *J Proteome Res* **6**: 3054-3061.

Hirsch, W., Schagger, H., and Fuchs, G. (1998) Phenylglyoxylate:NAD^+ oxidoreductase (CoA benzoylating), a new enzyme of anaerobic phenylalanine metabolism in the denitrifying bacterium *Azoarcus evansii*. *Eur J Biochem* **251**: 907-915.

Hoberman, H.D., and Rittenberg, D. (1943) Biological catalysis of the exchange reaction between water and hydrogen. *J Biol Chem* **147**: 211-227.

Hoehler, T. (2004) Biological energy requirements as quantitative boundary conditions for life in the subsurface. *Geobiol* **2**: 205-215.

Horvath, P., Coute-Monvoisin, A.C., Romero, D.A., Boyaval, P., Fremaux, C., and Barrangou, R. (2009) Comparative analysis of CRISPR loci in lactic acid bacteria genomes. *Int J Food Microbiol* **131**: 62-70.

Houwen, F.P., Plokker, J., Stams, A.J.M., and Zehnder, A.J.B. (1990) Enzymatic evidence for involvement of the methylmalonyl-CoA pathway in propionate oxidation by *Syntrophobacter wolinii*. *Arch Microbiol* **155**: 52-55.

Husain, M., and Steenkamp, D.J. (1985) Partial purification and characterization of glutaryl-coenzyme A dehydrogenase, electron transfer flavoprotein, and electron transfer flavoprotein-Q oxidoreductase from *Paracoccus denitrificans*. *J Bacteriol* **163**: 709-715.

Ishii, S., Kosaka, T., Hotta, Y., and Watanabe, K. (2006) Simulating the contribution of coaggregation to interspecies hydrogen fluxes in syntrophic methanogenic consortia. *Appl Environ Microbiol* **72**: 5093-5096.

Ishii, S., Kosaka, T., Hori, K., Hotta, Y., and Watanabe, K. (2005) Coaggregation facilitates interspecies hydrogen transfer between *Pelotomaculum thermopropionicum* and *Methanothermobacter thermautotrophicus*. *Appl Environ Microbiol* **71**: 7838-7845.

Jackson, B.E., and McInerney, M.J. (2002) Anaerobic microbial metabolism can proceed close to thermodynamic limits. *Nature* **415**: 454-456.

Jackson, B.E., Bhupathiraju, V.K., Tanner, R.S., Woese, C.R., and McInerney, M.J. (1999) *Syntrophus aciditrophicus* sp. nov., a new anaerobic bacterium that degrades fatty acids and benzoate in syntrophic association with hydrogen-using microorganisms. *Arch Microbiol* **171**: 107-114.

Jormakka, M., Tornroth, S., Byrne, B., and Iwata, S. (2002) Molecular basis of proton motive force generation: structure of formate dehydrogenase-N. *Science* **295**: 1863-1868.

Kaden, J., A, S.G., and Schink, B. (2002) Cysteine-mediated electron transfer in syntrophic acetate oxidation by cocultures of *Geobacter sulfurreducens* and *Wolinella succinogenes*. *Arch Microbiol* **178**: 53-58.

Kato, S., Kosaka, T., and Watanabe, K. (2009) Substrate dependent transcriptomic shifts in *Pelotomaculum thermopropionicum* grown in syntrophic co culture with *Methanothermobacter thermautotrophicus*. *Microbial Biotechnology* **2**: 575-584.

Kendall, M.M., Liu, Y., and Boone, D.R. (2006) Butyrate- and propionate-degrading syntrophs from permanently cold marine sediments in Skan Bay, Alaska, and description of *Algorimarina butyrica* gen. nov., sp. nov. *FEMS Microbiol Lett* **262**: 107-114.

Kosaka, T., Kato, S., Shimoyama, T., Ishii, S., Abe, T., and Watanabe, K. (2008) The genome of *Pelotomaculum thermopropionicum* reveals niche-associated evolution in anaerobic microbiota. *Genome Res* **18**: 442-448.

Krumholz, L.R., and Bryant, M.P. (1986) *Syntrophococcus sucromutans* sp. nov. gen. nov. uses carbohydrates as electron donors and formate, methoxymonobenzenoids or *Methanobrevibacter* as electron acceptor systems. *Arch Microbiol* **143**: 313-318.

Kuntze, K., Shinoda, Y., Moutakki, H., McInerney, M.J., Vogt, C., Richnow, H.H., and Boll, M. (2008) 6-Oxocyclohex-1-ene-1-carbonyl-coenzyme A hydrolases from obligately anaerobic bacteria: characterization and identification of its gene as a functional marker for aromatic compounds degrading anaerobes. *Environ Microbiol* **10**: 1547-1556.

Leang, C., Coppi, M.V., and Lovley, D.R. (2003) OmcB, a c-Type Polyheme Cytochrome, Involved in Fe (III) Reduction in *Geobacter sulfurreducens*. *J Bacteriol* **185**: 2096-2103.

Leang, C., Qian, X., Mester, T., and Lovley, D.R. (2010) Alignment of the c-type cytochrome OmcS along pili of *Geobacter sulfurreducens*. *Appl Environ Microbiol* **76**: 4080-4084.

Lee, M.J., and Zinder, S.H. (1988) Isolation and characterization of a thermophilic bacterium which oxidizes acetate in syntrophic association with a methanogen and which grows acetogenically on H_2-CO_2. *Appl Environ Microbiol* **54**: 124-129.

Li, F., Hagemeier, C.H., Seedorf, H., Gottschalk, G., and Thauer, R.K. (2007) Re-citrate synthase from *Clostridium kluyveri* is phylogenetically related to homocitrate synthase and isopropylmalate synthase rather than to *Si*-citrate synthase. *J Bacteriol* **189**: 4299-4304.

Li, F., Hinderberger, J., Seedorf, H., Zhang, J., Buckel, W., and Thauer, R.K. (2008) Coupled ferredoxin and crotonyl coenzyme A (CoA) reduction with NADH catalyzed by the butyryl-CoA dehydrogenase/Etf complex from *Clostridium kluyveri*. *J Bacteriol* **190**: 843-850.

Liu, Y., and Whitman, W.B. (2008) Metabolic, phylogenetic, and ecological diversity of the methanogenic archaea. In *Incredible Anaerobes From Physiology to Genomics to Fuels* Wiegel, J., Maier, R.J., and Adams, M.W. (eds): Ann N Y Acad Sci, pp. 171–189.

Logan, B.E., and Regan, J.M. (2006) Electricity-producing bacterial communities in microbial fuel cells. *Trends Microbiol* **14**: 512-518.

Lorowitz, W.H., Zhao, H., and Bryant, M.P. (1989) *Syntrophomonas wolfei* subsp. *saponavida* subsp. nov., a long-chain fatty-acid-degrading, anaerobic, syntrophic bacterium. *Int J Syst Bacteriol* **39**: 122–126.

Ludwig, W., Strunk, O., Westram, R., Richter, L., Meier, H., Yadhukumar et al. (2004) ARB: a software environment for sequence data. *Nucleic Acids Res* **32**: 1363-1371.

Mahadevan, R., and Lovley, D.R. (2008) The degree of redundancy in metabolic genes is linked to mode of metabolism. *Biophys J* **94**: 1216-1220.

McCarty, P.L. (1971) Energetics and kinetics of anaerobic treatment. In *Anaerobic Biological Treatment Processes*. Gould, R.F. (ed). Washington, D. C.: American Chemical Society, pp. 91-107.

McInerney, M.J. (1992) The genus *Syntrophomonas* and other syntrophic anaerobes. In *The Prokaryotes: an evolving electronic resource for the microbiological community*. Balows, A., Trüper, H.G., Dworkin, M., Harder, W., and Schleifer, K.H. (eds). New York: Springer–Verlag, pp. 2048–2057.

McInerney, M.J., and Bryant, M.P. (1981a) Anaerobic degradation of lactate by syntrophic associations of *Methanosarcina barkeri* and *Desulfovibrio* species and effect of H_2 on acetate degradation. *Appl Environ Microbiol* **41**: 346-354.

McInerney, M.J., and Bryant, M.P. (1981b) Basic principles of anaerobic degradation and methane production. In *Biomass Conversion Processes for Energy and Fuels*. Sofer, S.S., and Zaborsky, O.R. (eds). New York: Plenum Publishing Corp., pp. 277-296.

McInerney, M.J., and Wofford, N.Q. (1992) Enzymes involved in crotonate metabolism in *Syntrophomonas wolfei*. *Arch Microbiol* **158**: 344-349.

McInerney, M.J., Bryant, M.P., and Pfennig, N. (1979) Anaerobic bacterium that degrades fatty acids in syntrophic association with methanogens. *Arch Microbiol* **122**: 129-135.

McInerney, M.J., Mackie, R.I., and Bryant, M.P. (1981a) Syntrophic association of a butyrate-degrading bacterium and methanosarcina enriched from bovine rumen fluid. *Appl Environ Microbiol* **41**: 826-828.

McInerney, M.J., Sieber, J.R., and Gunsalus, R.P. (2009) Syntrophy in anaerobic global carbon cycles. *Curr Opin Biotechnol* **20**: 623-632.

McInerney, M.J., Bryant, M.P., Hespell, R.B., and Costerton, J.W. (1981b) *Syntrophomonas wolfei* gen. nov. sp. nov., an anaerobic, syntrophic, fatty acid-oxidizing bacterium. *Appl Environ Microbiol* **41**: 1029-1039.

McInerney, M.J., Struchtemeyer, C.G., Sieber, J., Mouttaki, H., Stams, A.J.M., Schink, B. et al. (2008) Physiology, ecology, phylogeny, and genomics of microorganisms capable of syntrophic metabolism. In *Incredible Anaerobes From Physiology to Genomics to Fuels* Wiegel, J., Maier, R.J., and Adams, M.W. (eds): Ann N Y Acad Sci, pp. 58-72.

McInerney, M.J., Rohlin, L., Mouttaki, H., Kim, U., Krupp, R.S., Rios-Hernandez, L. et al. (2007) The genome of *Syntrophus aciditrophicus*: life at the thermodynamic limit of microbial growth. *Proc Natl Acad Sci U S A* **104**: 7600-7605.

Merkel, S.M., Eberhard, A.E., Gibson, J., and Harwood, C.S. (1989) Involvement of coenzyme A thioesters in anaerobic metabolism of 4-hydroxybenzoate by *Rhodopseudomonas palustris*. *J Bacteriol* **171**: 1-7.

Miller, M., Holder, M., Vos, R., Midford, P., Liebowitz, T., Chan, L. et al. (2009). The CIPRES Portals. URL http://www.phylo.org/sub_sections/portal.

Moore, R., Young, M., and Lee, T. (2002) Qscore: an algorithm for evaluating SEQUEST database search results. *J Am Soc Mass Spectrom* **13**: 378-386.

Mountfort, D.O., and Bryant, M.P. (1982) Isolation and characterization of an anaerobic syntrophic benzoate-degrading bacterium from sewage sludge. *Arch Microbiol* **133**: 249-256.

Mouttaki, H., Nanny, M.A., and McInerney, M.J. (2007) Cyclohexane carboxylate and benzoate formation from crotonate in *Syntrophus aciditrophicus*. *Appl Environ Microbiol* **73**: 930-938.

Mouttaki, H., Nanny, M.A., and McInerney, M.J. (2008) Use of benzoate as an electron acceptor by *Syntrophus aciditrophicus* grown in pure culture with crotonate. *Environ Microbiol* **10**: 3265-3274.

Mouttaki, H., Nanny, M.A., and McInerney, M.J. (2009) Metabolism of hydroxylated and fluorinated benzoates by *Syntrophus aciditrophicus* and detection of a fluorodiene metabolite. *Appl Environ Microbiol* **75**: 998-1004.

Müller, N., Schleheck, D., and Schink, B. (2009) Involvement of NADH: acceptor oxidoreductase and butyryl-CoA dehydrogenase in reversed electron transport during syntrophic butyrate oxidation by *Syntrophomonas wolfei*. *J Bacteriol* **191**: 6167-6177.

Odom, J.M., and Peck, H.D., Jr. (1981) Localization of dehydrogenases, reductases, and electron transfer components in the sulfate-reducing bacterium *Desulfovibrio gigas*. *J Bacteriol* **147**: 161-169.

Oksanen, J., Blanchet, F.G., Kindt, R., Legendre, P., O'Hara, R.B., Simpson, G.L. et al. (2011) vegan: Community Ecology Package. In.

Pavlostathis, S.G., and Giraldo-Gomez, E. (1991) Kinetics of anaerobic treatment: A critical review. *Crit Rev Environ Control* **21**: 411-490.

Peters, F., Rother, M., and Boll, M. (2004) Selenocysteine-containing proteins in anaerobic benzoate metabolism of *Desulfococcus multivorans*. *J Bacteriol* **186**: 2156-2163.

Peters, F., Shinoda, Y., McInerney, M.J., and Boll, M. (2007) Cyclohexa-1,5-diene-1-carbonyl-coenzyme A (CoA) hydratases of *Geobacter metallireducens* and *Syntrophus aciditrophicus*: Evidence for a common benzoyl-CoA degradation pathway in facultative and strict anaerobes. *J Bacteriol* **189**: 1055-1060.

Pfaffl, M.W. (2001) A new mathematical model for relative quantification in real-time RT-PCR. *Nucleic Acids Res* **29**: e45.

RDevelopmentCoreTeam (2011) R: A language and environment for statistical computing. In. Vienna, Austria: R Foundation for Statistical Computing.

Reguera, G., McCarthy, K.D., Mehta, T., Nicoll, J.S., Tuominen, M.T., and Lovley, D.R. (2005) Extracellular electron transfer via microbial nanowires. *Nature* **435**: 1098-1101.

Ren, Q., Chen, K., and Paulsen, I. (2007) TransportDB: a comprehensive database resource for cytoplasmic membrane transport systems and outer membrane channels. *Nucleic Acids Res* **35**: D274-279.

Rocha, E. (2002) Is there a role for replication fork asymmetry in the distribution of genes in bacterial genomes? *Trends Microbiol* **10**: 393-395.

Rosenthal, A.Z., Matson, E.G., Eldar, A., and Leadbetter, J.R. (2011) RNA-seq reveals cooperative metabolic interactions between two termite-gut spirochete species in co-culture. *ISME J* **5**: 1133-1142.

Sato, K., Nishina, Y., Setoyama, C., Miura, R., and Shiga, K. (1999) Unusually high standard redox potential of acrylyl-CoA/propionyl-CoA couple among enoyl-CoA/acyl-CoA couples: a reason for the distinct metabolic pathway of propionyl-CoA from longer acyl-CoAs. *J Biochem* **126**: 668-675.

Schink, B. (1997) Energetics of syntrophic cooperation in methanogenic degradation. *Microbiol Mol Biol Rev* **61**: 262-280.

Schink, B. (2000) Microbial ecology--a late developing field in science. *FEMS Microbiol Rev* **24**: 553.

Schink, B. (2006) Syntrophic associations in methanogenic degradation. *Prog Mol Subcell Biol* **41**: 1-19.

Schink, B., and Friedrich, M. (1994) Energetics of syntrophic fatty acid oxidation. *FEMS Microbiol Rev* **15**: 85-94.

Schink, B., and Stams, A.J.M. (2006) Syntrophism among prokaryotes. In *The Prokaryotes: an evolving electronic resource for the microbiological community*. Dworkin, M., Falkow, S., Rosenberg, E., Schleifer, K.H., and Stackebrandt, E. (eds). New York: Springer-Verlag, pp. 309-335.

Schirawski, J., and Unden, G. (1998) Menaquinone-dependent succinate dehydrogenase of bacteria catalyzes reversed electron transport driven by the proton potential. *Eur J Biochem* **257**: 210-215.

Schöcke, L., and Schink, B. (1997) Energetics of methanogenic benzoate degradation by *Syntrophus gentianae* in syntrophic coculture. *Microbiology* **143**: 2345-2351.

Schöcke, L., and Schink, B. (1998) Membrane-bound proton-translocating pyrophosphatase of *Syntrophus gentianae*, a syntrophically benzoate-degrading fermenting bacterium. *Eur J Biochem* **256**: 589-594.

Scholten, J.C., and Conrad, R. (2000) Energetics of syntrophic propionate oxidation in defined batch and chemostat cocultures. *Appl Environ Microbiol* **66**: 2934-2942.

Schut, G., and Adams, M. (2009) The iron-hydrogenase of *Thermotoga maritima* utilizes ferredoxin and NADH synergistically: a new perspective on anaerobic hydrogen production. *J Bacteriol* **191**: 4451-4417.

Seitz, H.J., Schink, B., and Conrad, R. (1988) Thermodynamics of hydrogen metabolism in methanogenic cocultures degrading ethanol or lactate. *FEMS Microbiology Letters* **55**: 119-124.

Seitz, H.J., Schink, B., Pfennig, N., and Conrad, R. (1990) Energetics of syntrophic ethanol oxidation in defined chemostat cocultures. *Archives of Microbiology* **155**: 82-88.

Sekiguchi, Y., Kamagata, Y., Nakamura, K., Ohashi, A., and Harada, H. (1999) Fluorescence in situ hybridization using 16S rRNA-targeted oligonucleotides reveals localization of methanogens and selected uncultured bacteria in mesophilic and thermophilic sludge granules. *Appl Environ Microbiol* **65**: 1280-1288.

Sekiguchi, Y., Kamagata, Y., Nakamura, K., Ohashi, A., and Harada, H. (2000) *Syntrophothermus lipocalidus* gen. nov., sp. nov., a novel thermophilic, syntrophic, fatty-acid-oxidizing anaerobe which utilizes isobutyrate. *Int J Syst Evol Microbiol* **50** 771-779.

Shimoyama, T., Kato, S., Ishii, S., and Watanabe, K. (2009) Flagellum mediates symbiosis. *Science* **323**: 1574.

Sieber, J.R., McInerney, M.J., Plugge, C.M., Schink, B., and Gunsalus, R.P. (2010a) Methanogenesis: Syntrophic Metabolism. In *Handbook of Hydrocarbon and Lipid Microbiology*. Timmis, K.N. (ed): Springer Berlin Heidelberg, pp. 337-355.

Sieber, J.R., Sims, D.R., Han, C., Kim, E., Lykidis, A., Lapidus, A.L. et al. (2010b) The genome of *Syntrophomonas wolfei*: new insights into syntrophic metabolism and biohydrogen production. *Environ Microbiol* **12**: 2289-2301.

Sobieraj, M., and Boone, D.R. (2006) *Syntrophomonadaceae*. In *The Prokaryotes: an evolving electronic resource for the microbiological community*. Dworkin, M., Falkow, S., Rosenberg, E., Schleifer, K.H., and Stackebrandt, E. (eds). New York: Springer-Verlag, pp. 1041-1046.

Sorek, R., Kunin, V., and Hugenholtz, P. (2008) CRISPR--a widespread system that provides acquired resistance against phages in bacteria and archaea. *Nat Rev Microbiol* **6**: 181-186.

Sousa, D.Z., Smidt, H., Alves, M.M., and Stams, A.J. (2007) *Syntrophomonas zehnderi* sp. nov., an anaerobe that degrades long-chain fatty acids in co-culture with *Methanobacterium formicicum*. *Int J Syst Evol Microbiol* **57**: 609-615.

Sperotto, R.A., Gross, J., Vedoy, C., Passaglia, L.M., and Schrank, I.S. (2004) The electron transfer flavoprotein *fixABCX* gene products from *Azospirillum brasilense* show a *NifA*-dependent promoter regulation. *Curr Microbiol* **49**: 267-273.

Stamatakis, A., Hoover, P., and Rougemont, J. (2008) A rapid bootstrap algorithm for the RAxML Web servers. *Syst Biol* **57**: 758-771.

Stams, A.J., and Dong, X. (1995) Role of formate and hydrogen in the degradation of propionate and butyrate by defined suspended cocultures of acetogenic and methanogenic bacteria. *Antonie Van Leeuwenhoek* **68**: 281-284.

Stams, A.J., and Plugge, C.M. (2009) Electron transfer in syntrophic communities of anaerobic bacteria and archaea. *Nat Rev Microbiol* **7**: 568-577.

Strittmatter, A.W., Liesegang, H., Rabus, R., Decker, I., Amann, J., Andres, S. et al. (2009) Genome sequence of *Desulfobacterium autotrophicum* HRM2, a marine sulfate reducer oxidizing organic carbon completely to carbon dioxide. *Environ Microbiol* **11**: 1038-1055.

Summers, Z.M., Fogarty, H.E., Leang, C., Franks, A.E., Malvankar, N.S., and Lovley, D.R. (2010) Direct exchange of electrons within aggregates of an evolved syntrophic coculture of anaerobic bacteria. *Science* **330**: 1413-1415.

Svetlitshnyi, V., Rainey, F., and Wiegel, J. (1996) *Thermosyntropha lipolytica* gen. nov., sp. nov., a lipolytic, anaerobic, alkalitolerant, thermophilic bacterium utilizing short- and long-chain fatty acids in syntrophic coculture with a methanogenic archaeum. *Int J Syst Bacteriol* **46**: 1131-1137.

Szewzyk, U., and Schink, B. (1989) Degradation of hydroquinone, gentisate, and benzoate by a fermenting bacterium in pure or defined mixed culture. *Arch Microbiol* **151**: 541-545.

Tabb, D.L., McDonald, W.H., and Yates, J.R., 3rd (2002) DTASelect and contrast: tools for assembling and comparing protein identifications from shotgun proteomics. *J Proteome Res* **1**: 21-26.

Takamiya, A. (1953) Studies on the formic dehydrogenase of *Escherichia coli* III. Determination of the quantity of the enzyme within the cell by using hypophosphite as a specific inhibitor. *J Biochem* **40**: 407-414.

Thauer, R.K., Jungermann, K., and Decker, K. (1977) Energy conservation in chemotrophic anaerobic bacteria. *Bacteriol Rev* **41**: 100-180.

Thiele, J.H., and Zeikus, J.G. (1988) Control of interspecies electron flow during anaerobic digestion: significance of formate transfer versus hydrogen transfer during syntrophic methanogenesis in flocs. *Appl Environ Microbiol* **54**: 20-29.

Thompson, M.R., Chourey, K., Froelich, J.M., Erickson, B.K., VerBerkmoes, N.C., and Hettich, R.L. (2008) Experimental approach for deep proteome

measurements from small-scale microbial biomass samples. *Anal Chem* **80**: 9517-9525.

Van Kuijk, B.L., Schlosser, E., and Stams, A.J. (1998) Investigation of the fumarate metabolism of the syntrophic propionate-oxidizing bacterium strain MPOB. *Arch Microbiol* **169**: 346-352.

Vignais, P.M., Billoud, B., and Meyer, J. (2001) Classification and phylogeny of hydrogenases. *FEMS Microbiol Rev* **25**: 455-501.

Wallrabenstein, C.S., Bernhard (1994) Evidence of reversed electron transport in syntrophic butyrate or benzoate oxidation by *Syntrophomonas wolfei* and *Syntrophus buswellii*. *Arch Microbiol* **162**: 136-142.

Walt, A., and Kahn, M.L. (2002) The fixA and fixB genes are necessary for anaerobic carnitine reduction in *Escherichia coli*. *J Bacteriol* **184**: 4044-4047.

Warikoo, V., McInerney, M.J., Robinson, J.A., and Suflita, J.M. (1996) Interspecies acetate transfer influences the extent of anaerobic benzoate degradation by syntrophic consortia. *Appl Environ Microbiol* **62**: 26-32.

Washburn, M.P., Wolters, D., and Yates, J.R., 3rd (2001) Large-scale analysis of the yeast proteome by multidimensional protein identification technology. *Nat Biotechnol* **19**: 242-247.

Weidenhaupt, M., Rossi, P., Beck, C., Fischer, H.M., and Hennecke, H. (1996) *Bradyrhizobium japonicum* possesses two discrete sets of electron transfer flavoprotein genes: *fixA, fixB* and *etfS, etfL. Arch Microbiol* **165**: 169-178.

Wilson, K. (2001) Preparation of genomic DNA from bacteria. In *Curr Prot Mol Bio*. Ausubel, F.M., Brent, R., Kingston, R.E., Moore, D.D., Seidman, J.G., Smith, J.A., and Struhl, K. (eds). New York: Greene Publishing Associates and Wiley-Interscience, p. Unit 2.4.

Wischgoll, S., Heintz, D., Peters, F., Erxleben, A., Sarnighausen, E., Reski, R. et al. (2005) Gene clusters involved in anaerobic benzoate degradation of *Geobacter metallireducens*. *Mol Microbiol* **58**: 1238-1252.

Wofford, N.Q., Beaty, P.S., and McInerney, M.J. (1986) Preparation of cell-free extracts and the enzymes involved in fatty acid metabolism in *Syntrophomonas wolfei*. *J Bacteriol* **167**: 179-185.

Wolters, D.A., Washburn, M.P., and Yates, J.R., 3rd (2001) An automated multidimensional protein identification technology for shotgun proteomics. *Anal Chem* **73**: 5683-5690.

Worm, P., Stams, A.J.M., Cheng, X., and Plugge, C.M. (2011) Growth- and substrate-dependent transcription of formate dehydrogenase and hydrogenase coding genes in *Syntrophobacter fumaroxidans* and *Methanospirillum hungatei*. *Microbiology* **157**: 280-289.

Wu, C., Liu, X., and Dong, X. (2006a) *Syntrophomonas erecta* subsp. sporosyntropha subsp. nov., a spore-forming bacterium that degrades short chain fatty acids in co-culture with methanogens. *Syst Appl Microbiol* **29**: 457-462.

Wu, C., Liu, X., and Dong, X. (2006b) *Syntrophomonas cellicola* sp. nov., a spore-forming syntrophic bacterium isolated from a distilled-spirit-fermenting cellar, and assignment of *Syntrophospora bryantii* to *Syntrophomonas bryantii* comb. nov. *Int J Syst Evol Microbiol* **56**: 2331.

Wu, C., Dong, X., and Liu, X. (2007) *Syntrophomonas wolfei* subsp. methylbutyratica subsp. nov., and assignment of *Syntrophomonas wolfei* subsp. saponavida to *Syntrophomonas saponavida* sp. nov. comb. nov. *Syst Appl Microbiol* **30**: 376-380.

Zhang, C., Liu, X., and Dong, X. (2004) *Syntrophomonas curvata* sp. nov., an anaerobe that degrades fatty acids in co-culture with methanogens. *Int J Syst Evol Microbiol* **54**: 969-973.

Zhang, C., Liu, X., and Dong, X. (2005) *Syntrophomonas erecta* sp. nov., a novel anaerobe that syntrophically degrades short-chain fatty acids. *Int J Syst Evol Microbiol* **55**: 799-803.

Zhao, H.X., Yang, D.C., Woese, C.R., and Bryant, M.P. (1990) Assignment of *Clostridium bryantii* to *Syntrophospora bryantii* gen. nov., comb. nov. on the basis of a 16S rRNA sequence analysis of its crotonate-grown pure culture. *Int J Syst Bacteriol* **40**: 40-44.

Zindel, U., Freudenberg, W., Rieth, M., Andreesen, J.R., Schnell, J., and Widdel, F. (1988) *Eubacterium acidaminophilum* sp. nov., a versatile amino acid-degrading anaerobe producing or utilizing H_2 or formate. *Arch Microbiol* **150**: 254-266.

Zybailov, B., Mosley, A.L., Sardiu, M.E., Coleman, M.K., Florens, L., and Washburn, M.P. (2006) Statistical analysis of membrane proteome expression changes in Saccharomyces cerevisiae. *J Proteome Res* **5**: 2339-2347.